DEFORMATIONAL BEHAVIOUR OF SANDSTONES

AN EXPERIMENTAL INVESTIGATION INTO THE INFLUENCE OF ENVIRONMENTAL AND FABRIC PARAMETERS ON THE DEFORMATIONAL BEHAVIOUR OF SANDSTONES

By

ROGER JOSEPH RECTOR, B.Sc., B.Sc. (Hons.), M.Sc.

A Thesis

Submitted to the School of Graduate Studies

in Partial Fulfilment of the Requirements

for the Degree

Doctor of Philosophy

McMaster University

September 1970

DOCTOR OF PHILOSOPHY (1970)
(Geology)

McMASTER UNIVERSITY
Hamilton, Ontario.

TITLE: An Experimental Investigation into the Influence of Environmental and Fabric Parameters on the Behaviour of Sandstones

AUTHOR: Roger J. Rector, B.Sc., B.Sc.(Hons.), M.Sc. (Manitoba)

SUPERVISOR: Dr. P.M. Clifford

NUMBER OF PAGES: xviii, 190.

SCOPE AND CONTENTS: An experimental study has been carried out to determine the effects of environmental and fabric parameters on the deformational behaviour of sandstones. Confining pressures ranged from 1-2500 bars, total strains 0.5-20.0 percent, and strain rates 10^{-5} - 10^{-7} per second.

The modes of deformation are found to be strongly dependent on confining pressure, total strain, and composition. All rocks tested show the customary increase in strength with increasing confining pressure. The ultimate strength is found to be inversely proportional to the mean grain size of the framework, and calcite content. Unconfined compressive strengths and elastic properties are strongly dependent on porosity. Ductility is enhanced by increasing calcite content and increasing confining pressure, but is not influenced by clast variation in the framework.

The deformational mechanisms are shown to be functions of the rock's fabric and confining pressure. Extensional microfracturing in the quartz grains of a calcareous sandstone and an arenaceous carbonate are controlled by the Poisson's ratio of quartz and calcite, and the volume fraction of the quartz grains.

ACKNOWLEDGEMENTS

I wish to express my sincere gratitude to Dr. P.M. Clifford who not only suggested the research topic, but also provided guidance and assistance throughout the work. I am also indebted to Mr. D.H. Underhill who provided unpublished experimental data on the calcareous Blairmore sandstone, and helped the writer develop the experimental facilities and techniques used in the investigation. Dr. G.V. Middleton and Mr. N. Wilson have also been generous with time and advice throughout the project. My thanks also go to many other members of the Geology Department, too numerous to mention individually, for their assistance and many stimulating discussions. My wife, Bobbie, has been a quiet but constant source of encouragement throughout the course of my studies.

The essential financial support was provided by the Mines Branch of the Department of Energy, Mines and Resources (1966-70), the National Research Council (1966-70), Chevron Standard Fellowships (1967-69), Ontario Graduate Fellowships (1967-70), and a bursary from the Bickell Foundation (1970).

ABSTRACT

An experimental study has been carried out to investigate the effects of composition, rock fabric, confining pressure, and total strain on the deformational behaviour of sandstones. The rocks selected for the investigation included an orthoquartzite, two calcareous sandstones, a greywacke, and an arenaceous carbonate. Differences in rock properties and in the nature and distribution of strain have been shown by triaxial compression experiments in the range of 1-2500 bars confining pressure, 0.5-20.0 percent strain at the nominal strain rate of 10^{-5} per second.

All the rocks show the customary increase in strength and ductility with increasing confining pressure. Unconfined compressive strengths are strongly dependent on porosity variations. In general, the ultimate strength of the materials increases with diminishing mean grain size of the framework, and decreasing carbonate content. Ductility is not strongly controlled by framework variation, but rather by the calcite content. Static Young's moduli are significantly lowered by porosity. None of the rocks tested approached theoretical values of Young's modulus predicted by the intrinsic properties of the constituent minerals.

At low confining pressures, the orthoquartzite fails along narrow fault surfaces. At elevated confining pressures, the orthoquartzite deforms along broad cataclastic zones. In contrast to the orthoquartzite, the greywacke fails along narrow faults at all confining pressures. The calcareous sandstone and the arenaceous carbonate deform by cataclasis at low confining pressures. Microfracturing of the quartz grains and intracrystalline deformation accommodate the deformation in the calcareous Oriskany sandstone. In the arenaceous carbonate all of the deformation is accommodated by intracrystalline deformation. The absence of microfracturing in the quartz grains even at relatively high total strains (10%) can be attributed to the low volume fraction of quartz grains. The nature of deformation in the calcareous sandstones and the arenaceous carbonate is discussed in terms of a continuum mechanic model of deformed composite materials.

TABLE OF CONTENTS

LIST OF FIGURES

LIST OF PLATES

Page

Page

LIST OF TABLES

Chapter 1

INTRODUCTION

General Statement

A knowledge of the deformational behaviour of rocks has considerable importance in the fields of mining engineering, petroleum engineering, engineering geology, geophysics, and structural geology. In structural geology, there exists a considerable quantity of field data on the geometry and kinematics of deformed rock structures; however, the processes of deformation and the nature of the stresses responsible for deformation cannot be observed in the field. The nature of these deformational processes and the factors which influence the deformational behaviour of rocks can best be studied in controlled laboratory experiments which attempt to simulate natural deformational environments.

In the past three decades, experimental work in rock mechanics has been largely devoted to evaluating the influence of environmental parameters on the deformational modes and mechanisms of a variety of rocks and minerals. In more recent years, considerable effort has been expended on theoretical and experimental investigations of fracture initiation fracture propagation, and evaluation of various failure criteria.

Investigations of the fabric in natural tectonites have been confined largely to petrofabric studies of twin lamellae in calcite and dolomite, quartz deformation lamellae, quartz microfractures, and kink bands which are used to deduce the orientation of the principal stresses. The validity of this type of analysis has been verified by laboratory investigations on experimentally produced fabrics. For example, petrofabric analyses of experimentally deformed "sand crystals" (single crystals of calcite that poikilitically enclose a number of sand grains), and some calcite cemented sandstones indicate that twin lamellae in calcite and microfracturing in the detrital grains can be used to infer the orientation of the principal stresses (Friedman, 1963).

Experimental investigations on the influence of a rock's initial fabric on deformational behaviour have lagged behind studies on environmental effects and petrofabric analyses. Although numerous sandstones have been experimentally deformed by various workers, at present no systematic descriptions of rock fabric are sufficiently detailed to allow a comprehensive study on the effects of rock parameters.

Purpose and Scope of the Investigation

The mechanical properties of rocks for the most part are dependent on the state of stress to which they are subjected and their deformational environment. Rock parameters such as composition, grain size, anisotropy, porosity, etc. can modify and in some cases control the deformational properties in a particular stress field and environment. The present investigation was undertaken to evaluate the deformational and failure characteristics of sandstones subjected to triaxial compression as a function of composition, sedimentary fabric, cement content, confining pressure and total strain.

During the period 1966-1969, the investigation required the writer, in conjunction with P. M. Clifford and D. H. Underhill, to develop a suitable triaxial testing apparatus, test procedures and data processing methods. Using the techniques developed, a study was carried out to investigate the deformational behaviour of sandstones. Environmental conditions and variations in composition and fabric should lead to differences in the nature and distribution of strain. The writer concentrated his major research effort on these particular aspects.

Approach used in the Investigation

Extensive research has been carried out by previous workers on the effects of confining pressure, pore pressure, temperature, and time on rock behaviour (Bredthauer, 1957; Handin and Hager, 1957; Handin and Hager, 1958; Handin *et al.*, 1963; Heard, 1963). A number of investigations have been devoted to assessing the individual effects of grain size, porosity, and anisotropy (Trask, 1959; Borg et al., 1960; Brace, 1961; Donath, 1964). For this reason, the present research involves the investigation of a number of rock parameters and their interrelationships.

Initially it was hoped that "model sandstones" comprised of sand and plaster of Paris or concrete would be made such that each independent rock parameter could be studied in turn. Porosity and homogeneity variations in the artificial sandstones could not be reasonably controlled and this aspect of the project was discontinued.

In lieu of the model sandstones, five natural rocks were selected for this study. In natural rocks, it is difficult to isolate individual fabric parameters. Therefore, samples were chosen such that wide compositional variations and a moderate range of grain sizes were obtained. These rocks included an orthoquartzite, greywacke, two calcareous sandstones, and an arenaceous limestone.

To evaluate the effects of rock fabric, a careful characterization was made of each test material prior to deformation (Chapter 3). Using carefully standardized experimental procedures (Appendix A), a study was made of the strengths, ductilities and deformational modes of the five rocks. Standardization of experimental procedures allows the comparative data thus obtained to be used to sort out the influence of various rock parameters.

All together, 150 room temperature triaxial compression experiments on four of the test materials were conducted by the writer in the range of 1-2500 bars confining pressure, 0.5 - 20.0 percent total strain, at nominal strain rates of 10^{-5} to 10^{-7} per second (Appendix-C). The pertinent data from an additional 45 experiments on the calcareous Blairmore sandstone were provided by D. Underhill.

The experimental strength data were examined with reference to the Mohr-Coulomb, Griffith, and maximum octahedral shear stress criteria of failure.

In the final phase of the investigation, a number of experimentally deformed specimens were examined in thin section in an attempt to correlate between observed deformational textures and deformational processes.

Chapter 2

REVIEW OF LITERATURE

General Statement

An understanding of rock failure under stress is important both to the geologist unravelling the mechanics of folding and faulting, and to the mining engineer striving to maximize rock breakage and minimize hazards from explosive rock bursts. The influence of environmental and fabric parameters on deformational behaviour cannot be fully evaluated without a knowledge of rock failure and deformational mechanisms. Experimental and theoretical rock mechanics attempt to resolve these questions.

In experimental rock deformation, the stress-strain curve and the deformed specimen are the primary data sources. The stress-strain curve reflects, to some extent, the deformational mode and the deformational mechanisms within the test specimen. This chapter reviews the characteristic regions of the stress-strain curve, some of the prevalent theories of fracture, and the mechanisms of uniform flow (plastic deformation).

Stress-Strain Curve

Brace (1964) subdivided an idealized stress-strain curve into four regions (Figure 1). Microscopic behaviour of a homogeneous brittle rock material can be correlated with the various regions of this characteristic stress-strain curve.

In Region I, the stress-strain curve is characterized by a concave upward slope. The degree of curvature in Region I varies for different rocks, as it is a function of both the rock material and the amount of pore space (Brace, 1964). In general, compact rocks have a straight stress-strain curve in this region, whereas open structured rocks have a pronounced curvature. The application of confining pressure causes a straightening of Region I due to compaction and pore closure (Brace, 1964).

In Region II, the effective elastic moduli, Young's modulus and Poisson's ratio, have constant values (Brady, 1969b, 1969d). Region II terminates when the principal stress reaches a critical value, after which any further increase in load results in localized failure (Brady, 1969b, 1969d).

Important permanent changes in the microscopic character of the rock occur in Region III. These changes accompany a subtle, gradual flattening of the stress-strain curve. Microcracking occurs

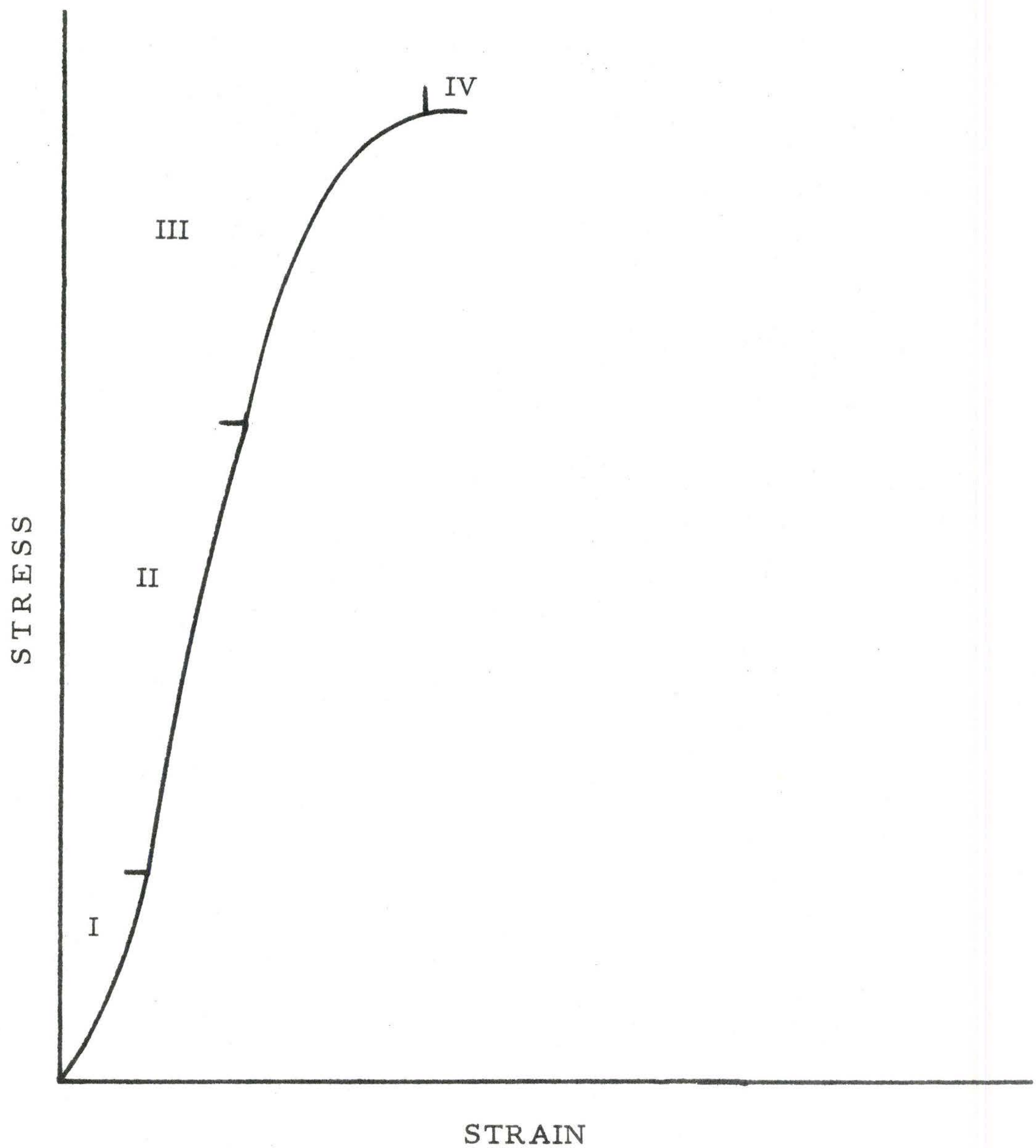

Figure 1. Idealized stress-strain curve.

and the ratio of lateral strain to axial strain increases rapidly, whereas in Regions I and II, it is nearly constant (Brace, 1964). The rock becomes lighter in color, apparently due to grains becoming unlocked at their boundaries (Brace, 1964).

Region IV is a very small region of constant stress in brittle rocks in which the lateral strain increases rapidly, cracks grow out of grain boundaries at many sites, and large through-going fractures grow out of an array of en échelon cracks (Brace, 1964; Bombolakis, 1968).

On the basis of theoretical and experimental data, Bieniawski (1967a, 1967b, 1967c) postulates stages of brittle fracture in multi-axial compression which can be correlated to the various regions of the stress-strain curve (Table I). In this study, Region V (maximum deformation) is extended to include ductile faulting and homogeneous deformation, as well as brittle fracture. Depending on the mode of deformation, Region V may be characterized by a number of deformational mechanisms - forking and coalescence of cracks, cataclasis, intracrystalline gliding, or recrystallization. In the final phase of this investigation, the mechanisms of deformation in Region V are examined in four of the test materials.

TABLE I. STAGES OF BRITTLE FRACTURE IN MULTIAXIAL COMPRESSION CORRELATED TO THE VARIOUS REGIONS OF THE STRESS-STRAIN CURVE

Stage	Stress-Strain Region
1. Closing of cracks	Region I. Crack closure
2. Linear elastic deformation	Region II. Fracture initiation
3. Stable fracture propagation	Region III. Critical energy release
4. Unstable fracture propagation	Region IV. Strength failure (maximum stress) - onset of forking
5. Forking and coalescence of cracks	Region V. Rupture (maximum deformation)

Brittle Deformation

The most familiar property of rocks is their brittleness at low temperatures and confining pressures. The characteristic feature of brittle solids is that they deform elastically up to a certain stress, then, suddenly break. Studies of brittle fracture stem from attempts to predict strengths of materials.

A criterion of failure for a given material may be defined as a quantitative statement which predicts that failure takes place when a definite relation characteristic of the material is satisfied. Most criteria are phenomenological. However, the Griffith criterion is a genetic failure mechanism. The conventional failure criteria are based on simple assumptions about the critical factor determining rupture. Some of the common phenomenological failure criteria are:

(1) maximum principal stress

(2) maximum principal strain

(3) maximum shear stress (Coulomb-Mohr)

(4) maximum strain energy

(5) maximum distortional strain energy or maximum octahedral shear stress.

The most important of these are summarized by Robertson (1955) and discussed in detail by Nadai (1950). Experimental and theoretical data for a number of rocks and rock-like materials have been examined with reference to the various failure criteria by a number of workers

(Robertson, 1955; Heard, 1960; Rhinehart, 1966; Cherry *et al.*, 1968; Hatano, 1968; Lundborg, 1968; Brady, 1969a, 1969c).

Although numerous theories for fracture have been suggested, the most useful for interpretation of experimental data are the Coulomb, the Mohr, the Griffith, and the maximum octahedral shear stress. The state of stress which causes fracture, fracture orientation, and to some extent the details of the fracture process are considered by the three former theories.

1. Coulomb Criterion

The Coulomb criterion postulates that the shear stress tending to cause failure across a plane is resisted by the cohesion of the material and by a constant times the normal stress across the plane. The criterion for shear failure in a plane is,

$$|\tau| = S_o + \mu\sigma \tag{2.1}$$

where σ and τ are the normal and shear stresses across a plane, S_o is regarded as an intrinsic constant for the material (the "cohesion" or cohesive shear strength of the soil scientists), and μ is the coefficient of internal friction. The coefficient of internal friction (μ), can be defined by the angle of internal friction (ϕ)

$$\mu = \tan \phi \tag{2.2}$$

where ϕ, is the angle between the "Mohr envelope" and the abscissa of the Mohr diagram (see discussion on Mohr criterion). The Coulomb criterion predicts that the direction of shear fracture is inclined at an acute angle to the direction of the maximum stress and can be determined by the expression,

$$\theta = (1/2)\tan^{-1}(1/\mu) \text{ or } \theta = \frac{90-\phi}{2} \tag{2.3}$$

where θ is the angle between the maximum principal stress and the fracture plane. The criterion does not involve σ_2 and is equivalent to the assumption of a linear Mohr envelope.

The Coulomb criterion has been widely applied in soil mechanics (Drucker and Prager, 1952; Drucker, 1954; Finn, 1967). The Coulomb hypothesis is generally regarded as the best description of the failure of rocks subjected to stress under low confining pressures (Brace, 1960).

2. Mohr Criterion

Mohr generalized the Coulomb criterion by extending it into three dimensions and by allowing for a variable coefficient of internal friction (Handin, 1969). The Mohr hypothesis postulates that material properties are a function of the state of stress and that shear failure occurs on those planes for which the shearing stresses (τ) are at a maximum and the normal stresses (σ) are at a minimum.

Experimentally determined values of the normal stresses at failure (σ_1, σ_2, σ_3) can be used to draw a series of "Mohr circles" in shear and normal stress space. The Mohr's envelope, the tangent to the family of Mohr circles, defines the yield surface of the solid under combined stress conditions. Failure will not take place if values of σ and τ are below the envelope, but failure will occur if values of σ and τ just touch or lie above the envelope.

The Mohr hypothesis carries two important implications:

(1) The value of the intermediate stress does not effect failure.

(2) The envelope is a function of the angle between the fracture plane and the maximum principal stress.

Combined triaxial compression or extension, and torsion experiments on the effects of the intermediate principal stress indicate that the shear strength of a material does depend on the relative magnitude of the intermediate stress (Handin et al., 1967; Mogi, 1967; Wiebols and Cook, 1968). As the mean stress $(1/2)(\sigma_1 + \sigma_3)$ is increased, the Mohr envelope becomes concave downward such that the predicted plane of fracture becomes inclined at an increasing angle to the direction of the maximum principal stress (Jaeger and Cook, 1969).

3. Griffith Criterion

The Griffith theory forms the basis of most analyses of the mechanism of brittle fracture (McClintock and Walsh, 1962; Murrell, 1963; Brady, 1969a, 1969c). The theory predicts that macroscopic fracture starts at the tips of pre-existing flaws (Griffith cracks) which enlarge and spread under the influence of applied stress, Griffith (1921) assumed that the cracks would propagate under applied stress when the strain energy released by extending the crack equals the energy to create new crack surfaces. The tensile fracture strength σ_f is related to the flaw dimension c, by the following equation,

$$\sigma_f = (2E\gamma/\pi c)^{1/2} \tag{2.4}$$

where E is the Young's modulus, γ is the fracture surface energy, and c is the half length of the Griffith crack. Room temperature uniaxial compressive strength σ_c, is eight times the tensile strength, or

$$\sigma_c = 8(2E\gamma/\pi c)^{1/2} \tag{2.5}$$

becomes the expression of the Griffith criterion for compressive strength (Brace, 1961). The Griffith criterion is expressed by Hoek and Bieniawski (1965) in terms of the maximum principal stress at fracture (σ_1), the principal stress ratio (σ_3/σ_1), and the uniaxial compressive strength (σ_c) as follows,

$$\sigma_1 = \sigma_3 + \sigma_c (2\sigma_3/\sigma_c + 1/4)^{1/2} + 1/4\,\sigma_c \tag{2.6}$$

In compression, the Griffith cracks probably close resulting in frictional forces developing on the crack surfaces. McClintock and Walsh (1962) modified the Griffith criterion to account for the closing of flaws in the following equation,

$$\sigma_1 = -4\sigma_t/((1-\sigma_3/\sigma_1)(1+\mu^2)^{1/2} - \mu(1+\sigma_3/\sigma_1)) \tag{2.7}$$

where μ is the coefficient of internal friction between crack faces and σ_t is the uniaxial tensile strength. Equation 2.7 can be expressed for uniaxial compression as,

$$\sigma_1 = \sigma_3((1+\mu^2+\mu)^{1/2}/(1+\mu^2-\mu)^{1/2}) + \sigma_c \tag{2.8}$$

where σ_c is the uniaxial compressive strength (Hoek and Bieniawski, 1966). The modified criterion can be represented as a Mohr envelope by the expression,

$$|\tau| = 2K - \mu\sigma \tag{2.9}$$

where K is the tensile strength, μ is the coefficient of sliding friction at the points of contact of crack surfaces (Brace, 1960). The modified Griffith and the Coulomb criterion are identical in the region of compression suggesting that the Griffith mechanism of crack growth is operative in the fracture of rocks at low confining pressure (Brace, 1960).

4. Maximum Octahedral Shear Stress Criterion

The maximum octahedral shear stress criterion predicts that yielding or rupture will occur when a constant amount of distortional strain energy is stored in a volume element. The failure condition is expressed in terms of stresses as,

$$\tau_{oct} = (1/3)((\sigma_1 - \sigma_2)^2 + (\sigma_1 - \sigma_3)^2 + (\sigma_2 - \sigma_3)^2)^{1/2} \qquad (2.10)$$

To account for all three principal stresses, but to avoid three dimensional diagramming, the stresses at failure are expressed in terms of the octahedral shear stress as a function of the octahedral normal stress (mean pressure). The mean pressure is related to dilational strain energy and is expressed in terms of the principal stresses by the following equation;

$$P_m = (1/3)(\sigma_1 + \sigma_2 + \sigma_3) \qquad (2.11)$$

Linearity of the octahedral shear stress with the mean pressure is an approximate empirical criterion of failure for rupture of silicate rocks and to some extent for limestones (Robertson, 1955; Handin et al. 1967).

Plastic Deformation

In the general sense, the ductility of a material is its capacity for undergoing permanent deformation without fracturing. Ductility commonly implies a capacity for plastic deformation by the mechanisms of crystal plasticity, slip, and twinning (Paterson, 1969). The term plastic deformation has many meanings because of disagreement amongst workers in various fields. In the geological context, the term plastic deformation is avoided and replaced by the concept of uniform flow, that is, macroscopically homogeneous deformation (Griggs and Handin, 1960). Uniform flow or permanent deformation is used in this study without any implications as to the shape of the stress-strain curve or the mechanisms responsible for the permanent deformation of the body. The three geological mechanisms of flow are intracrystalline gliding, cataclasis, and recrystallization.

In polycrystalline metals, ductility is achieved by crystallographic slip. The plane of densest packing and the widest spacing is the slip plane, and the slip direction is confined to the densest row of atoms (Hull, 1965). In ceramics, the slip planes and directions are affected by electrostatic forces and directional bonding. Von Mises (1928) and Taylor (1938) determined that five independent slip systems are required for ductility of a polycrystalline material. A slip system is said to be independent if simple shear cannot be achieved by any combination of other available slip systems (Groves and Kelley, 1963). The criterion is based on the assumption that in a polycrystalline aggregate, no discontinuities of displacement occur at the grain boundaries. This means that an individual grain undergoes the same homogeneous deformation as the neighbouring assemblage of grains. The Von Mises criterion has been used to explain the ductility of a number of compositionally simple ceramic materials (Parker, 1963; Nabarro _et al._, 1964; Wachtman, 1967). In studying the deformational behaviour of sandstones, the possibility of achieving flow by intracrystalline gliding in calcite and quartz should be evaluated.

At room temperature and atmospheric confining pressure $(01\bar{1}2)\langle 0\bar{1}11\rangle$ twinning (= e-twinning) commonly occurs in calcite. This provides three independent slip systems if the crystal is favourably oriented for twinning, but does not satisfy the Von Mises requirement. The translation gliding systems $(10\bar{1}1)\langle \bar{1}012\rangle$ (= r-translation) and $(02\bar{2}1)\langle \bar{1}012\rangle$ (= f-translation) may become operative, providing five independent slip systems, satisfying Von Mises requirement, and enabling calcite to deform in a ductile manner by crystalline gliding (Turner _et al._, 1954). Room temperature critical resolved shear stress at the yield point for e-twinning, r-translation and f-translation are approximately 80, 1100 bars and 2200 bars respectively (Turner _et al._, 1954, Borg & Handin, 1967). Under the experimental conditions of this study the initial resolved shear stresses for e-twinning, r-translation and f-translation may be achieved. This may account for the homogeneous deformation of favourably oriented calcite grains.

Quartz deformed under the conditions of temperature, confining pressure and strain rate in this investigation does not have five independent slip systems; therefore the flow mechanism cannot be intracrystalline gliding (Heard and Carter, 1968).

"Cataclastic flow involves displacements of constituent grains of an aggregate relative to one another accompanied by mechanical granulation, breaking, or crushing of grains" (Handin and Hager, 1957). In cataclasis, grain rotation and fracturing occur, resulting in the loss of cohesion on a small scale; but the body of material as a whole does not lose cohesion. Cataclasis is an active mechanism of flow on all scales from grain to grain up to sections several thousand feet thick (Stearns, 1969). Cataclastic deformation of both calcite and quartz can be expected under the experimental conditions encountered in this investigation.

The third active mechanism of uniform flow is recrystallization. Significant recrystallization of calcite is not achieved at temperatures under 500°C (Griggs *et al.*, 1960). Recrystallization of quartz also requires high temperatures and confining pressures in the order of 6Kb (Griggs *et al.* 1960; Green, 1967). The recrystallization mechanism clearly is not operative at the low temperatures, confining pressures and high strain rates at which the present series of experiments were conducted.

In summary, uniform flow in sandstones deformed under the environmental conditions of this study can be achieved in the following manner:

(1) cataclasis of the quartz grains.

(2) cataclasis of the calcite grains,

and (3) twinning and intracrystalline gliding in calcite.

Chapter 3

EXPERIMENTAL INVESTIGATION

General Statement

The prime object of this experimental investigation is to evaluate the influence of composition, and sedimentary fabric on the deformational behaviour of sandstones under varying conditions of confining pressure, total strain, and strain rate. Test materials are described in a standardized semi-quantitative manner to facilitate analysis and possible future comparisons with results of other investigators. Results of triaxial compression experiments are discussed with reference to the effects of environmental and fabric parameters on rock properties such as deformational mode, strength, ductility, elastic behaviour and deformational mechanisms.

Test Materials

1. Characterization of Test Materials

Changes in a rock's fabric parameters should lead to changes in deformational behaviour of sandstones. Therefore, rock descriptions must be standardized in a semi-quantitative manner.

Griffiths (1961) has defined the basic properties of sedimentary rocks which he feels are necessary and sufficient for a unique description of the rock, namely, particle composition, size, shape, orientation, and packing. However, it is convenient to determine other properties, e.g. porosity, fracture index and anisotropy in order to specify a material's mechanical properties. (Table II).

The composition of the undeformed test materials has been determined by modal analysis of thin sections. Effective porosity measurements have been made by Core Laboratories - Canada Ltd. of Edmonton.

Grain sizes of the samples used are based on measurements in thin section. Grains for measurement are selected by traversing the thin section in a manner similar to modal analysis so that the size frequency distributions obtained reflect a volume frequency rather than a weight percent. Maximum and minimum apparent diameters of each grain are measured. The maximum diameter is the largest intercept across the grain. In ambiguous grains the largest symmetrical axis is measured (Middleton, 1962). The minimum diameter is defined as the largest intercept perpendicular to the maximum diameter.

TABLE II

MATERIAL PARAMETERS OF SANDSTONES DETERMINED IN THIS STUDY

(1) COMPOSITION (MODAL ANALYSIS)

(2) POROSITY

(3) GRAIN SIZE AND SORTING

(4) GRAIN SHAPE

ROUNDNESS (VISUAL ESTIMATE)

SPHERICITY (THIN SECTION MEASURE)

(5) GRAIN ORIENTATION

(6) CONTACTS PER GRAIN

(7) "STRAIN INDEX" OF FRAMEWORK AND CEMENT

(FRACTURE INDEX, LAMELLAE/MM)

(8) ANISOTROPY

The size measure obtained by this type of analysis is a function of size, shape, composition, orientation, and packing of the grains (Griffiths, 1967). A single mineral, quartz, is used as the basis of measurement so that compositional effects are eliminated. No other adjustments are made for the other variables.

Two thin sections cut normal to the bedding were made of each sandstone. Fifty quartz grains were measured in each thin section; the results from each thin section were compared to those of the other thin section, and the two later combined to give a composite analysis.

Some of the quartz grains have been significantly modified by authigenic quartz overgrowths. If the quartz overgrowth is in optical continuity with the grain it is considered to be mechanically part of the grain and included in the grain size measurement. If the quartz grains have a preferred dimensional orientation, the orientation of the thin section is likely to affect size determinations (Middleton, 1962).

The size of the individual grains is calculated using the formula,

$$C = -\log_2 K(ab)^{1/2} \qquad (3.1)$$

where C = the size of the grain in Ø units

a = maximum grain diameter in thin section

b = minimum grain diameter in thin section

K = conversion factor to reduce measured values to millimeters.

The mean grain size is calculated by the method of moments by a computer program (Parkash, 1968). One standard deviation of the grain size is used as a measure of the sorting (Folk, 1961).

A description of the shape or geometric form of a particle is based on two measures, sphericity and roundness. A measure of the sphericity is obtained by the equation,

$$SPH = b/a \tag{3.2}$$

where b and a are the minimum diameter and maximum diameter in thin section respectively. Particle roundness is estimated by a visual comparison with standard roundness charts.

Grain orientation is defined as the angle between the observed long axis of a quartz grain and the inferred horizontal bedding direction (Mellon, 1964). Values of grain orientation are based on 100 quartz grain measurements for each of the test materials.

Packing is a measure of the degree to which grains are in contact with or interlocked among their neighbours (Krumbein and Sloss, 1963). The operational definition by which packing is estimated in this study is the number of contacts per grain. No allowance is made for the type of contact, i.e., point contact, surface contact or interpenetrative contact. The majority of grains in the sandstones studied have either point contacts or surface contacts.

The strain index of the framework and the cement is expressed by the fracture index and the twin lamellae spacing index respectively. The fracture index is based on the fracturing in one hundred grains per specimen as follows: Percent of unfractured grains X 1, plus percent of slightly fractured grains (1-3 fractures) X 2, plus percent moderately fractured grains (4-6 fractures) X 3, plus percent highly fractured grains (more than 6 fractures) X 4, plus percent demolished grains X 5 (Borg et al., 1960). Demolished grains are nests of fragments which retain the original grain outline or mylonitic zones. The index may vary from 100 to 500. The method is subjective but the indices determined can be used to compare relative amounts of fracturing between specimens. The twin lamellae spacing index is based on the number of lamellae per millimeter when viewed on edge and measured along a line normal to the twin planes (Friedman, 1963).

The effects of anisotropy on the deformational behaviour can be ignored because all specimens were compressed normal to bedding (McLamore and Gray, 1966).

2. Potsdam Sandstone

The Potsdam (Cambrian, Smith Falls, Ontario) is a white, flaggy (3 cms), very fine grained, very well sorted sandstone, with no visible fractures and an effective porosity of 8.2%. In thin section, the sandstone can be classified as a supermature orthoquartzite (Folk, 1961).

On the basis of a modal analysis of 100 points the rock consists of 97% quartz and 3% calcite. Extensive quartz overgrowths have modified the original clastic grains forming an interlocking but generally not interpenetrating texture (Plate 1A). Long axes of sixty-six percent of the quartz grains lie within 30° of the bedding (Figure 2). Untwinned calcite (lamellae index $<$ 10) occurs in small widely separated ovoid clots. A summary of the undeformed aggregate parameters is tabulated in Table III.

3. Oriskany Sandstone

The Oriskany (Lower Devonian, Cayuga, Ontario) is a white, massive (18 cms), fine grained, moderately well sorted, mature calcareous sandstone with an effective porosity of 6.3%. Small quartz overgrowths are present on a few of the grains and grain contacts are generally not penetrative (Plate 1B). Only fifty-six percent of the quartz grains lie within 30° of the bedding (Figure 2). Fine to cryptocrystalline calcite is interstitial to the quartz grains, but occasionally occurs as irregular lamina 1 mm thick. The rock consists of 80% quartz and 20% calcite. The observed roundness (subangular) of the quartz grains appears to have been significantly altered by calcite corrosion. Undeformed material parameters are summarized in Table III.

Plate 1

A. Photomicrograph of the Potsdam sandstone. Note the quartz overgrowths and the interlocking nature of the grain contacts. (polarized light, X 110)

B. Photomicrograph of the calcareous Oriskany sandstone. (polarized light, X 110)

A

B

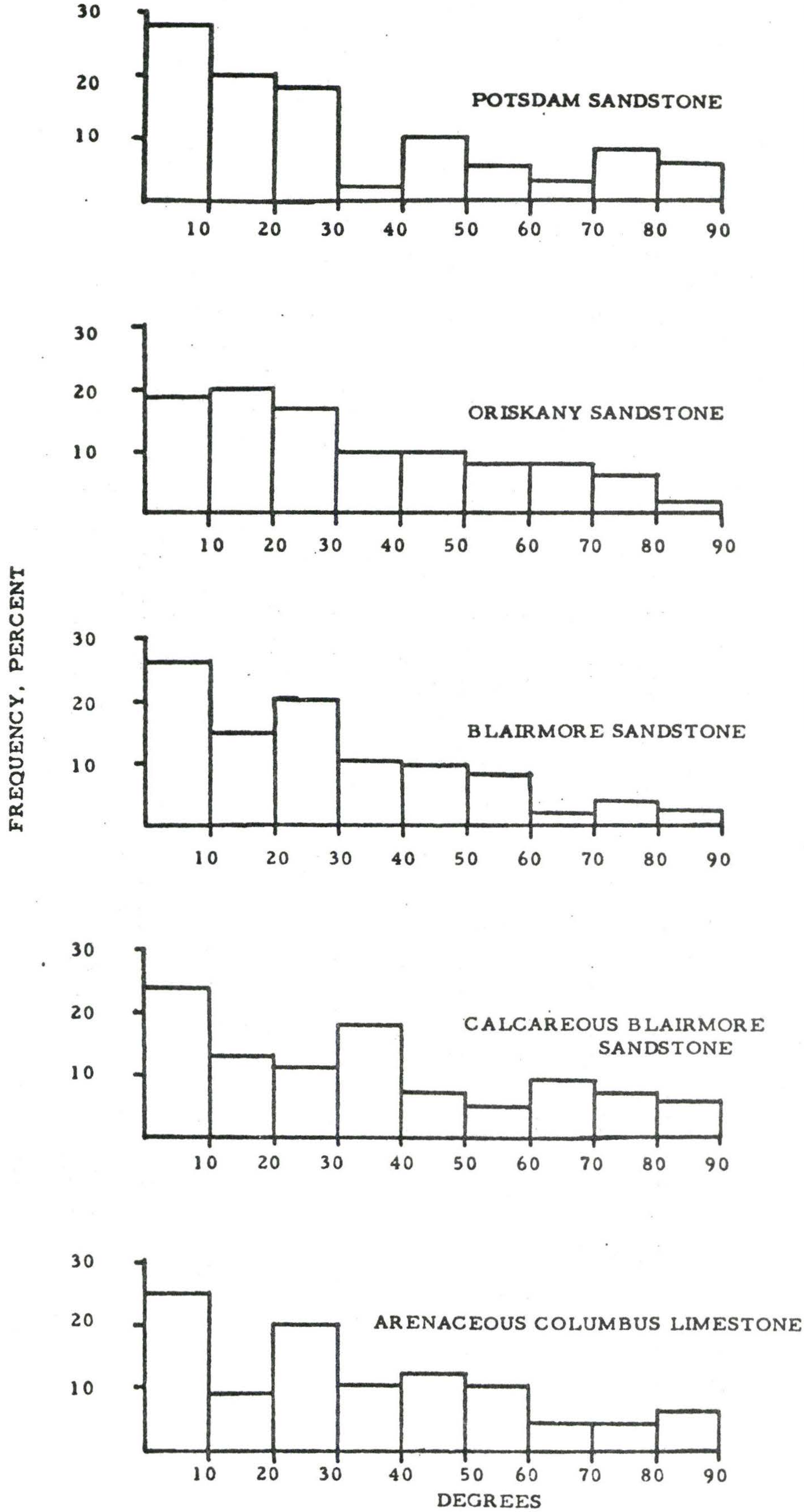

Figure 2. Grain orientation based on 100 quartz grains per sample.

TABLE III. COMPARISON OF CERTAIN PARAMETERS FOR UNDEFORMED SANDSTONES

	POTSDAM	ORISKANY	CALCAREOUS BLAIRMORE	BLAIRMORE	COLUMBUS "sand fraction"
Grain Size Ø	3.07	2.05	2.75	2.43	3.53
Sorting	0.26	0.54	0.22	0.25	0.15
Sphericity	0.63	0.69	0.61	0.62	0.65
Roundness	0.34	0.34	0.29	0.25	0.35
Calcite %	3.0	20.0	39.0	3.4	62.0
Contacts/Grain	5.45	4.72	2.09	4.39	1.24
Porosity %	8.2	6.3	1.6	4.5	14.9
Specific Gravity gms/cc	2.54	2.55	2.71	2.67	2.57
Fracture Index	120.0	116.0	140.0	110.0	101.0
Lamellae Spacing Index	10.0	10.0	10.0	10.0	10.0

4. Blairmore Sandstone

The Blairmore (Lower Cretaceous, Red Deer River, Alberta) is a grey "salt and pepper", flaggy (6 cms), fine grained, well sorted, sandstone with an effective porosity of 4.5%. The sandstone can be classified as an immature greywacke (Folk, 1961). Subangular to angular sand grains make up 73.6% of the rock and consist of: feldspar (23.2%), quartz (21.0%), rock fragments (13.0%), chert (10.8%) and composite quartz grains (5.6%). The clastic grains form a densely packed interlocking framework (Plate 2A). Long axes of sixty-one percent of the quartz grains lie within 30° of the inferred bedding (Figure 2). The matrix (20.4%) consists of fine grained inter-granular detritus biotite and authigenic silica (?) and chlorite. The distinction between rock fragments-matrix-authigenic cement is difficult to ascertain in this fine grained sandstone. Calcite (4%) occurs as random grains throughout the rock. Compositionally and texturally the rock is similar to the silicate cemented phase of the Mountain Park sandstone (Blairmore) described by Mellon (1964, 1967).

5. Calcareous Blairmore

This facies of the Blairmore (Lower Cretaceous, Red Deer River, Alberta) is a black to dark grey, massive, fine grained, very well sorted, submature subgreywacke (Folk, 1961). Modally the rock consists of calcite (39.4%), feldspar (24.7%), quartz(11.4%), rock

Plate 2

A. Photomicrograph of the Blairmore sandstone. Quartz, feldspar, chert, and rock fragments are the prominent detrital grains. Matrix consists of authigenic chlorite and silica as well as some fine detrital material. (polarized light, X 135)

B. Photomicrograph of the calcareous Blairmore sandstone. (polarized light, X 110)

A

B

fragments (10.7%), chert (8.3%), mica (0.8%), and other (5.1%) (Underhill, personal communication). Calcite grain sizes range from cryptocrystalline to coarse grains of irregular shape which enclose several sand grains (Plate 2B). In thin section, the elongate subangular to angular clastic grains and mica mark a distinct parallel lamination. However, only 48% of the quartz grains lie within 30^{o} of this lamination (Figure 2). Table III summarizes the characterizing parameters of the calcareous Blairmore sandstone.

6. <u>Columbus Limestone</u>

Thetest block of "Columbus" (Devonian, Ingersoll, Ontario) is a buff brown, medium crystalline, massive, arenaceous and dolomitic limestone with an effective porosity of 14.9%. Bedding in the test block is marked by a concentration of spirifer brachiopods and rugose corals.

In thin section the rock consists of very fine grained, subangular to subrounded, very well sorted, "floating" sand grains in a groundmass of recrystallized sparry calcite (Plate 3). Microscopic determinations of quartz grain size, sorting, etc. are summarized in Table III. Orientation of quartz grains vary between 0^{o} (parallel to bedding) and 90^{o} (normal to bedding) with only 54% within 30^{o} of the macroscopic bedding surface (Figure 2). Calcite grains range

Plate 3

Photomicrograph of the arenaceous and dolomitic Columbus limestone. The sand grains "float" in a cement of re-crystallized sparry calcite. Dolomite occurs as discrete rhombs. (polarized light, X 110)

in size from cryptocrystalline to 1 mm, with the majority of the grains (85%) 0.125 mm. Dolomite occurs as discrete rhombs (0.145 mm) scattered throughout the rock. Crinoid columnals and ossicles, fragments of brachiopod tests, and coral (?) fragments can be occasionally identified in some thin sections. Modally the rock consists of calcite (62.0%), quartz (21.0%) and dolomite (17.0%).

Influence of Environmental Parameters

1. General Statement

One of the prime purposes of experimental research in rock mechanics is to furnish information on the deformational modes and mechanisms so that this information can be related to observed rock structures in the field.

Griggs and Handin (1960) define three deformational modes - extension fracture, fault, and uniform flow. Donath (1968) extends the number of deformational modes to the following:

(1) extensional faulting

(2) brittle faulting

(3) ductile faulting

(4) homogeneous flow

(5) elastic (recoverable) deformation

Extensional faulting (longitudinal splitting of the specimen) is mainly observed at very low confining pressures. Although the mechanism of forming extensional faults in a compressive stress field is not known, it has been attributed to submicroscopic flaws which act as stress risers to produce local tensile stresses (Heard, 1968). Brittle shear faulting is defined as faulting with loss of cohesion, whereas ductile faulting is faulting without the loss of cohesion (Donath, 1968). The brittle-ductile transition of a number of rocks has been well documented by several workers (Von Karman, 1911; Adams, 1912; Heard, 1960; Handin *et al.*, 1963). Extensional and shear faulting are gradational and apparently form by the same process of internal fracturing (Brace, 1964). Homogeneous flow is defined as permanent deformation without any visible signs of faulting. Elastic deformation is defined as strain which occurs instantaneously when stress is applied and is fully and instantaneously recovered when stress is removed. This definition is not strictly applicable in this study, and the definition used here is that elastic deformation means that 60% or more of the total strain is recoverable within a very short time when the stress is removed.

A rock's mode of deformation is strongly affected by environmental factors such as confining pressure, total strain, pore pressures, temperature, strain rate, and the stress field in which it occurs. Besides these environmental parameters, material parameters such as grain size, anisotropy, porosity, composition, homogeneity, etc. should be considered. Apparatus effects must also be taken into account when one is evaluating deformational modes. Apparatus stiffness affects the rate at which energy is dissipated at failure (Bieniawski et al., 1969). A "soft" testing machine like the one used in this investigation tends to cause a rapid dissipation of energy at fracture. A force equalizer such as Paterson (1958) used in his apparatus prevents bending moments and lateral movements of the anvil, thus forcing symmetrical deformation. This results in conjugate fractures when the specimens fail by faulting. The flat anvil used in this study allows minute shifting, and produces less rigid boundary conditions with the result that only a single fault plane forms at failure.

2. Effect of Confining Pressure

(a) Deformational Modes. The Potsdam sandstone fails by brittle shear fracture over the entire range of confining pressures studied (1-2500 bars). At 1 bar the specimens are characterized by a number of narrow fracture surfaces subparallel to the core axis, and the occasional fracture surface inclined at 45^{o} to the core axis. The mode of deformation is transitional between extensional faulting and brittle shear faulting. At low strains ($\approx 3\%$) and confining pressures of 500, 1000, 1500, 2000 and 2500 bars the specimens exhibit narrow single faults of the brittle shear type. However, some less persistent conjugate faults are developed in some specimens (Plate 4).

Deformational modes of the Blairmore sandstone are essentially similar to those of the Potsdam sandstone. Extensional faulting characterizes specimens deformed at atmospheric confining pressures, whereas shear faulting occurs at higher confining pressures (Plate 5). At low strains the deformation is restricted to narrow, distinct faults with no development of conjugate faults.

Specimens of Oriskany sandstone deformed at confining pressures up to 1000 bars are characterized by shear faulting accompanied by a sudden release of stored elastic energy. Unconfined test specimens are characterized by extensional faulting. Both extensional and shear components are present in specimens tested at 250 bars confining pressure (Plate 6). At 1100 bars confining pressure, faulting is accompanied by a gradual release of stored elastic energy, and at low strains the faults are long but tend to be less distinct. At 1500 bars confining pressure and low strains ($\approx 4\%$) a number of short, barely discernible conjugate fractures inclined at 45° to the core axis appear in the deformed specimens (Plate 6). These "Luders Lines" are widely distributed throughout the sample, and a tendency toward barreling can be observed. The specimen fails without losing cohesion and its deforma-

Plate 4

Specimens of Potsdam sandstone deformed 2.51 to 4.89 percent strain at various confining pressures (X 3)

A. 1 bar, confining pressure (2.51 percent strain)

B. 500 bars, confining pressure (4.89 percent strain)

C. 1000 bars, confining pressure (3.60 percent strain)

D. 2500 bars, confining pressure (4.17 percent strain)

A

B

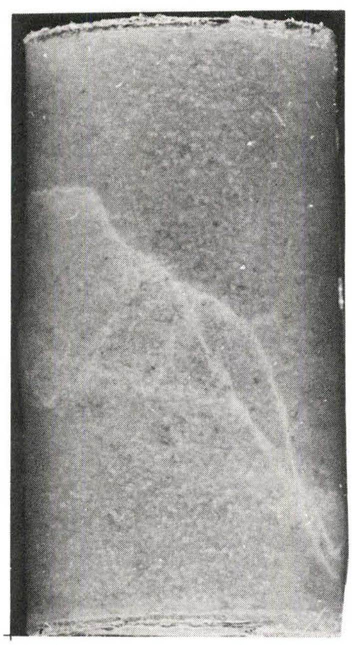

C

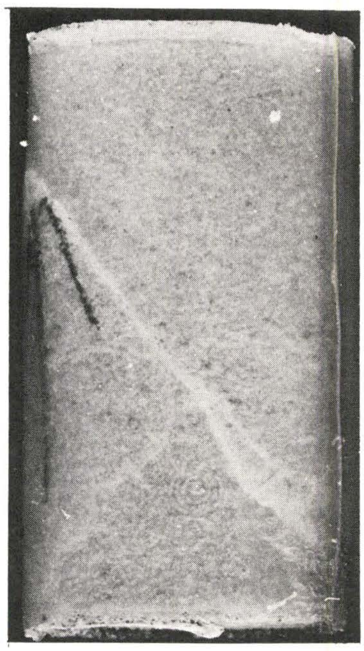

D

Plate 5

Specimens of Blairmore sandstone deformed 4.27 to 4.58 percent strain at various confining pressures (X 3).

A. 1 bar confining pressure (4.31 percent strain)

B. 500 bars confining pressure (4.27 percent strain)

C. 1500 bars confining pressure (4.49 percent strain)

D. 2500 bars confining pressure (4.58 percent strain)

A

B

C

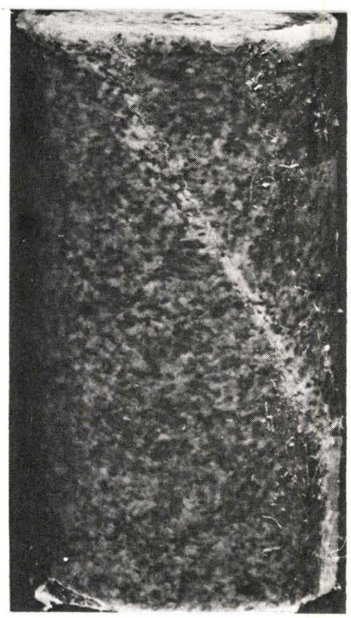

D

Plate 6

Specimens of Oriskany sandstone deformed 3.66 to 4.93 percent strain at various confining pressures (X 3)

A. 250 bars confining pressure (3.66 percent strain)

B. 1000 bars confining pressure (4.54 percent strain)

C. 1500 bars confining pressure (4.43 percent strain)

D. 2500 bars confining pressure (4.93 percent strain)

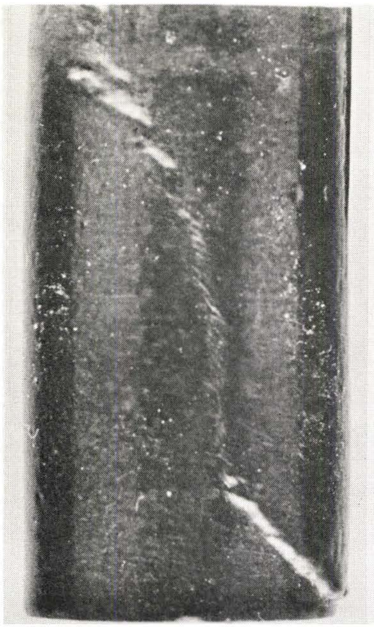

A

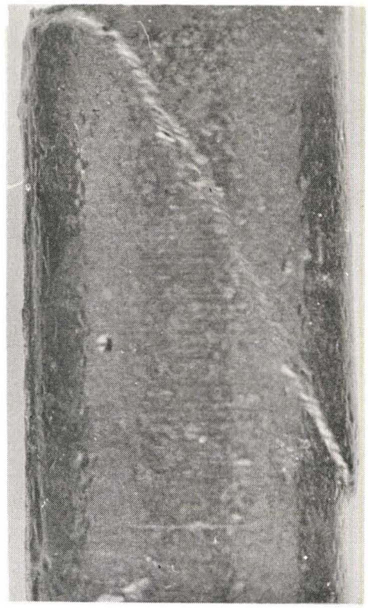

B

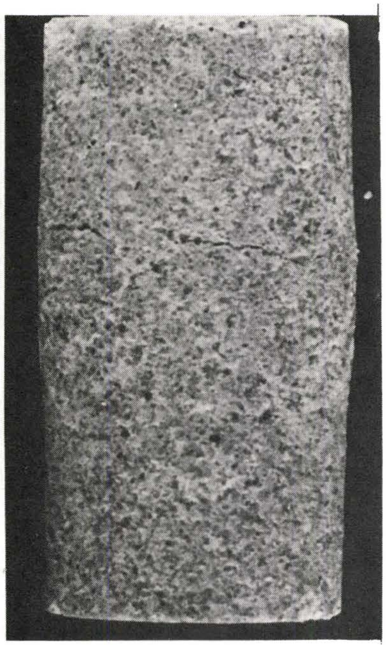

C

D

tional mode is ductile faulting. Luders Lines and slight bulging characterize samples deformed at 2000 and 2500 bars confining pressure.

Within the confining pressure range of this investigation, the permanent deformation of the Columbus limestone varies from extensional faulting at 1 bar to homogeneous flow at 2500 bars confining pressure (Plate 7). At 1 0 0 bars confining pressure, brittle fracture is accompanied by a sudden and substantial loss of elastic energy; the deformation is restricted to several parallel shear faults with minor development of conjugate slip surfaces (Plate 7). Numerous conjugate slip surfaces (Luders Lines) characterize the specimens deformed at 250 and 500 bars confining pressure. At higher confining pressures and low strains the specimens deform homogeneously and the permanent strain is distributed throughout the specimen. No visible faults occur in these specimens, but at low strains barreling cannot be observed.

(b) Strength. Two strength parameters can be used in considering the "strength" of a material as determined in experimental rock deformation, that is, "yield strength (stress)" and "ultimate strength" (Robertson, 1955). "Ultimate strength" is defined as the maximum differential stress sustained by the specimen. The "yield stress" is defined as the maximum stress that a specimen can withstand without undergoing permanent (plastic) deformation either by solid flow or rupture (Coates, 1965) Permanent deformation does not imply any-

Plate 7

Specimens of arenaceous Columbus limestone deformed 1.08 to 7.92 percent strain at various confining pressures (X 3)

A. 1 bar confining pressure (1.08 percent strain)

B. 100 bars confining pressure (1.32 percent strain)

C. 500 bars confining pressure (7.92 percent strain)

D. 2000 bars confining pressure (3.15 percent strain)

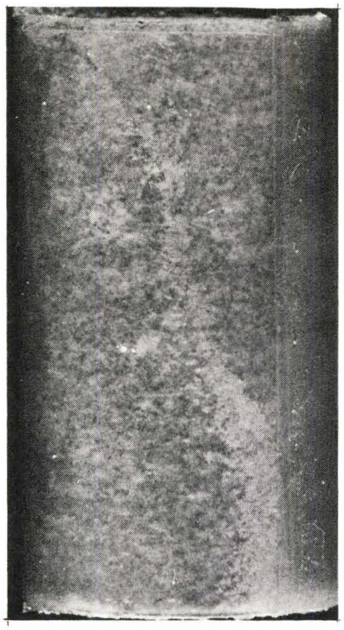

A

B

C

D

thing about the shape of the stress-strain curve or the mechanism of deformation. In this study the "ultimate strength" is used as the strength parameter.

The definition of ultimate strength becomes difficult to apply when a specimen work hardens during deformation as there is no true maximum differential stress, and the stress at which the test terminates determines the strength of the material. Apparatus design and deformational mode can affect the values of experimentally determined strengths (Appendix A). These factors must be taken into account in specifying strengths and comparing strength determinations between different laboratories.

Calculated average stress-strain curves for specimens of Potsdam sandstone deformed at various confining pressures are given in Figure 3. The initial portion of each curve is nearly linear up to the ultimate strength beyond which there is a sudden and abrupt drop in the differential stress. The rapid release of stored elastic energy during faulting is typical of brittle shear failure. Figure 4 shows that there is a large initial increase in the compressive strength between 1 and 500 bars confining pressure after which the strength continues to increase but at a reduced rate (150 bars for every 100 bars confining pressure). The large initial increase probably reflects closing of cracks and a general compaction of the specimen by the applied confining pressure.

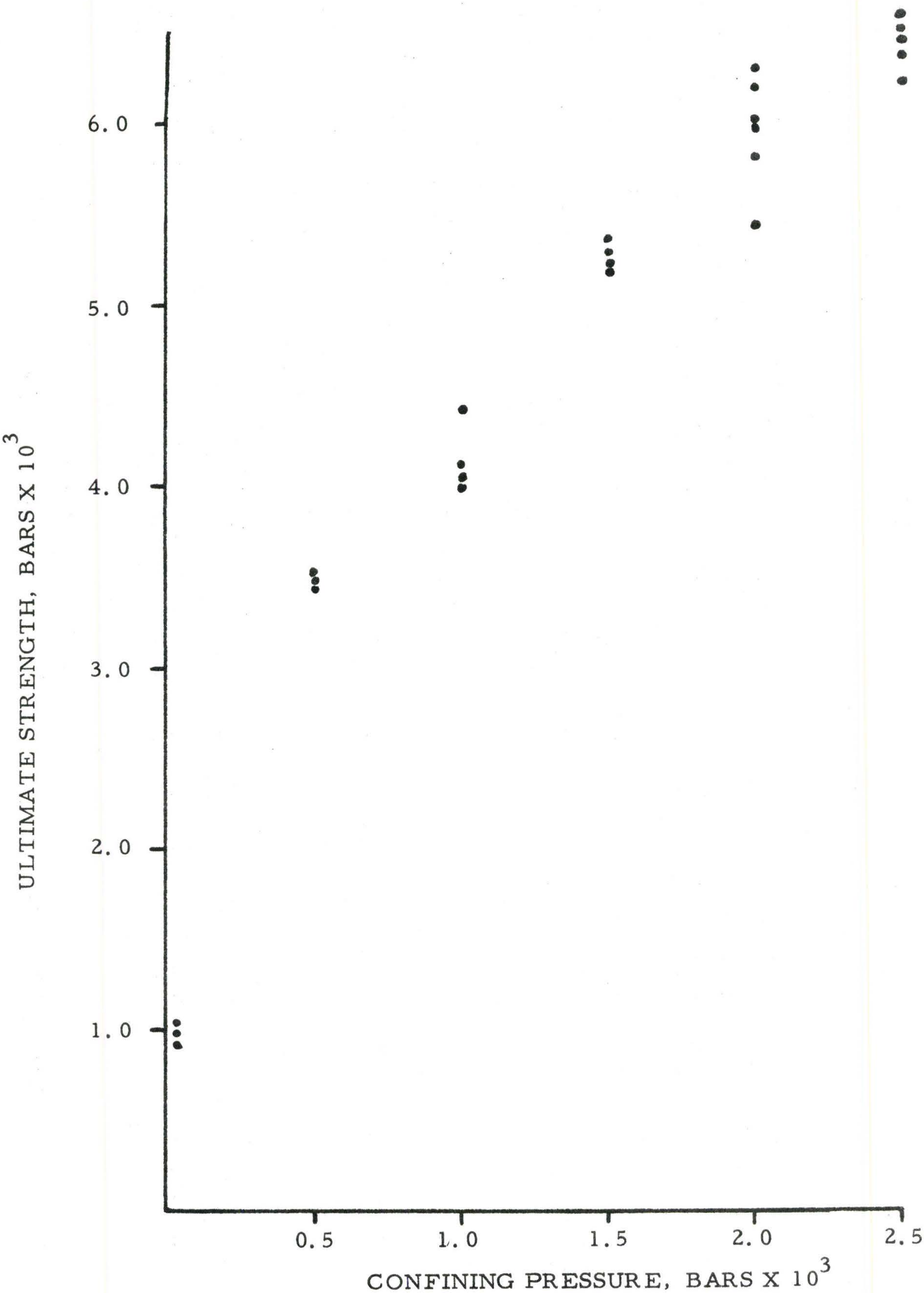

Figure 4. Maximum differential stress sustained by the Potsdam sandstone at various confining pressures.

Figure 5 shows the average stress-strain curves for the deformation of the Blairmore sandstone as a function of confining pressure. The curves are essentially similar to those obtained for the Potsdam sandstone, namely, increasing maximum differential stress at higher confining pressures, linear deformation up to the ultimate strength, and a sharp drop in the differential stress at rupture. At confining pressures greater than 500 bars the strength increases gradually, such that for every 100 bar increase in the confining pressure the strength is enhanced approximately 150 bars (Figure 6).

Figure 7 summarizes the stress-strain relationships of the Oriskany sandstone. The ultimate strength increases systematically with confining pressure except at 1100 bars confining pressure. In Figure 8 the effect of confining pressure on the ultimate strength of the Oriskany sandstone is illustrated. Scatter in the points reflects material differences between specimens, or in some cases slight differences in specimen end conditions. Above 500 bars confining pressure, the strength increases 100 bars per 120 bars increase in confining pressure.

Average stress-strain curves for the arenaceous Columbus limestone as a function of confining pressure are given in Figure 9. Unlike the stress-strain curves of the sandstones, these curves show a complete spectrum from brittle faulting to work hardening (rising

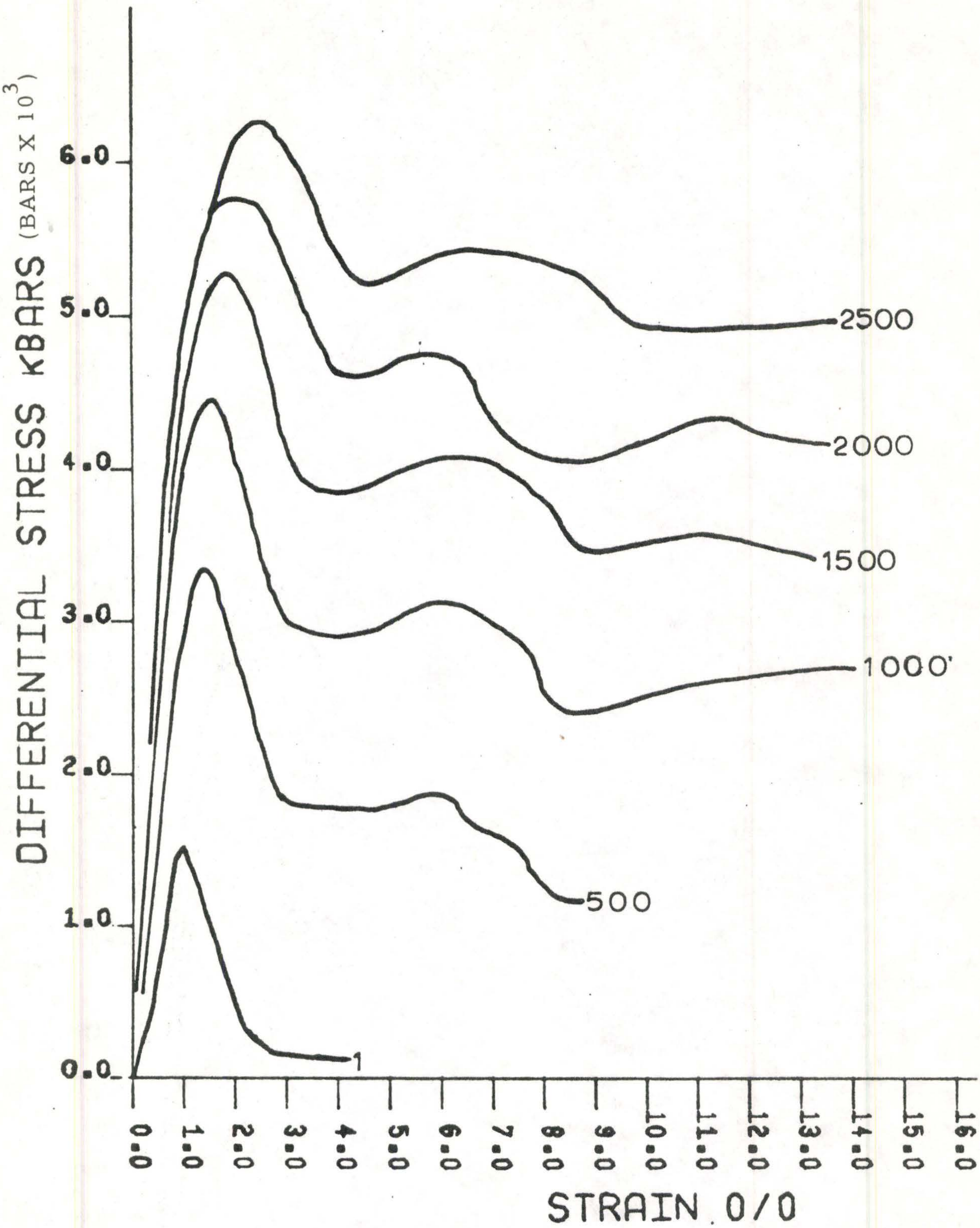

Figure 5. Average stress-strain curves for the Blairmore sandstone deformed at various confining pressures.

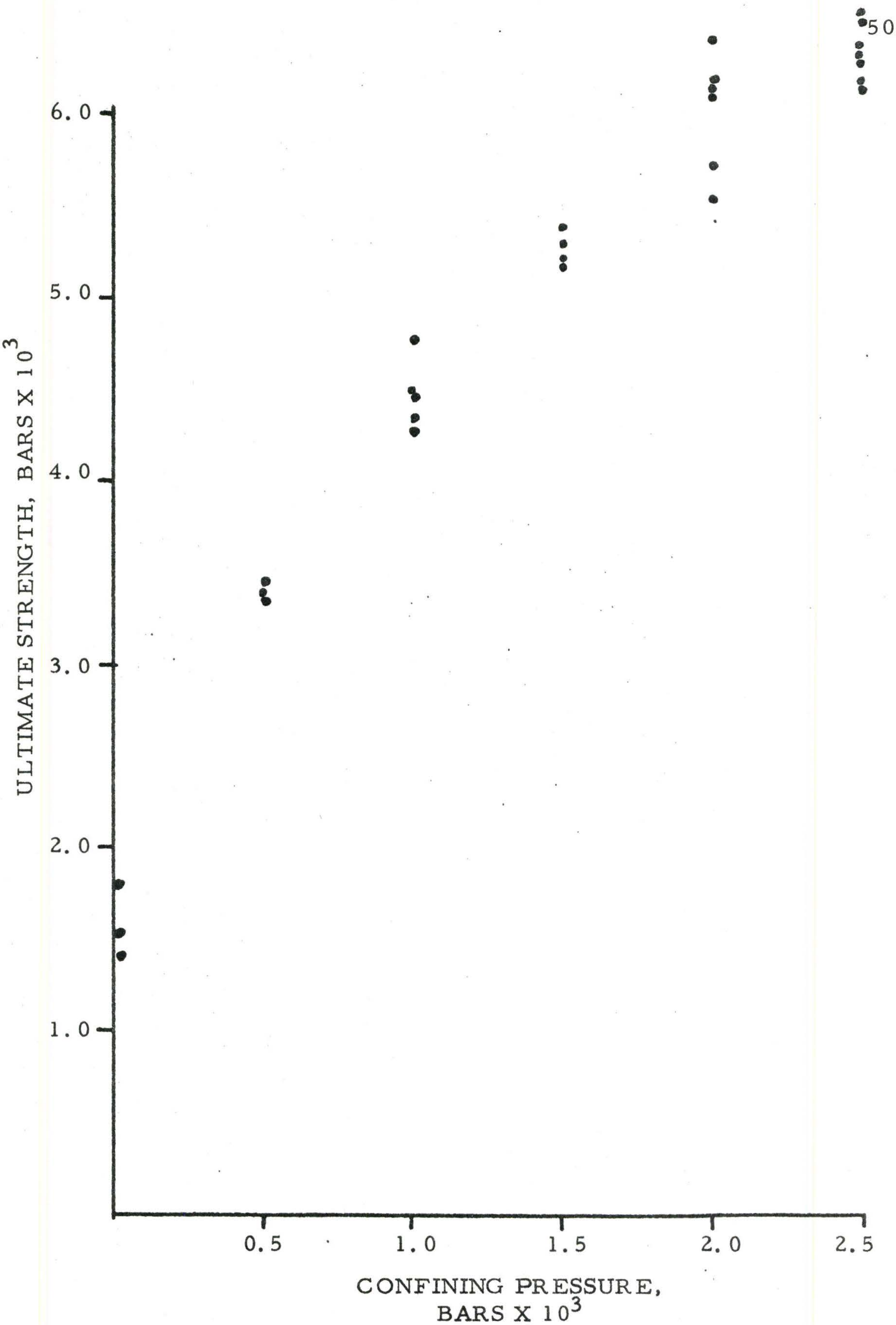

Figure 6. Maximum differential stress sustained by the Blairmore sandstone at various confining pressures.

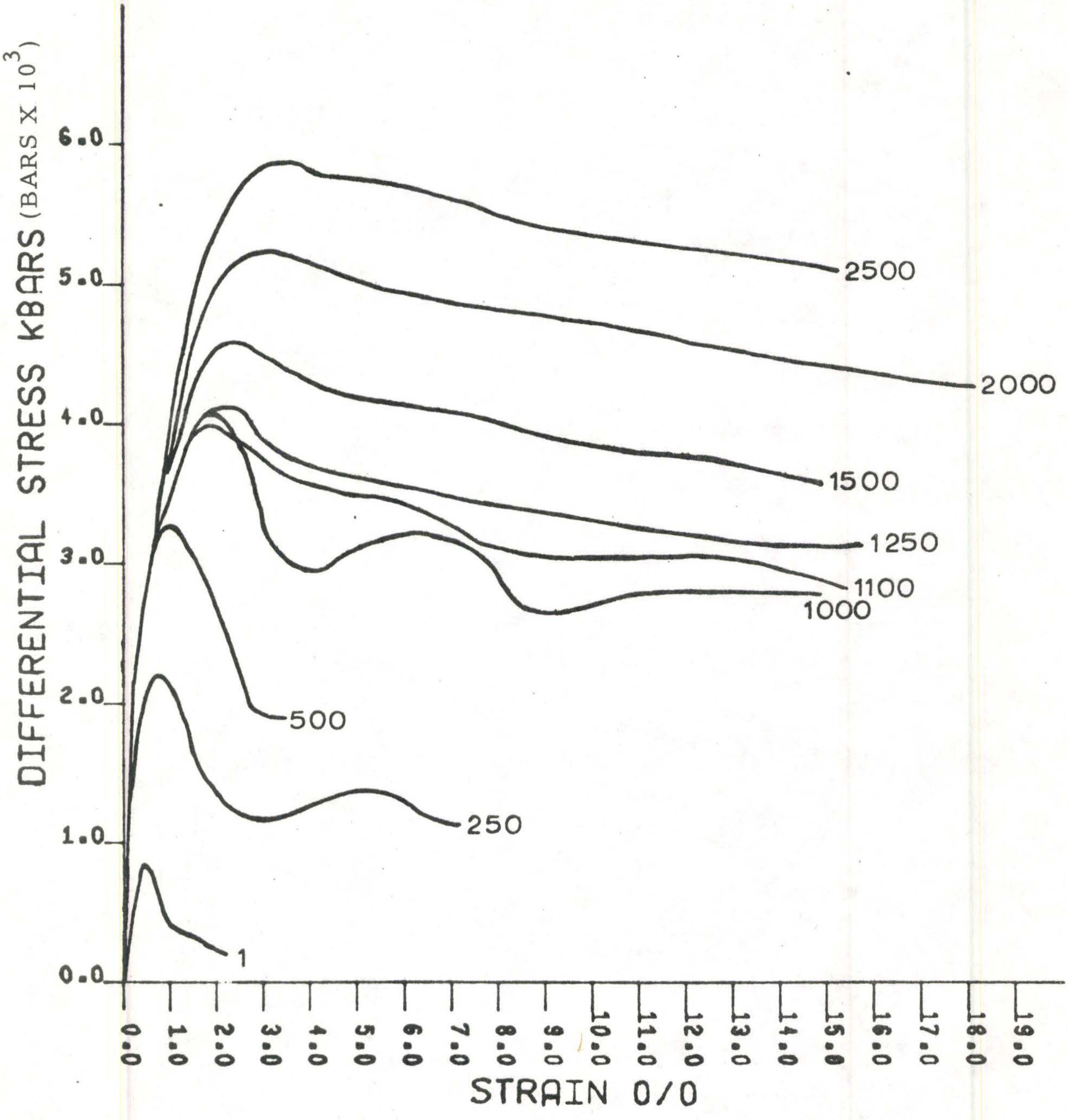

Figure 7. Average stress-strain curves for the Oriskany sandstone deformed at various confining pressures.

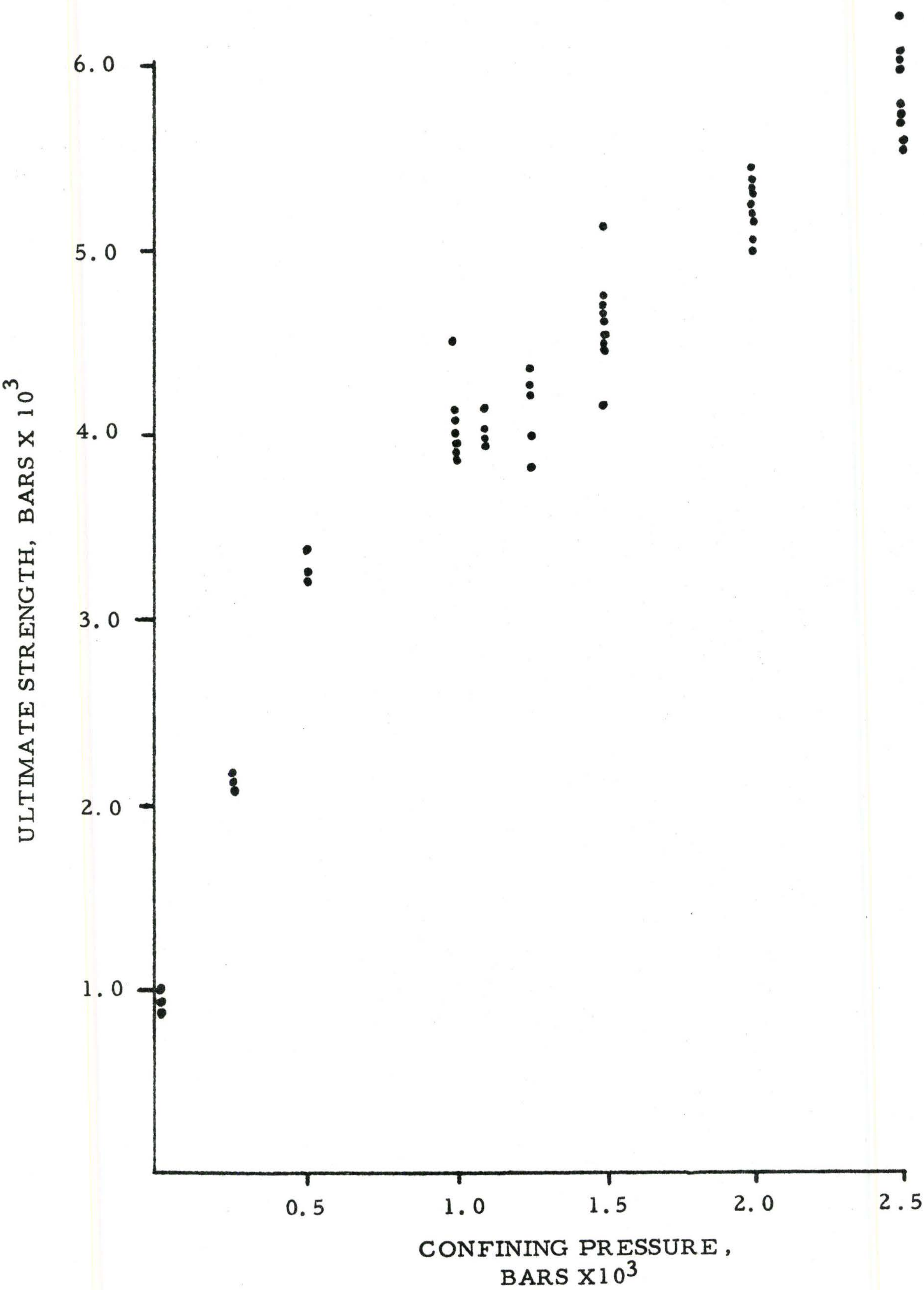

Figure 8. Maximum differential stress sustained by the Oriskany sandstone at various confining pressures.

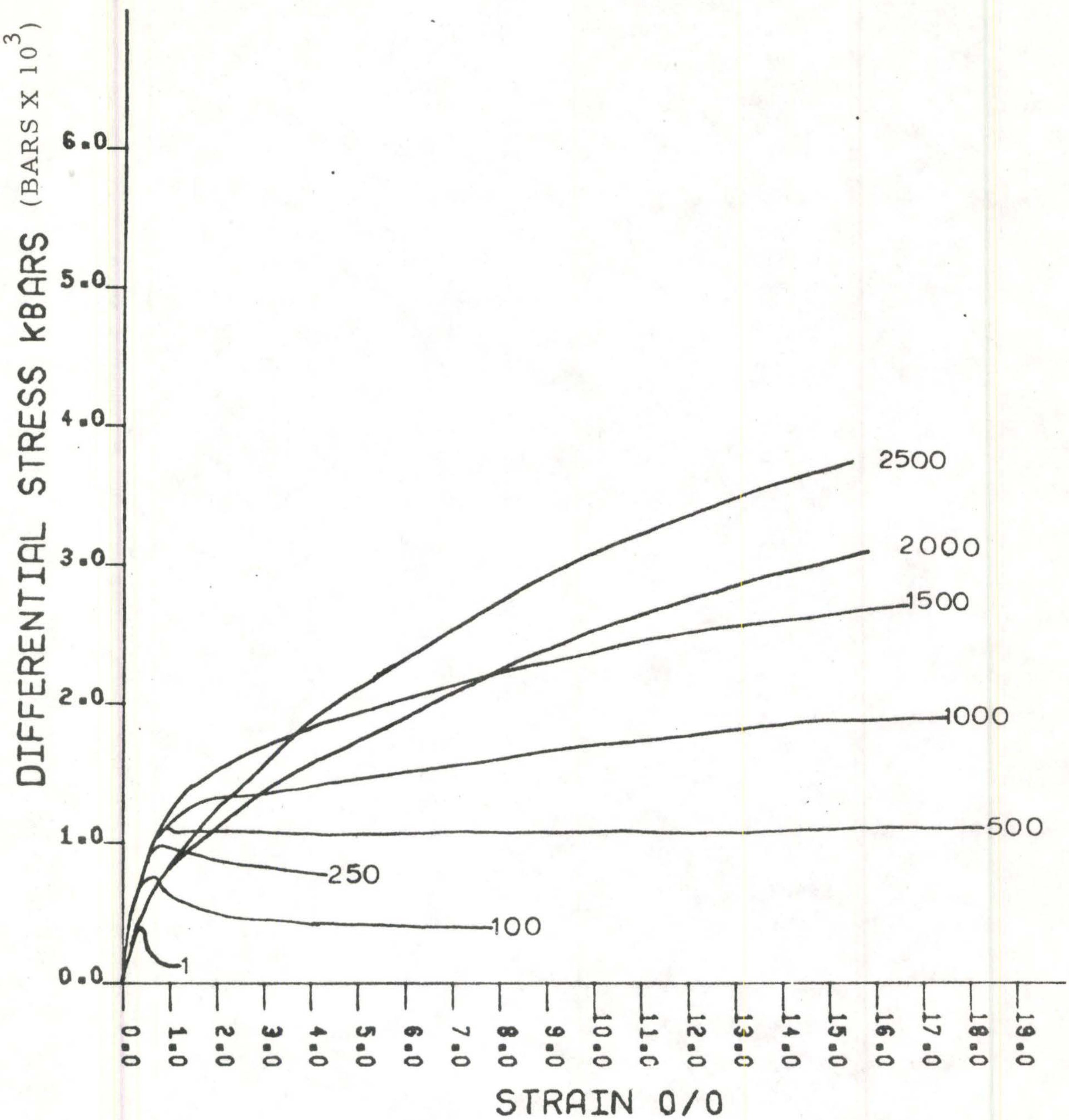

Figure 9. Average stress-strain curves for the arenaceous Columbus limestone deformed at various confining pressures.

stress-strain curve). Values of the ultimate strength of specimens deformed at confining pressures greater than 1000 bars are directly related to total strain. Figure 10 illustrates the variation of strength with confining pressure. For the puposes of this diagram, strengths at 1000, 1500, 2000 and 2500 bars confining pressure are based on total strains of 18%, 17%, 16% and 16% respectively.

(c) Evaluation of Failure Criteria. An extensive and rigorous evaluation of the various failure criteria is beyond the scope of this investigation. The following discussion is a qualitative examination of strength date of the various test materials and the Coulomb-Mohr, Griffith and the octahedral shear stress failure criteria.

The Coulomb-Mohr criterion postulates that failure will occur when the shearing stress exceeds the cohesion of the material plus the frictional resistance on the shear fracture planes. Mohr envelopes for the Potsdam, Blairmore, Oriskany sandstones, and the arenaceous Columbus limestone are illustrated in Figure 11. The maximum principal stress is the maximum differential stress plus confining pressure sustained by the specimen, and the minimum principal stress is equivalent to the confining pressure ($\sigma_2 = \sigma_3$). The fracture angle θ, is defined as the angle between the fracture surface or fault and the direction of maximum principal compression. The predicted angles of fracture derived from the Mohr diagrams for the confining pressure

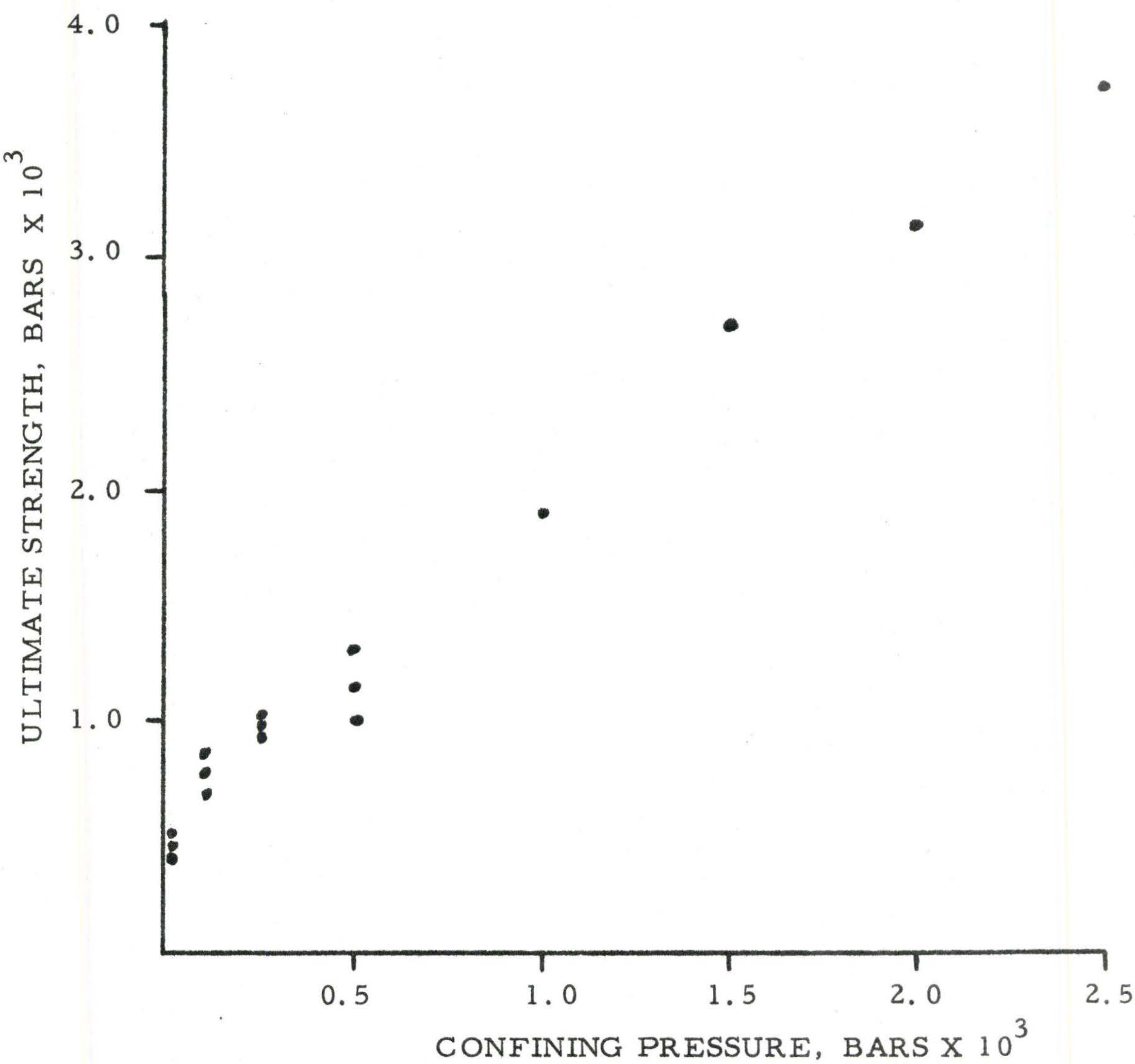

Figure 10. Maximum differential stress sustained by the arenaceous Columbus limestone at various confining pressures.

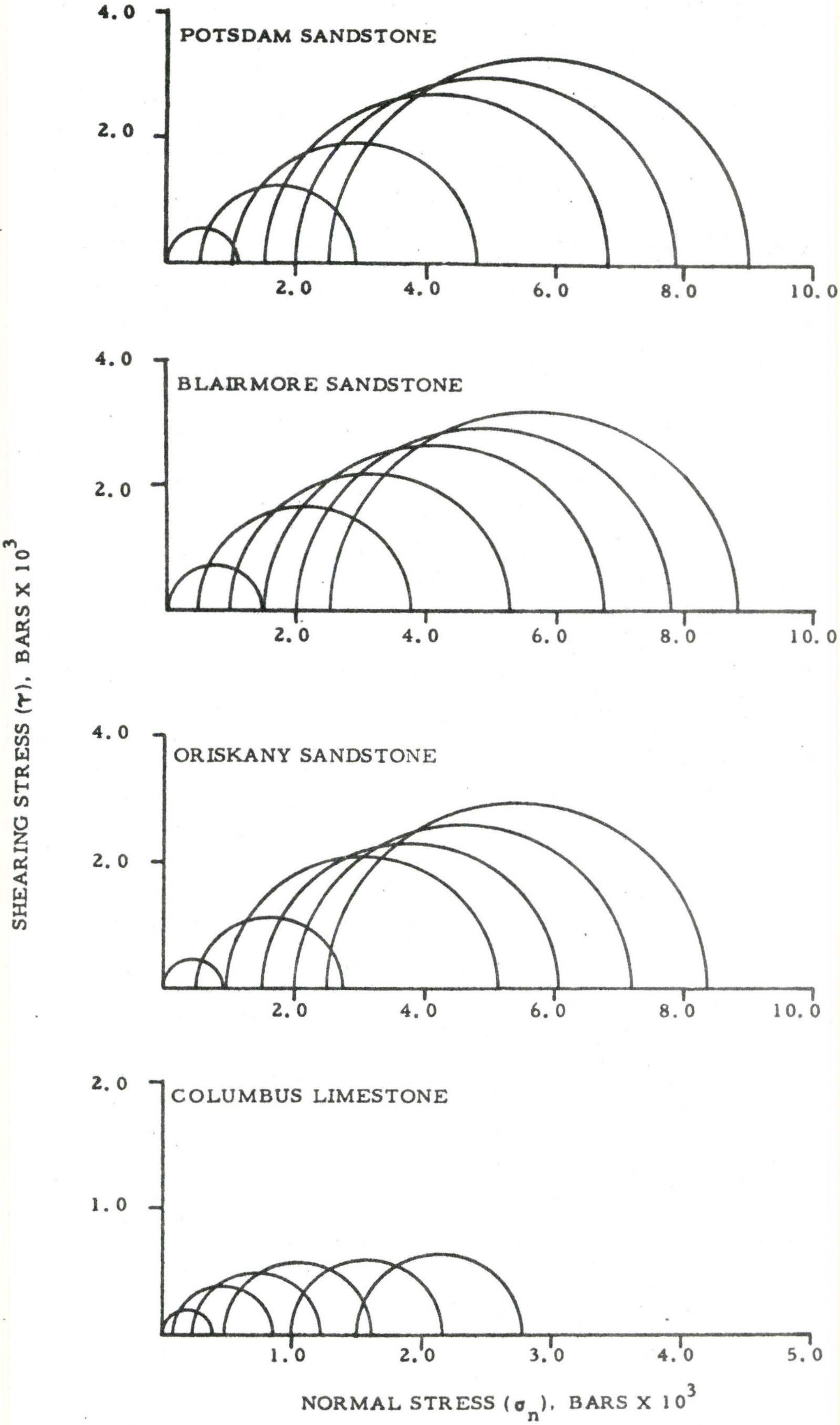

Figure 11. Mohr diagrams for the various test materials.

values of 1, 500, 1000, 1500, 2000 and 2500 bars are compared to the average experimentally observed fracture angles in Table IV. The experimental and the predicted fracture angles increase systematically as the principal stresses at failure increase (Table IV). The predicted orientation of the fracture angle differs from those observed (Table IV). The experimentally determined fracture angles can be influenced by the ratio of the specimen length to diameter of the test specimens, suggesting that the observed fracture angles may be a result of test procedures (Jaeger and Cook, 1969). Smaller fracture angles are related to larger length to diameter ratios. Although the Coulomb-Mohr criterion is not an adequate failure criterion here, it is widely and successfully applied in engineering problems and will remain useful in depicting experimental results until an adequate mechanistic theory of fracture is developed.

The Griffith criterion is the only mechanistic criterion available at this time. In order to establish whether the original or the modified Griffith theories adequately predict brittle rock failure, the test results are reduced to a dimensionless form by dividing each rock strength value by its uniaxial compressive strength (Hoek and Bieniawski, 1965). These dimensionless strength values are plotted in Figure 12 along with the various Griffith fracture loci from

TABLE IV. COMPARISON OF OBSERVED (θ_o) FRACTURE ANGLES AND THOSE PREDICTED (θ_p) BY THE COULOMB-MOHR CRITERION

	1 Bar		500 Bars		1000 Bars		1500 Bars		2000 Bars		2500 Bars	
	θ_p	θ_o	θ_p	θ_o	θ_p	θ_o	θ_p	θ_o	θ_p	θ_o	θ_p	θ_o
Potsdam	-	1	31	26	35	32	36	32	37	34	39	35
Blairmore	-	3	29	26	31	29	37	30	38	33	40	34
Oriskany	-	0	31	28	35	30	36	35	37	37	39	≈ 40
Columbus	-	8	34	38	41	≈ 40	43	≈ 40	-	≈ 40	-	-

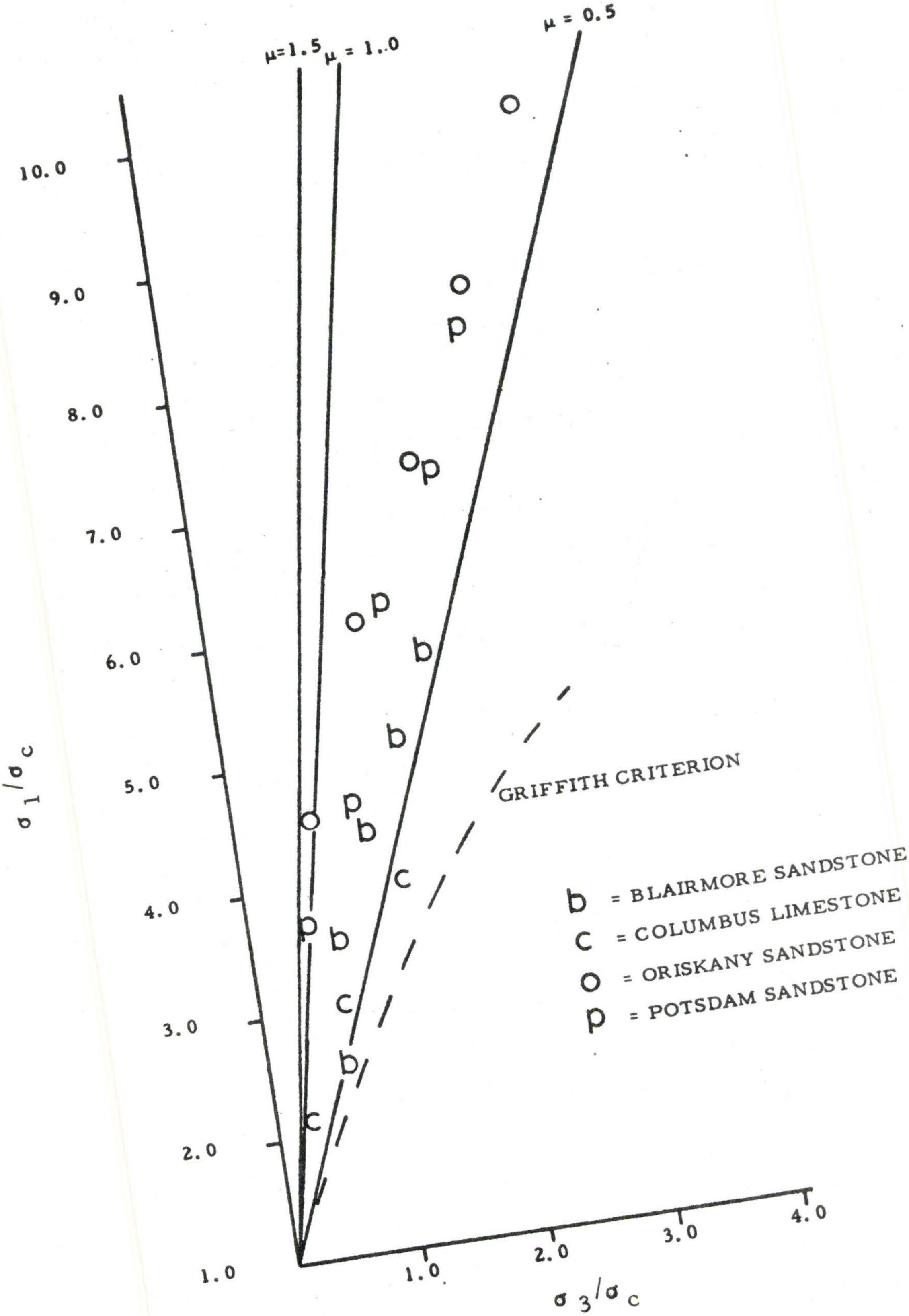

...re 12. Triaxial fracture data for the various test materials.

equations 2.6 and 2.7. A comparison of the experimental results with the various predicted loci of the Griffith criterion suggest that the modified Griffith criterion with coeffcients of internal friction of 0.5 to 1.0 predicts fracture of most of the test materials. Hoek and Bieniawski (1965) point out that although the Griffith "... theory of brittle fracture offers a reliable prediction of fracture initiation stress, ... the resulting fracture propagation from a single crack cannot account for the macroscopic fracture of a specimen.".

The octahedral shear stress criterion has been used as an approximate empirical criterion for a number of rocks (Robertson, 1955; Handin et al.,1967). Plots of the octahedral shear stress versus the mean pressure for failure of the Potsdam, Blairmore and Oriskany sandstones are shown in Figures 13, 14 and 15. The values of the octahedral shear stress for these rocks are essentially similar and are approximately linear with increasing principal stresses at failure. The values of the octahedral shear stress versus the mean pressure for the Oriskany sandstone can be divided into two populations. The first population is representative of samples which have failed in a brittle manner (1 to 1000 bars confining pressure), whereas the second population is representative of samples which have failed by ductile faulting (1100 to 2500 bars confining pressure).

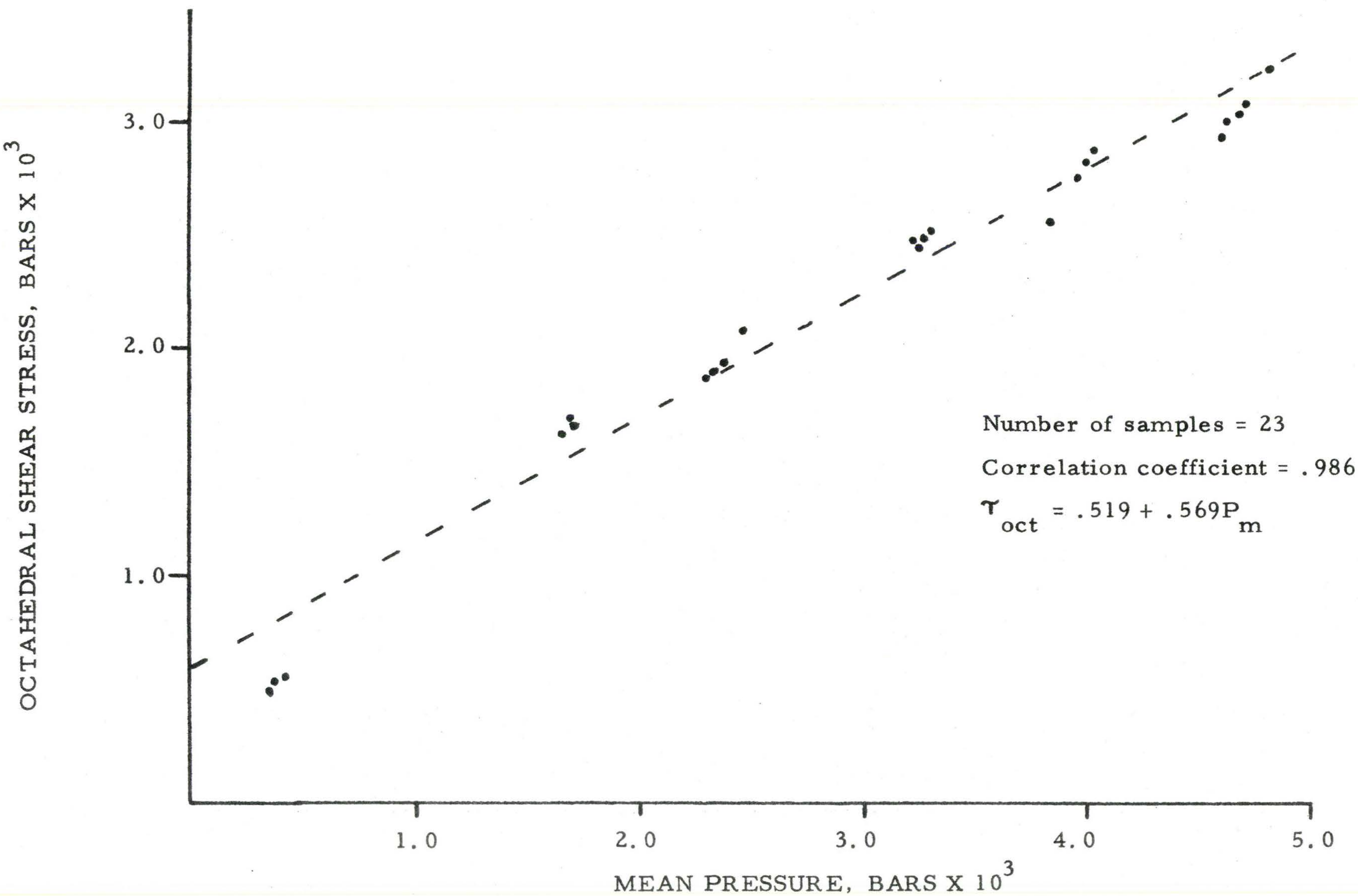

Figure 13. Octahedral shear stress versus mean pressure for failure of Potsdam sandstone.

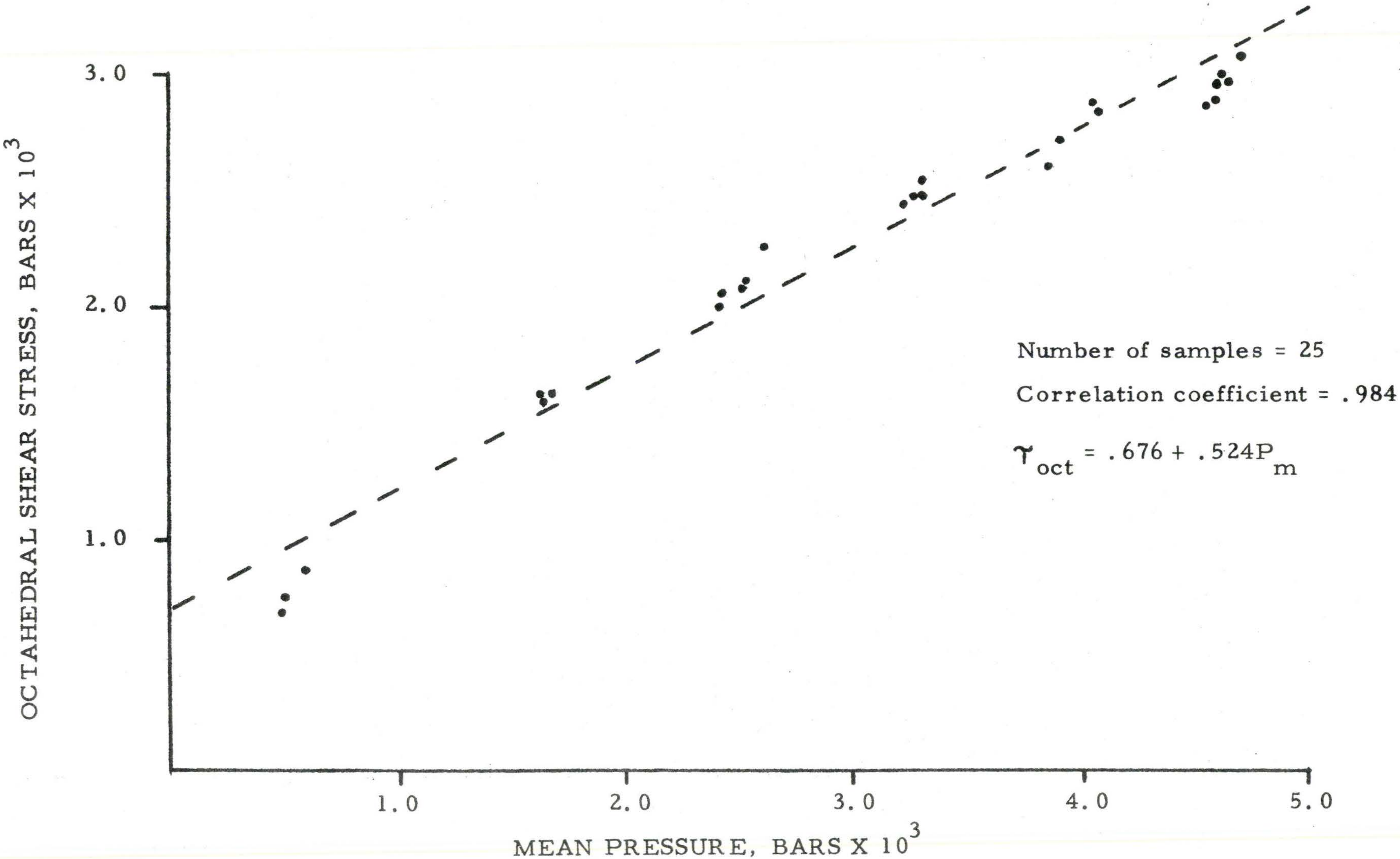

Figure 14. Octahedral shear stress versus mean pressure for failure of Blairmore sandstone.

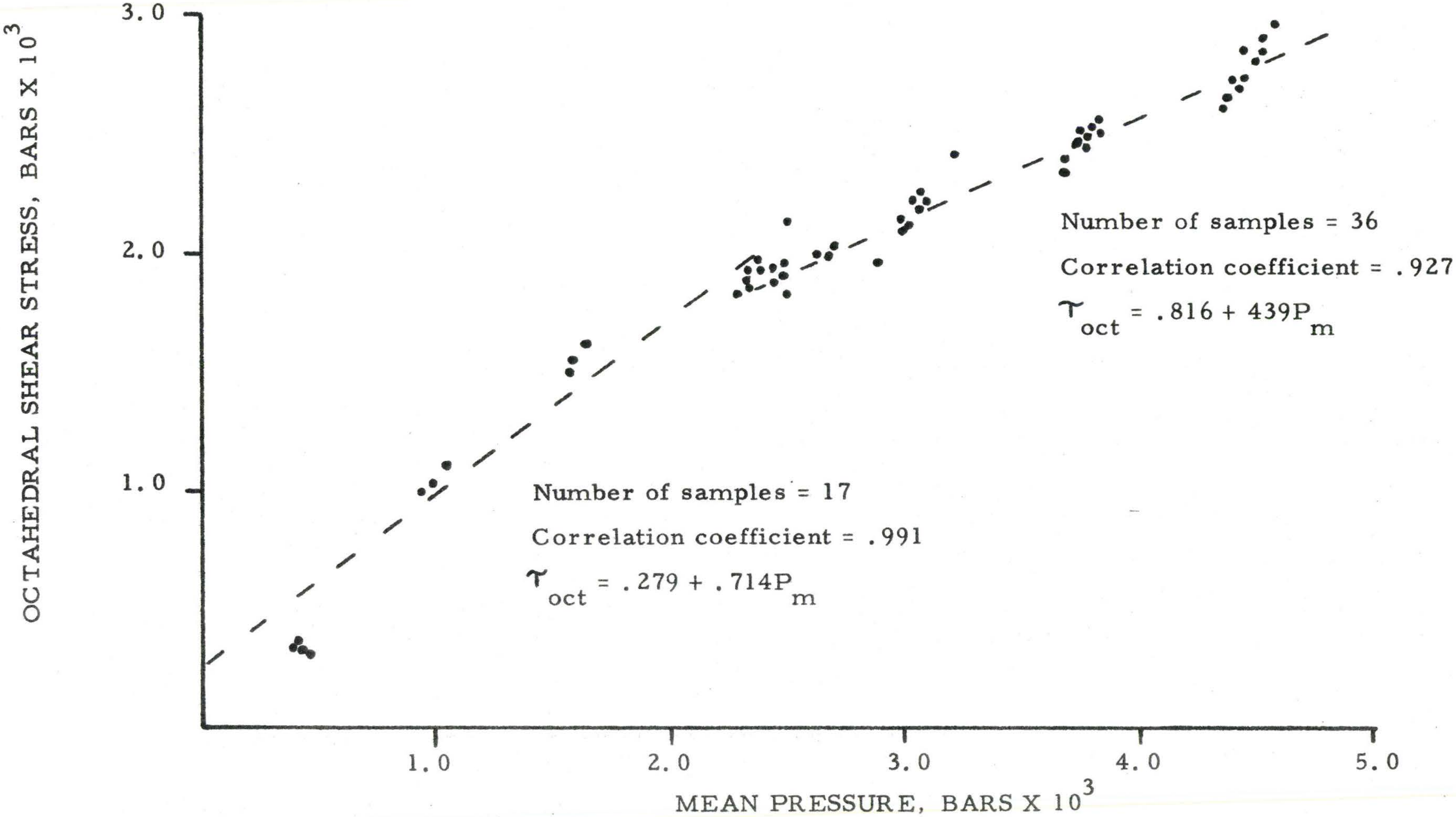

Figure 15. Octahedral shear stress versus mean pressure for failure of Oriskany sandstone.

The octahedral shear stress criterion may be used to predict yielding in the arenaceous Columbus limestone, but the onset of plastic flow from the stress-strain record is difficult to ascertain. In this investigation, the ultimate strength at 1, 100, 250, 500 bars confining pressure, and the differential stress at 1% total for 1000 and 1500 bars confining pressure are arbitrarily chosen as the yield stresses. No values are used for the tests run at 2000 and 2500 bars confining pressure because permanent deformation apparently occurs close to the onset of axial loading. The plot of the octahedral shear stress for the Columbus limestone tends to flatten with increasing mean pressure (Figure 16). This behaviour is a reflection of the transition between brittle and homogeneous deformational behaviour.

(d) Elastic Properties. The elastic limit is the point on the stress-strain curve at which the deformation ceases to be linear and totally recoverable (Region II). The elastic limit is difficult to detect and its choice is strongly dependent on instrument sensitivity; moreover, for porous sedimentary rocks the application of a confining pressure may produce irrecoverable strain due to pore collapse (Handin and Hager, 1957). Values of elastic moduli are strongly influenced by the conditions under which they are obtained, namely, stress-strain region, a loading or unloading cycle, and strain rate (Brace, 1964; Brady, 1968).

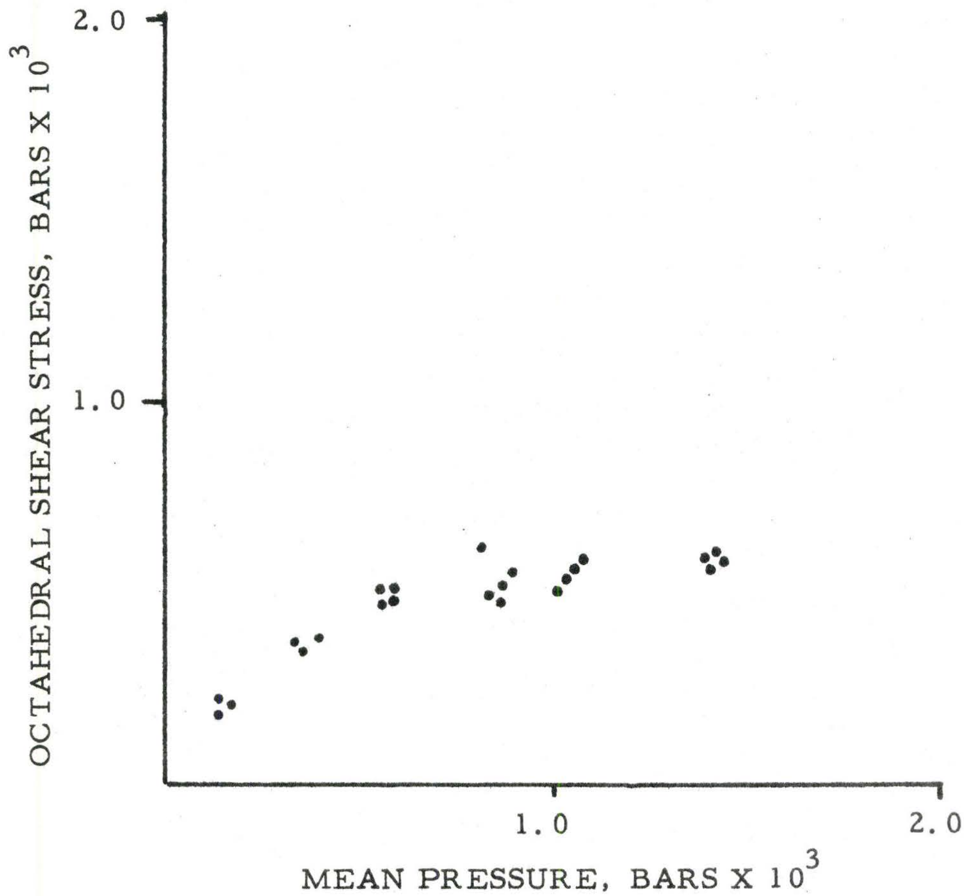

Figure 16. Octahedral shear stress versus mean pressure for failure of the Columbus limestone.

The Potsdam, Blairmore and Oriskany sandstones behave essentially elastically up to the onset of faulting (60% of the total strain is recoverable). The static Young's modulus is calculated on a loading cycle over the same interval of strain (0 to 1%) in order to facilitate comparison between tests. This interval of strain customarily lies within Region II of the stress-strain curve except in atmospheric tests where Region I is also present. Strain rates in this interval of strain are in the order of 10^{-5}.

Figures 17, 18, 19 and 20 illustrate the effect of confining pressure on the static Young's modulus. The open circles 0, represent calculated means, the horizontal bars $\overline{\underline{\;}}$, represent the limits of observed variation. Values of the Young's modulus for the Potsdam, Blairmore and Oriskany sandstones have a large initial increase be- between 1-500 bars confining pressure and then increase gradually or are approximately constant at confining pressures greater than 1000 bars. Literature values of the Young's Moduli for sandstones range from 0.088×10^6 bars to $.975 \times 10^6$ bars. The large initial increase in Young's modulus is generally attributed to a general compaction of the specimen (Brace, 1964).

The effect of confining pressure on the Young's modulus of the Columbus limestone (Figure 20) differs markedly from the behaviour observed in the sandstones. Although there is a general increase in the Young's modulus at low and moderate confining pres-

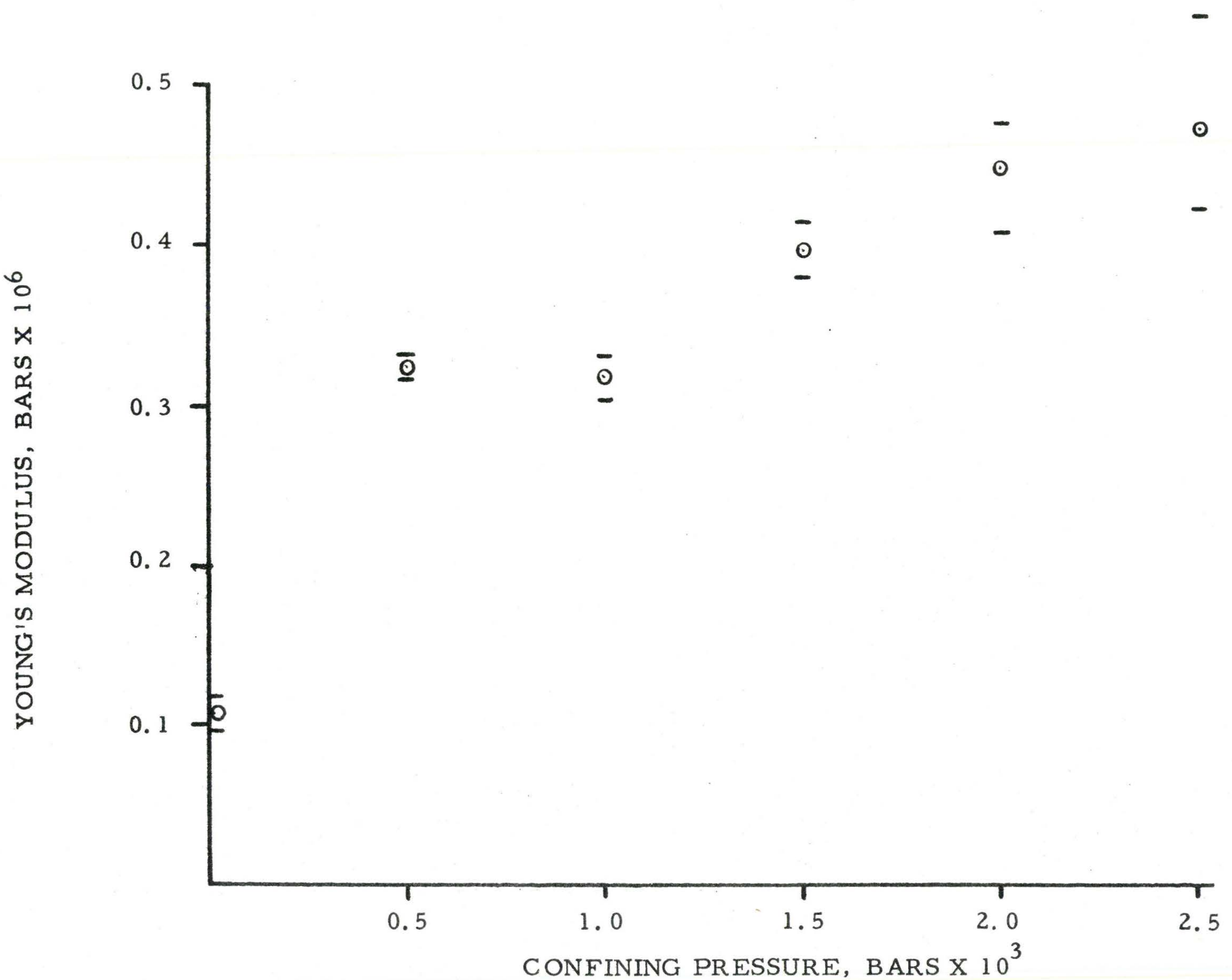

Figure 17. Young's modulus as a function of confining pressure for the Potsdam sandstone.

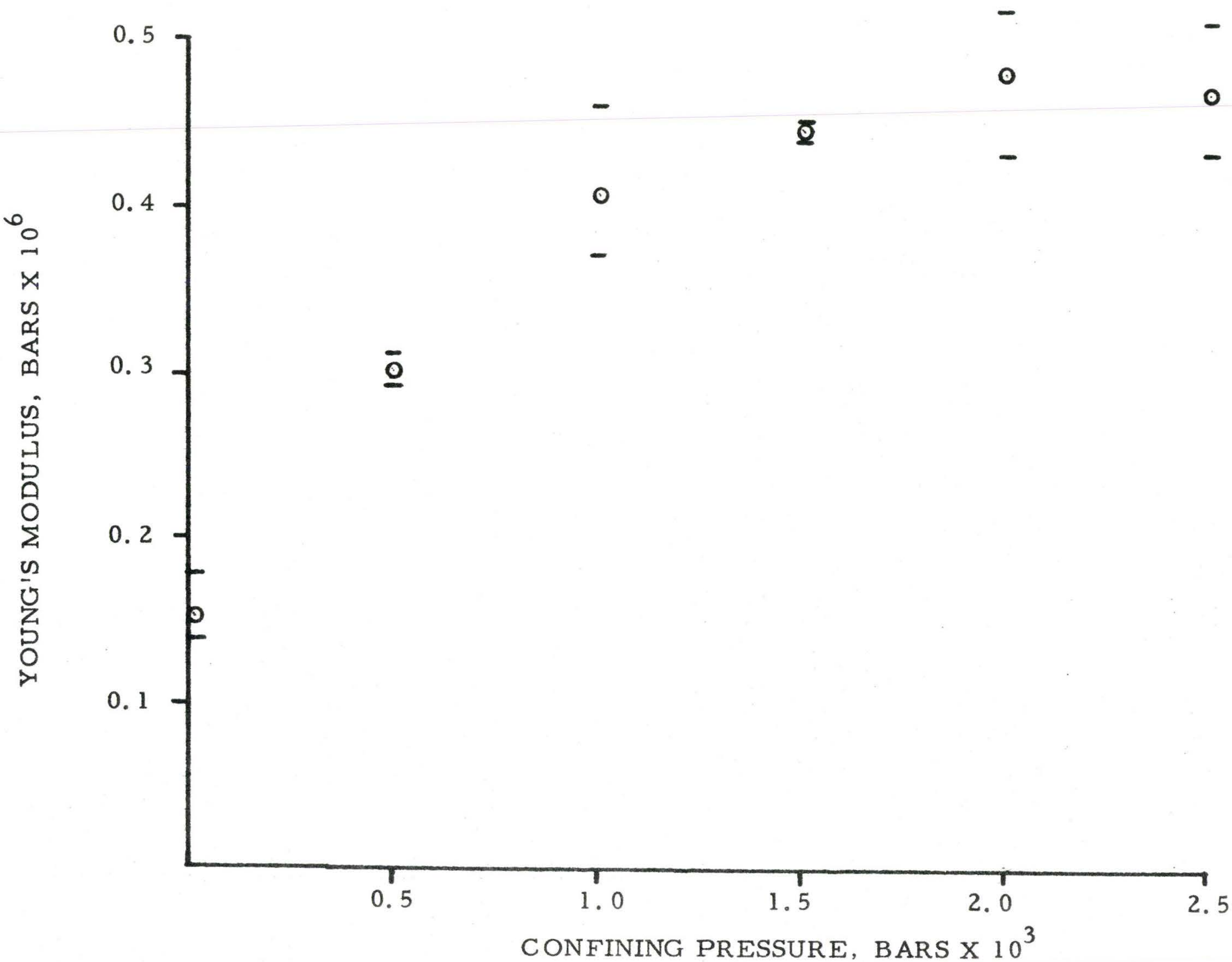

Figure 18. Young's modulus as a function of confining pressure for the Blairmore sandstone.

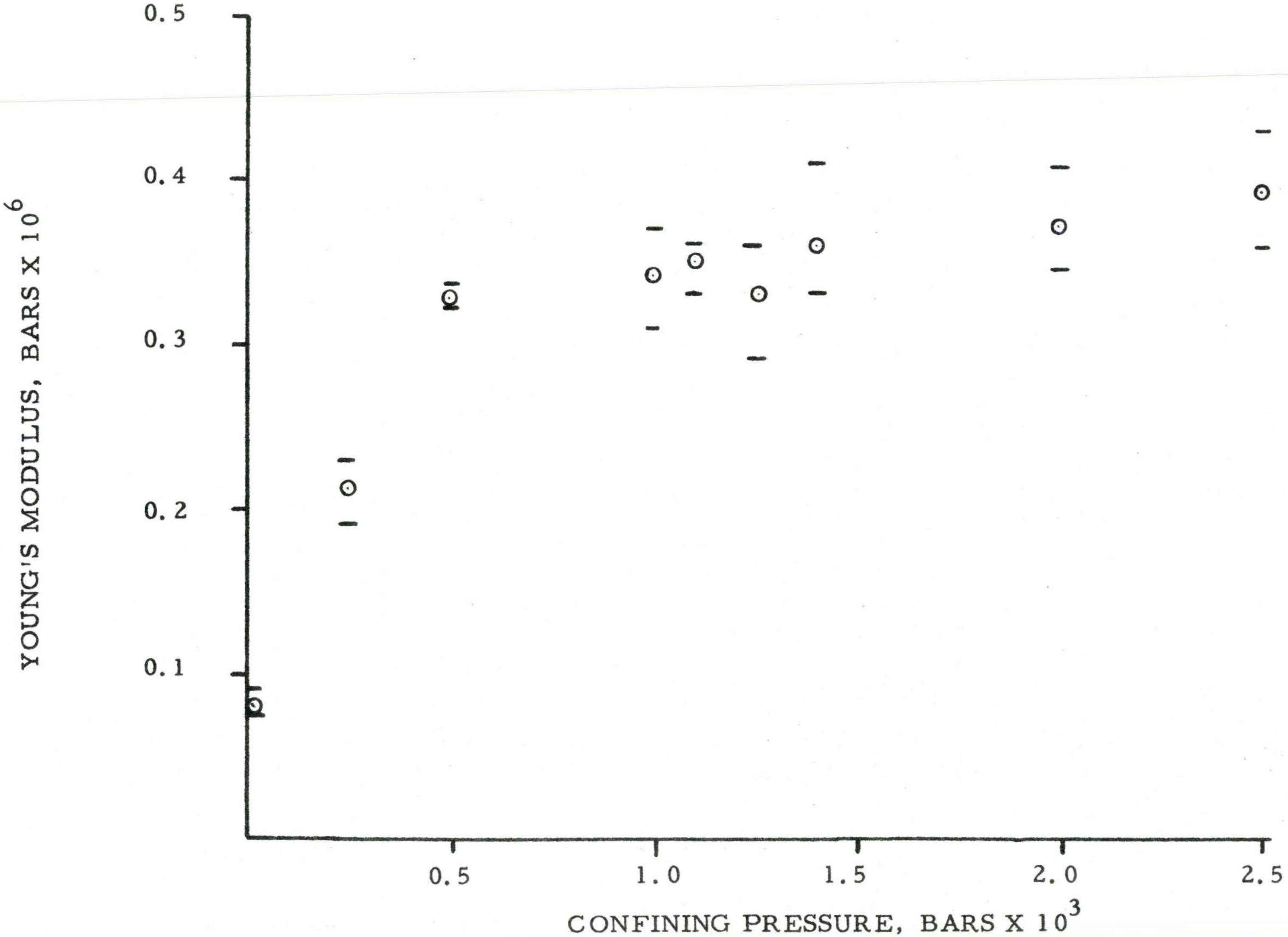

Figure 19. Young's modulus as a function of confining pressure for the Oriskany sandstone.

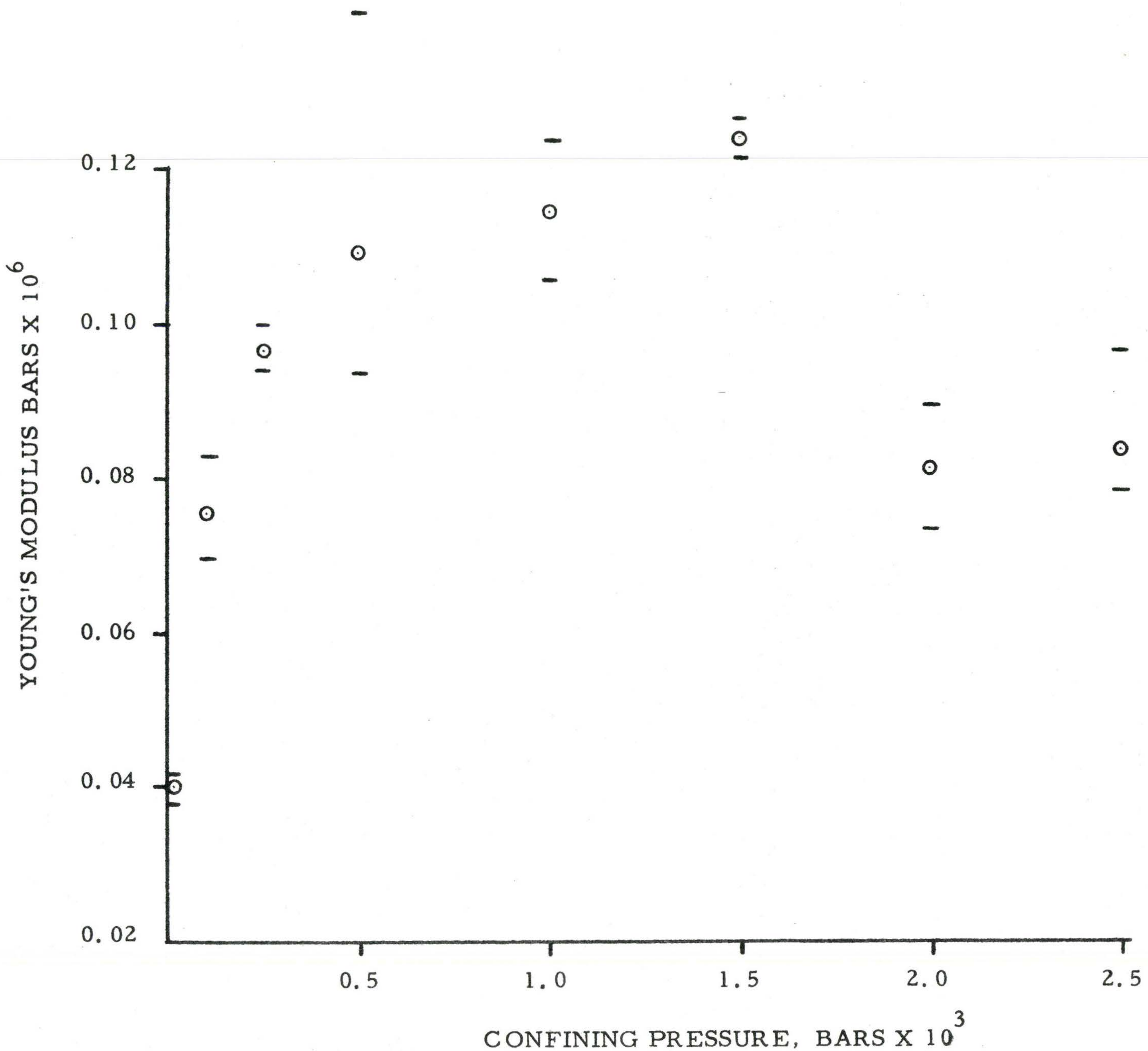

Figure 20. Young's Modulus as a function of confining pressure for the Columbus sandstone

sures, at 2000 and 2500 bars confining pressure there is a sharp and substantial decrease. The stress-strain curves for the Columbus limestone (Figure 9) also indicate that the truly elastic region has diminished substantially and is in fact negligible at confining pressures of 2000 and 2500 bars. Values of Young's modulus determined at these confining pressures are virtually meaningless because permanent deformation occurs close to the onset of axial loading.

3. Effect of Total Strain

(a) Deformational Modes. It is obvious that the mode of deformation is strongly dependent on the amount of strain to which a rock is subjected. At very low strains most rocks are essentially elastic whereas at higher strains they can undergo uniform flow, brittle fracture or ductile faulting.

Plate 8 illustrates different specimens of Potsdam sandstone deformed to various amounts of strain at a confining pressure of 2500 bars. At low strains ($\approx 2\%$) the mode of deformation is brittle shear faulting along a single narrow fault. At higher strains a second fault is formed in a conjugate orientation. The formation of the second fault can be correlated to a sharp drop in the differential stress on the stress-strain curve (Plate 9). The magnitude of the drop in the differential stress is less than that associated with the first fault. As was pointed out earlier the generation of the second fault may be entirely related to apparatus constraints. The effects of total strain and confining pressure

Plate 8

Specimens of Potsdam sandstone deformed at 2500 bars confining pressure to various percent strains (X 3)

A. 2.39 percent strain

B. 4.17 percent strain

C. 7.00 percent strain

D. 8.71 percent strain

A

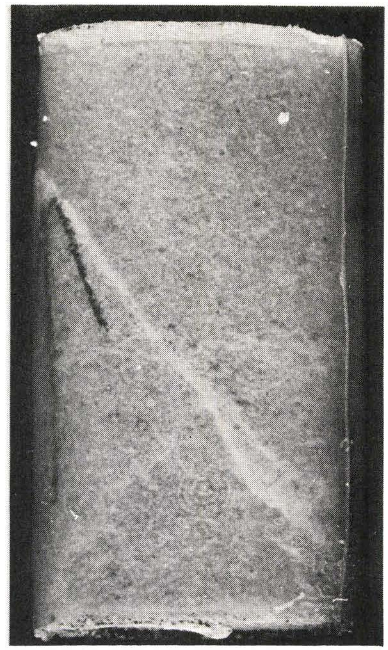

B

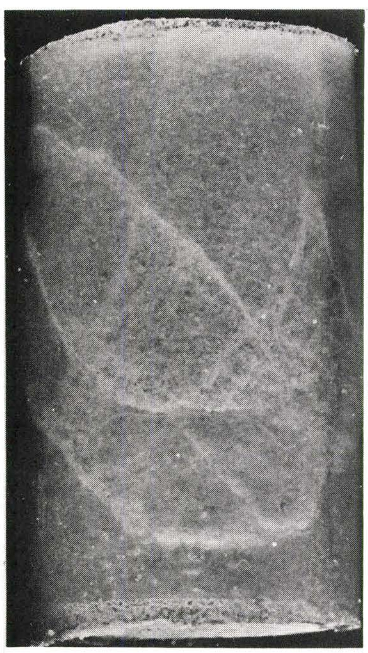

C

D

Plate 9

Stress-strain record for the Potsdam sandstone deformed at 2000 bars confining pressure to various percent strains with associated deformational modes.

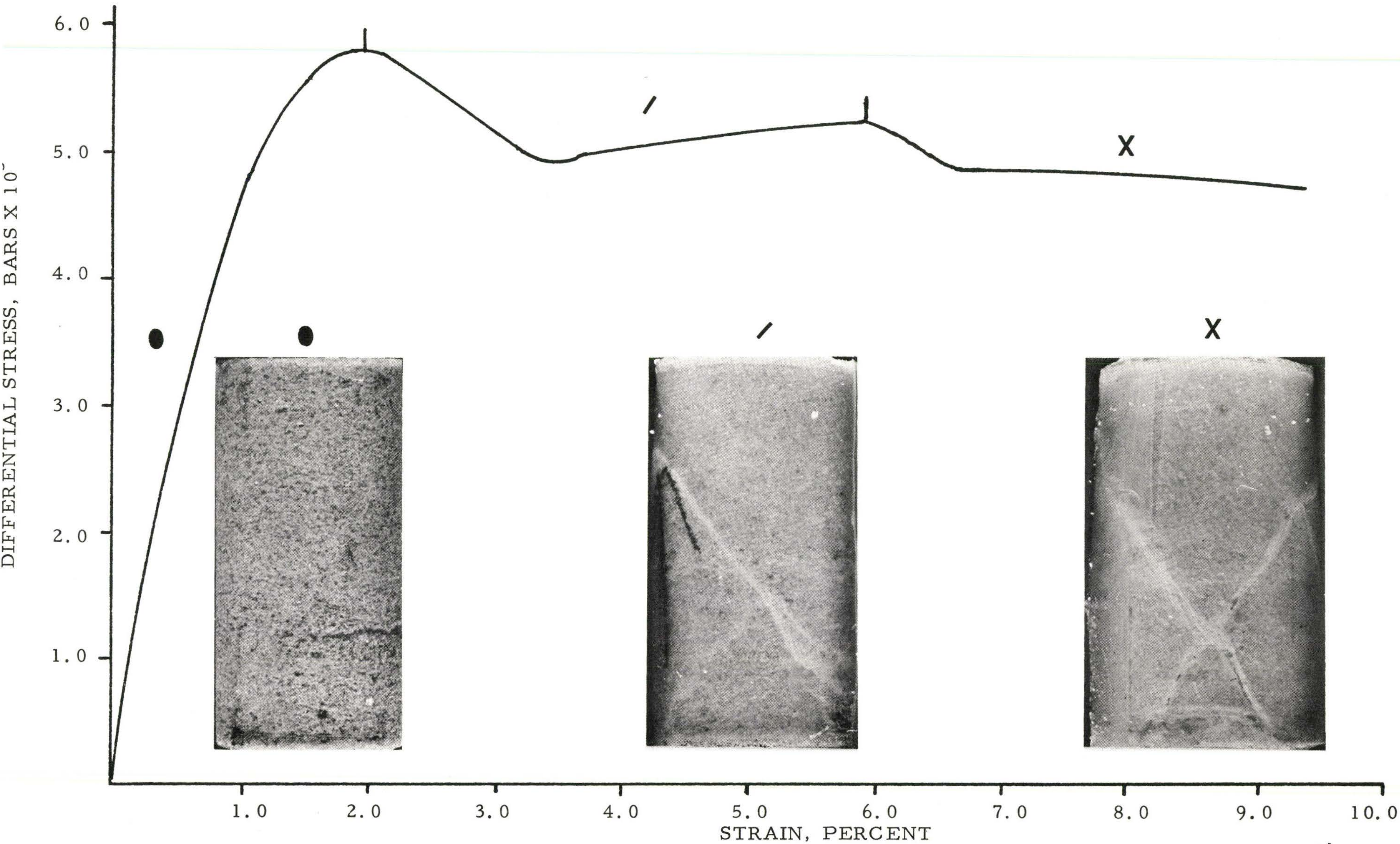
DIFFERENTIAL STRESS, BARS X 10
6.0
5.0
4.0
3.0
2.0
1.0
1.0
2.0
3.0
4.0
5.0
6.0
7.0
8.0
9.0
10.0
STRAIN, PERCENT
X
X

can best be illustrated by a diagram of total strain versus confining pressure (Figure 21). In this type of diagram and others of a similar nature, a specimen's deformational mode is characterized by a number of standard symbols, namely, extensional faults (+), single brittle shear faults (/), conjugate shear faults (X), ductile faults (Δ), permanent homogeneous deformation (0), and elastic deformation (●). Boundaries between the various fields are based on the deformational mode of individual specimens and to some extent the stress-strain curve (e.g., Plate 9).

The deformational modes of the Blairmore sandstone as a function of total strain are similar to those of the Potsdam sandstone (Figure 22). Unlike the Potsdam sandstone the Blairmore is characterized by more distinct faults with little or no apparent cataclasis visible in the test specimens (Plate 10).

At confining pressures less than 1100 bars the effect of total strain on the deformational behaviour of the Oriskany sandstone is similar to that observed in the Potsdam and Blairmore sandstones (Figure 23). At confining pressures greater than 1000 bars no abrupt drop in the differential stress accompanies faulting (Figure 7). At 1500 bars confining pressure and total strains less than 2% the mode of deformation is elastic; at 3% total strain ductile faulting occurs; at 5%

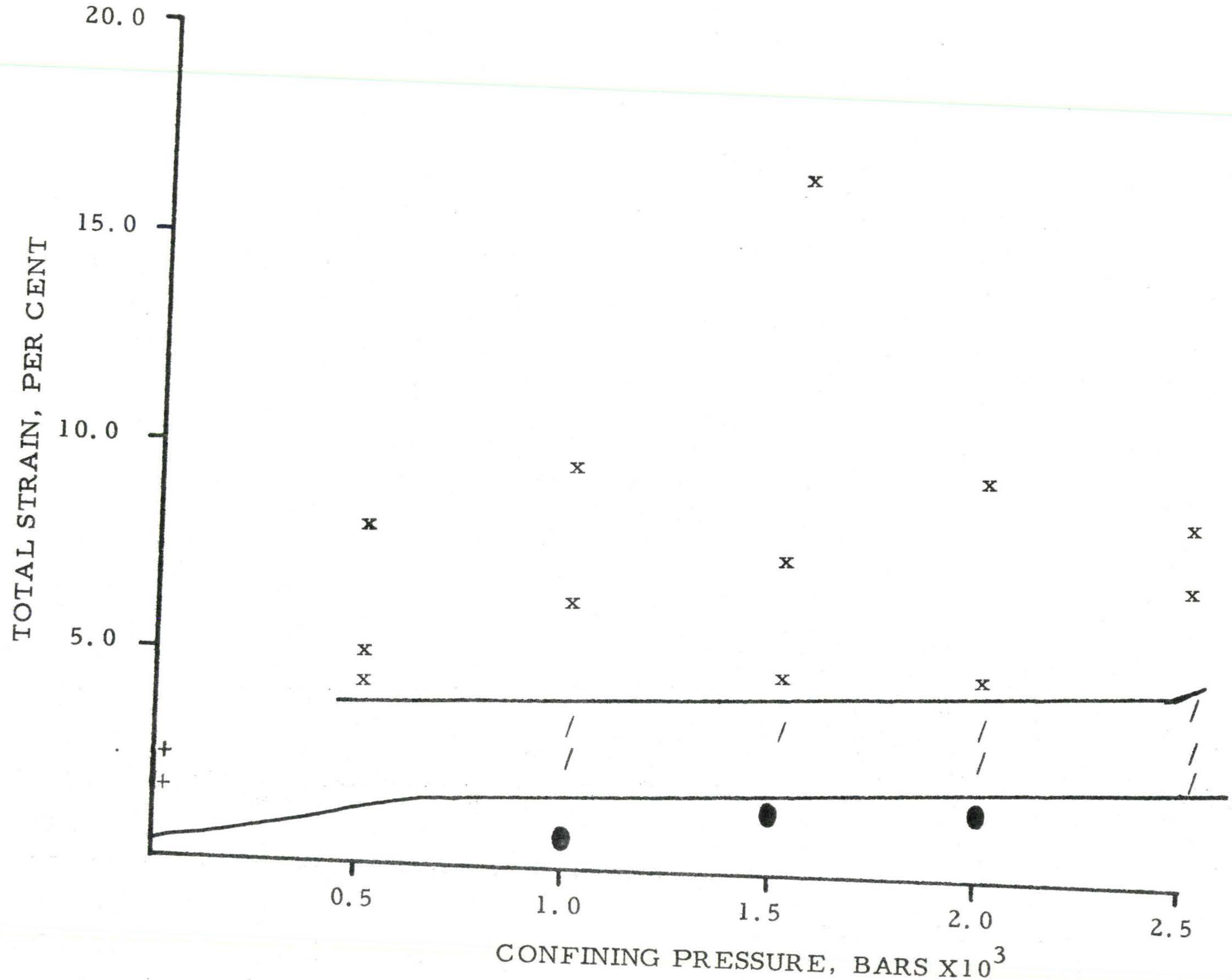

Figure 21. Deformational mode fields for the Potsdam sandstone

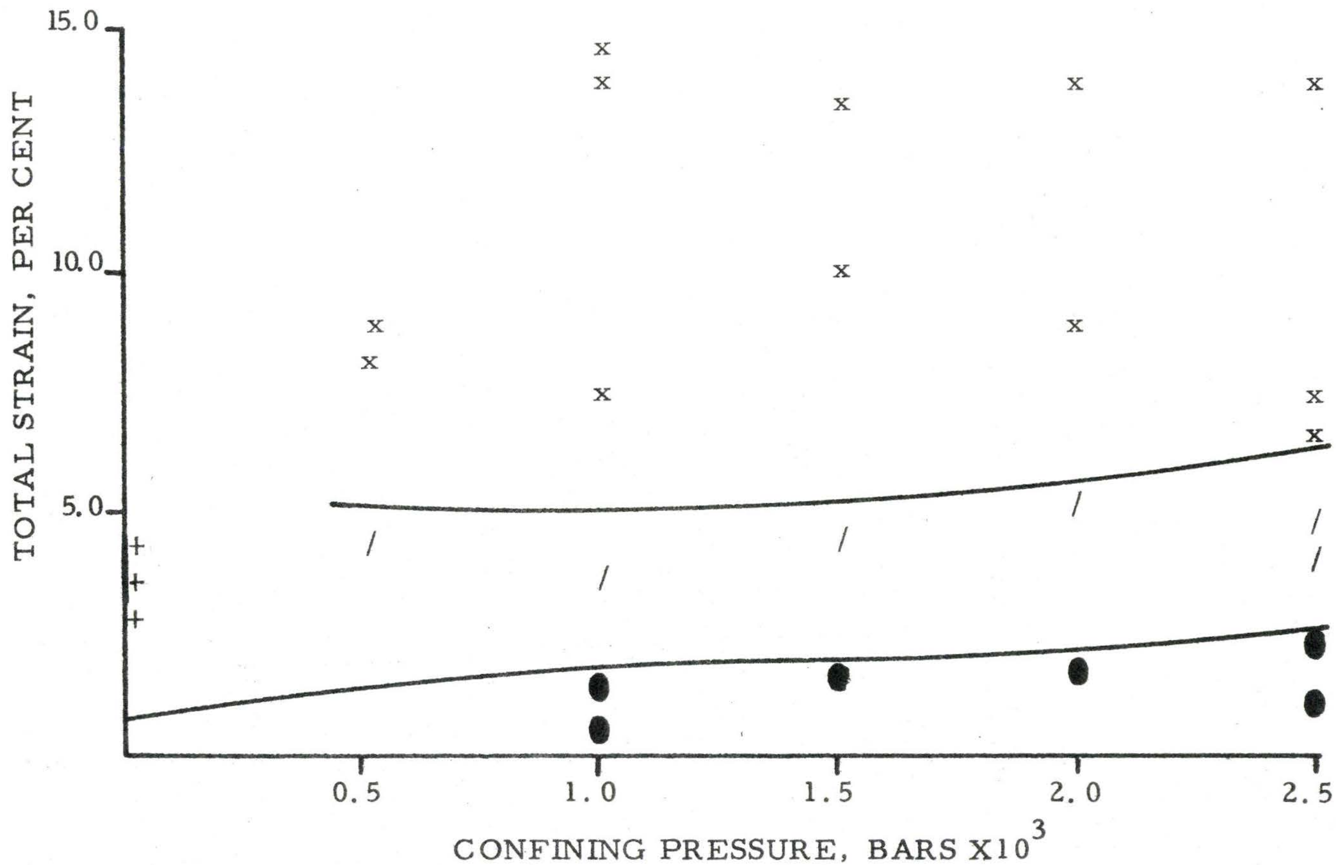

Figure 22. Deformational mode fields for the Blairmore Sandstone

Plate 10

Specimens of Blairmore sandstone deformed at 2500 bars confining pressure to various percent strains (X 3)

A. 1.03 percent strain

B. 2.48 percent strain

C. 4.81 percent strain

D. 13.89 percent strain

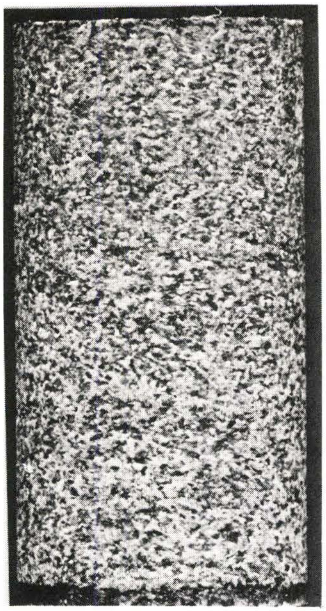

A

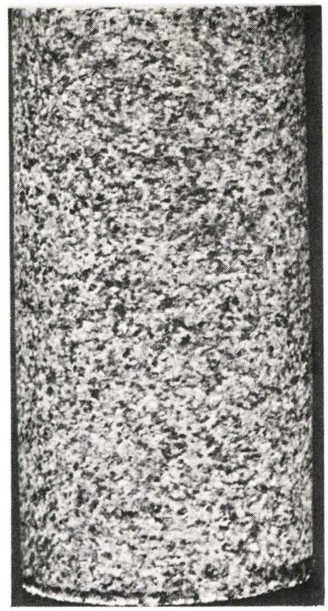

B

C

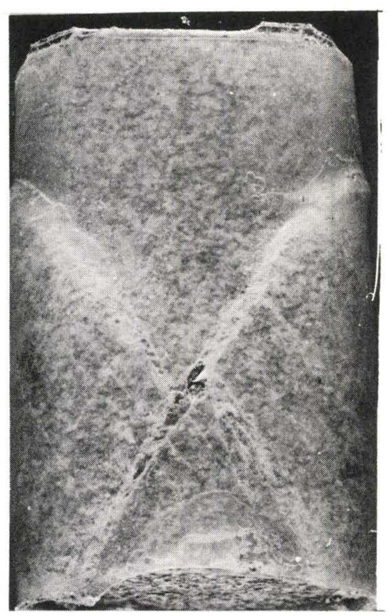

D

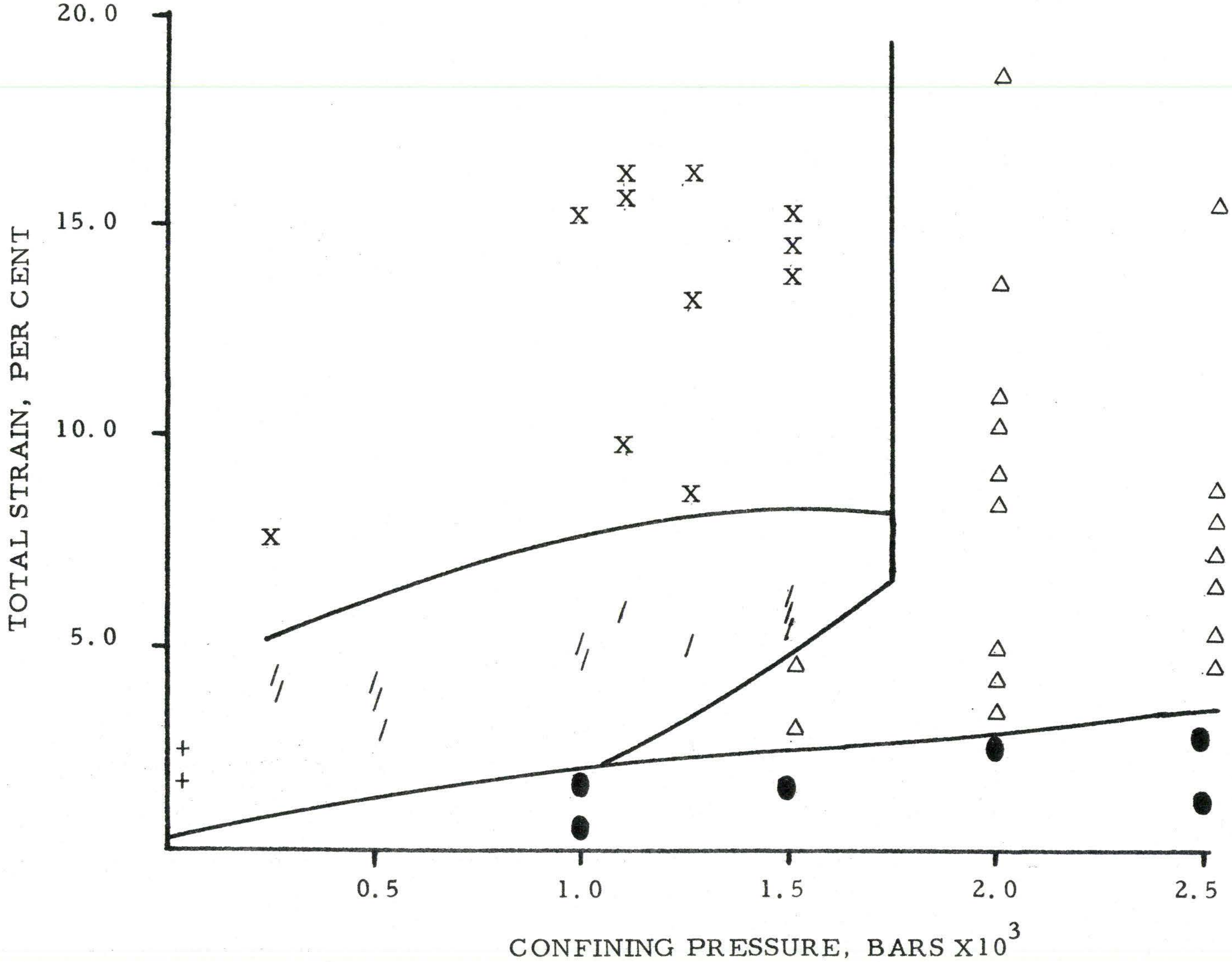

Figure 23. Deformational mode fields for the Oriskany sandstone

total strain a single shear fault occurs, and at total strains greater than 7% conjugate shear faults characterize the specimen (Plate 11). At 2000 and 2500 bars confining pressure numerous, barely discernible slip surfaces (Luders Lines) uniformly distributed throughout the specimens appear at total strains of approximately 3%. With increasing strain the specimens barrel and more prominent fault surfaces develop.

At low confining pressures and low strains the Columbus limestone is characterized by brittle deformation. Ductile faulting is the characteristic mode of deformation at total strains greater than 1% at 250 and 500 bars confining pressure. At 1000 bars confining pressure the Columbus limestone deforms elastically up to total strains of approximately 1%; undergoes permanent homogeneous deformation between 1-2% total strain; ductile faulting occurs at total strains greater than 2% (Figure 24). At high confining pressures no field of elastic deformation can be detected and the specimens deform homogeneously up to relatively high total strains before the onset of ductile faulting (Figure 24 and Plate 12).

During impregnation of the deformed cores prior to thin sectioning some specimens of the arenaceous Columbus limestone broke into a series of approximately equal thickness disks along planes perpendicular to the compressional axis (Plate 13). This disk-type of

Plate 11

Specimens of Oriskany sandstone deformed at 1500 bars confining pressure to various percent strains (X 3)

A. 1.73 percent strain

B. 2.65 percent strain

C. 4.43 percent strain

D. 6.15 percent strain

E. 14.50 percent strain

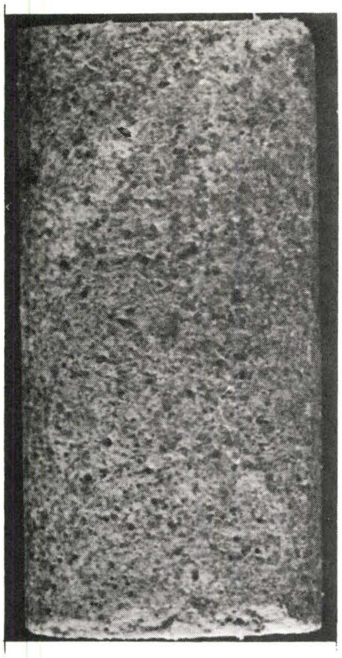

A

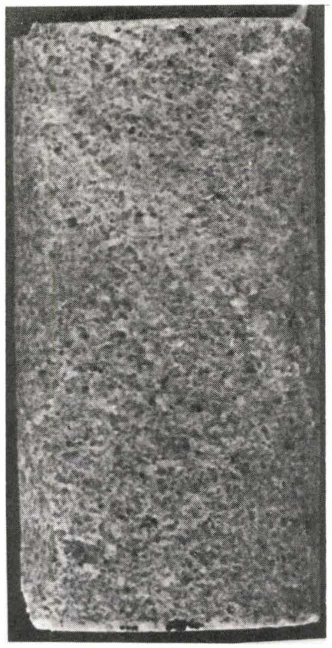

B

C

D

E

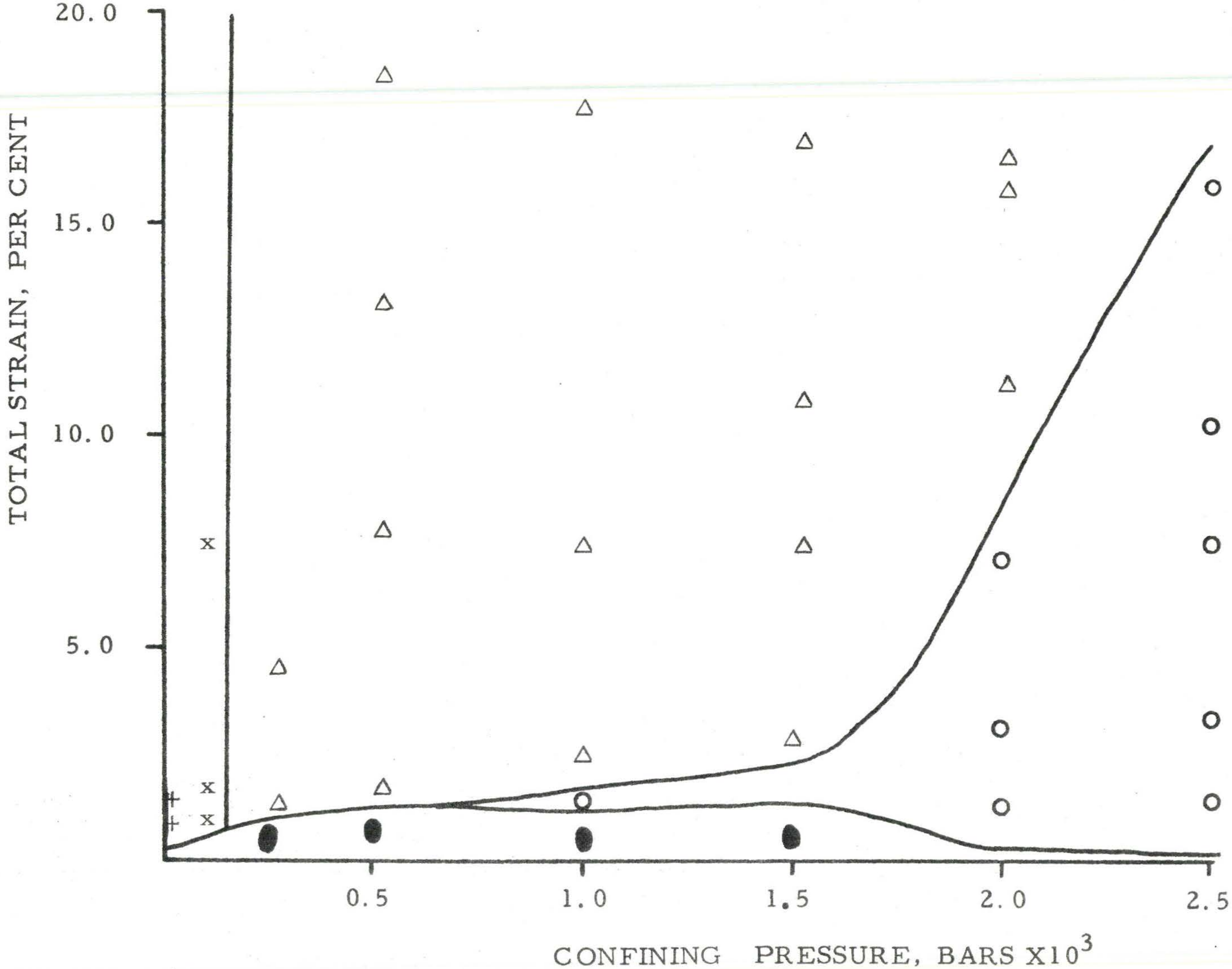

Figure 24. Deformational mode fields for the arenaceous Columbus limestone

Plate 12

Specimens of arenaceous Columbus limestone deformed at 2000 bars confining pressure to various percent strains (X 3)

A. 3.15 percent strain

B. 7.00 percent strain

C. 11.21 percent strain

D. 15.61 percent strain

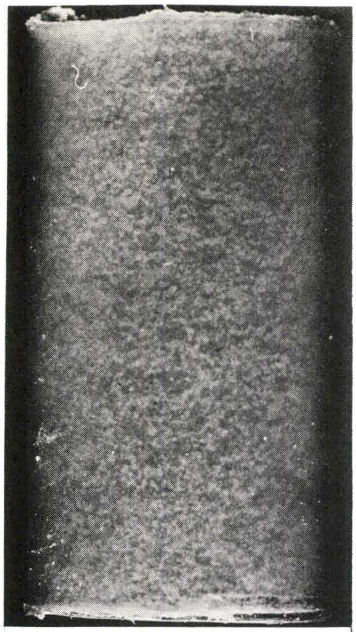

A

B

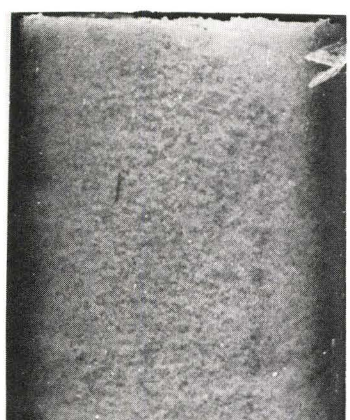

C

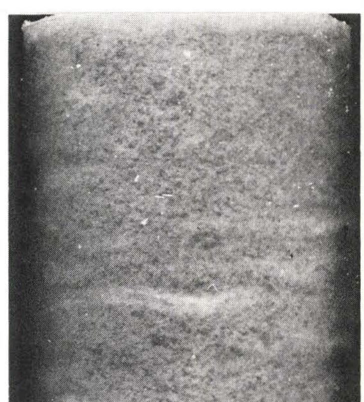

D

Plate 13

Disk-type failure in the arenaceous Columbus limestone deformed at 1500 bars confining pressure to 16.95 percent strain (X 3.2)

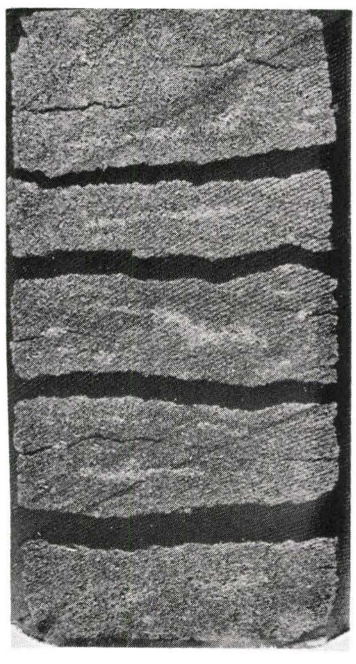

failure characterizes specimens which had been subjected to total strains of greater than 7%. Similar behaviour also occurs in saturated and jacketed specimens of sandy shale and is apparently related to pore pressures in rocks of low permeability (Bredthauer, 1957). In the Columbus limestone a possible explanation of this type of behaviour is that, upon impregnation and setting, the epoxy cement causes failure along incipient but invisible planes of weakness normal to the compressional axis. These incipient planes may be similar to dendritic markings observed in alabaster deformed to strains greater than 15% (Boyd and Currie, 1969). Another possibility is that the disk-type failure is a relaxation phenomenon. Murrell (1966) interprets disk-type fractures "... as a result of inhomogeneous plastic deformation in the rock specimen internal stresses exist in it after the external loads are removed, and these are sufficient to open up microscopic cracks and even cause the specimen to fracture in some cases.".

(b) Ductility. Handin and Hager (1957) define ductility qualitatively as the total percent deformation before fracture. In this investigation, ductility is defined as the total strain a rock undergoes before fracture or faulting. No distinction is made between faulting with or without loss of cohesion. Ideally one would like to base ductility on the basis of permanent strain rather than total strain, but it is difficult to specify the elastic limit on the stress-strain curve. The "ductility" of a rock is a function of the conditions of deformation and rock parameters. There is no universally applicable measure of ductility, but a relative classification based on total strain before faulting has been used as a basis of comparison between materials. A material is said to be very brittle, brittle, moderately brittle (transitional), moderately ductile, and ductile if the total strain before faulting or fracture is less than 1, 1 to 5, 2 to 8, 5 to 10, and greater than 10 percent respectively (Handin, 1966). In this study, the five-fold classification of ductility is not useful in comparing the relative ductilities of the test materials. For example, the onset of ductile faulting in the Columbus limestone at 1500 bars confining pressure occurs at 2% total strain (moderately brittle), but the specimen continues to deform in a ductile manner up to total strains of 17% (Figure 24).

Ductility as a function of confining pressure is plotted in Figures 25, 26, 27 and 28 for each of the four rocks tested by the writer. All the rocks show the customary increase in ductility with increasing confining pressure. The Columbus limestone is clearly the most ductile of the four rocks. Ductilities of the Potsdam and the non-calcareous Blairmore sandstones are essentially similar. The ductility of the calcareous Oriskany sandstone is generally greater than the ductilities of the Potsdam and the Blairmore sandstones, but usually less than the ductility of the Columbus limestone.

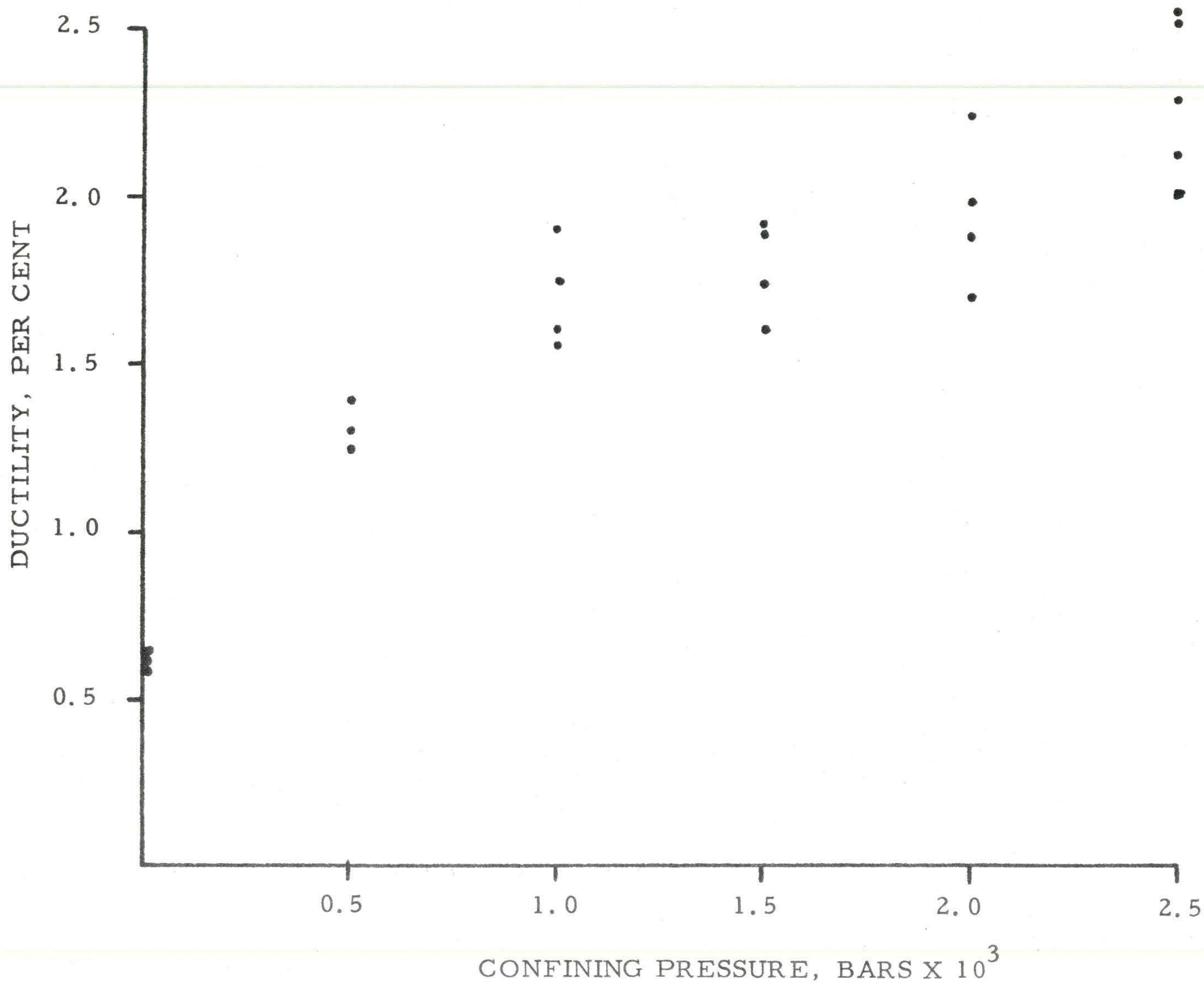

Figure 25. Ductility (percent strain before faulting) of Potsdam sandstone as a function of confining pressure.

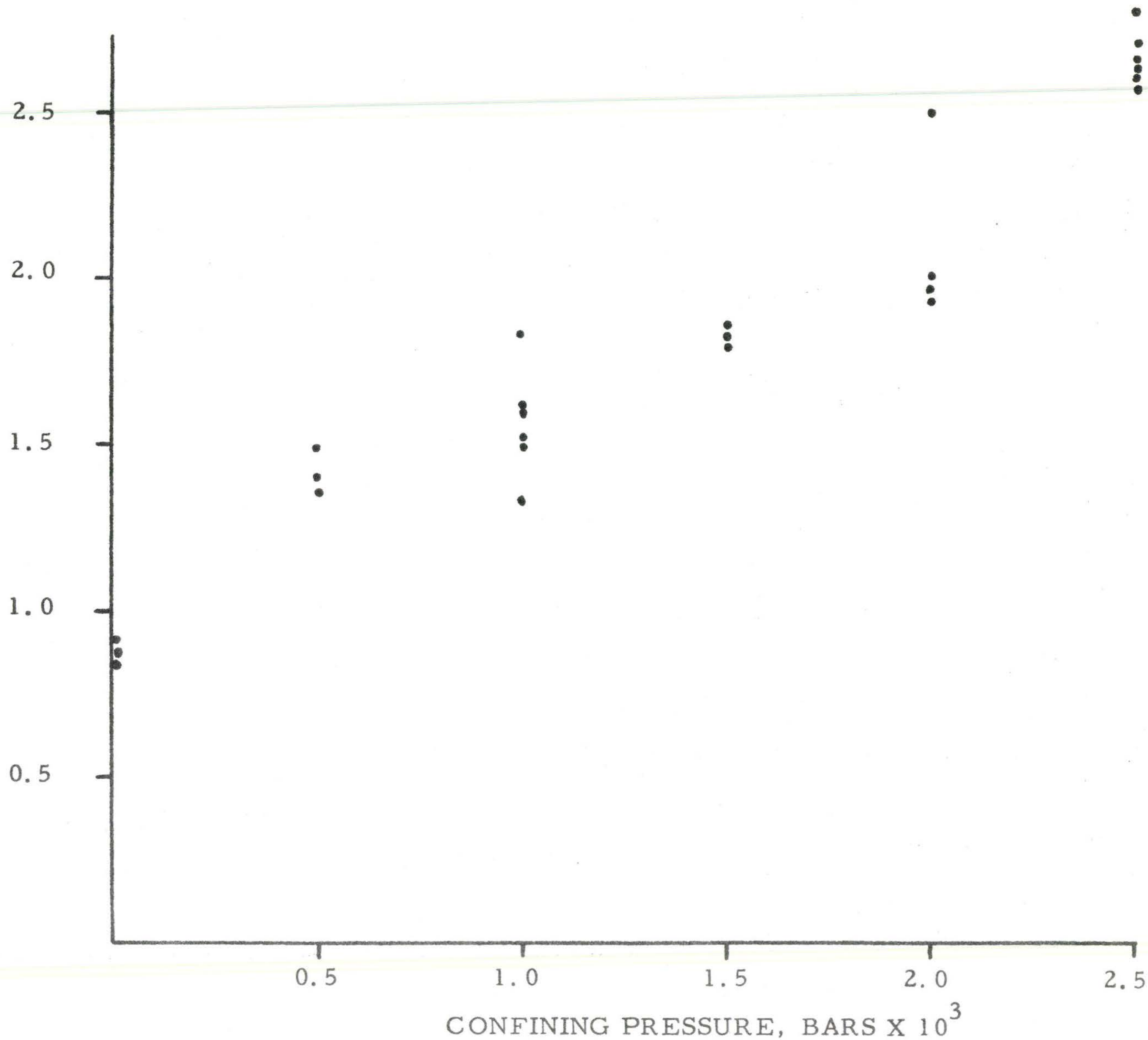

Figure 26. Ductility (percent strain before faulting) of the Blairmore sandstone as a function of confining pressure.

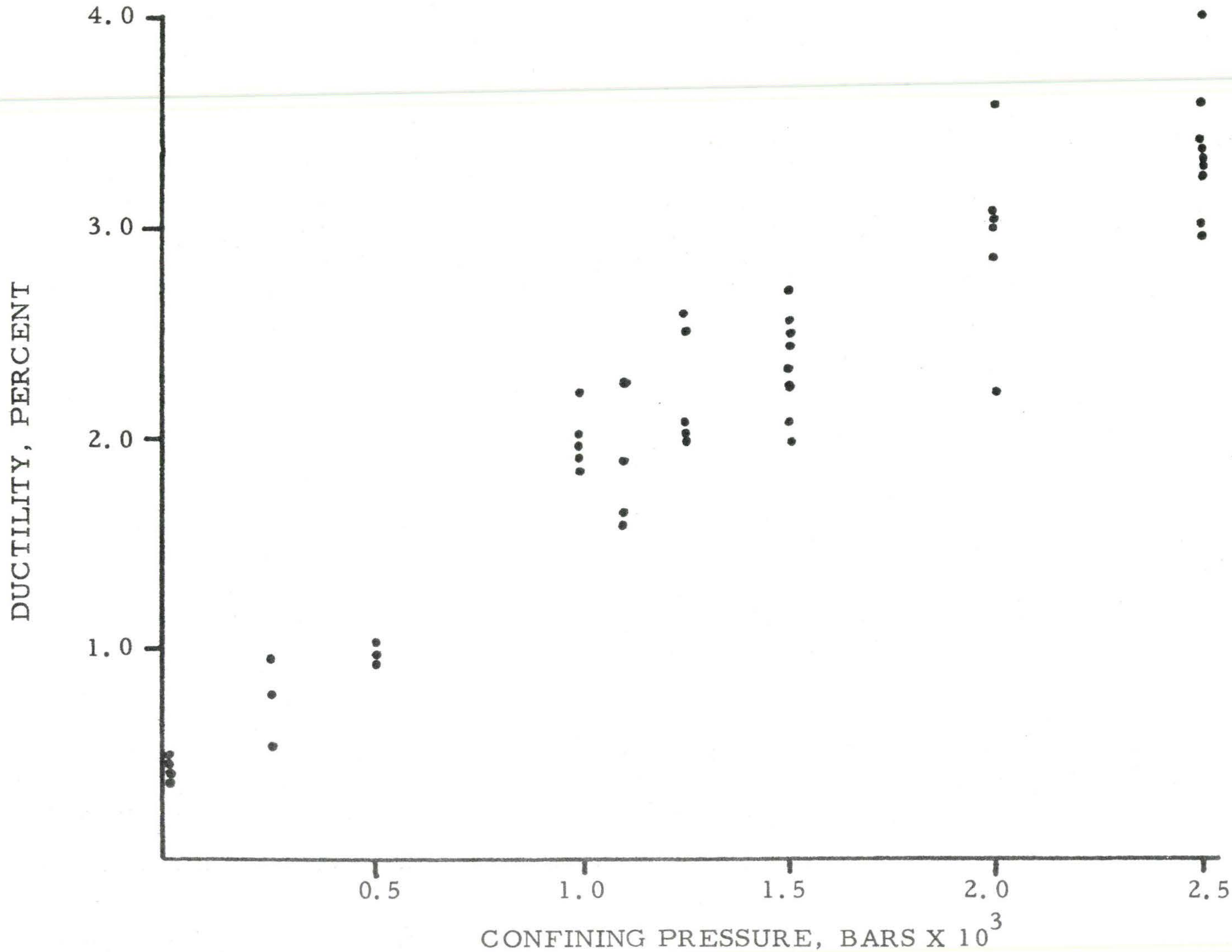

Figure 27. Ductility (percent strain before faulting) of the Oriskany sandstone as a function of confining pressure.

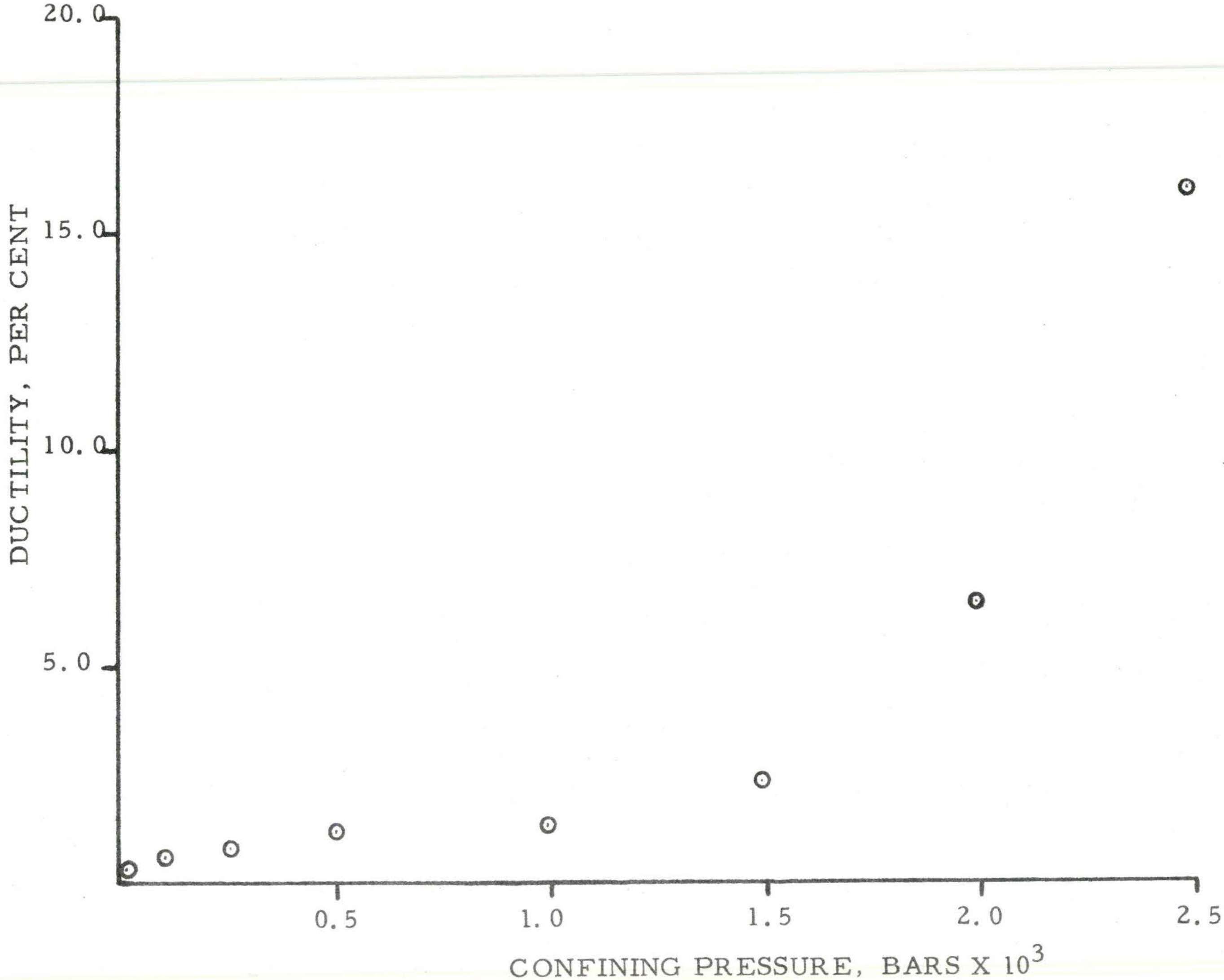

Figure 28. Mean ductility (percent strain before faulting) of the arenaceous Columbus limestone as a function of confining pressure.

4. Effect of Strain Rate

(a) General Statement. The most common types of tests which explore the relationships between differential stress, strain, and time are the creep, constant strain rate, and constant loading rate tests. In a constant strain rate test, the differential stress applied to the sample varies with the strain such that the rate of strain remains constant. In a creep test, the rate of strain varies with time while a constant stress difference is maintained. A continuous build up of the differential stress with time occurs in a constant loading rate test.

Unlike the constant strain rate test, the rate of strain is variable in a creep test and the constant loading rate test. Constant strain rate and creep tests are thought to be more akin to natural deformational conditions (Heard, 1968).

The apparatus used in this study provides a constant loading rate, therefore a material's behaviour is reflected by changes in the strain rate related to changes in the mode of deformation. The strain rate specified in this study refers only to the rate of strain in the elastic region, and not to a strain rate over the entire test.

(b) Strength and Ductility. Previous experimental work at room temperature on the Yule marble indicates a slight but systematic decrease in strength which is directly related to decreasing strain rate

(Heard, 1963). On the other hand, the strength of a quartz sandstone does not vary systematically with decreasing strain rate (Donath, 1968). The effect of strain rate on a calcite cemented sandstone on the basis of these experimental results is not easily predictable.

Some preliminary tests were performed on the calcareous Oriskany sandstone to evaluate the capabilities of the "strain-pump" and to clarify experimental procedures at reduced rates of strain. The results of these experiments are tabulated in Table V. The non-systematic variation in strength and ductility probably reflects insufficient data and to some extent sample variation. Additional experiments will have to be run before any conclusions regarding the effect of strain rate on the strength and ductility of calcite cemented sandstones can be made.

Influence of Fabric Parameters

1. General Statement

The mechanical properties of rocks for the most part depend on the state of stress to which they are subjected. Other than generalizations as to rock composition, rock fabric parameters are usually considered to have minor effects, and are generally ignored in experimental rock mechanics. By using standardized techniques of rock description and testing procedures, it was hoped that the influence of composition

TABLE V. SUMMARY OF TRIAXIAL COMPRESSION TESTS ON THE ORISKANY SANDSTONE DEFORMED AT CONFINING PRESSURES OF 1000 AND 2500 BARS AND VARIOUS STRAIN RATES

Confining Pressure, Bars	Nominal Strain Rate	Ultimate strength, Bars	Ductility, Percent	Number of Tests
1000	10^{-5}	4081	2.00	8
1000	10^{-6}	3602	2.00	3
2500	10^{-5}	5849	3.40	10
2500	10^{-7}	5890	5.76	1

and sedimentary fabric on the deformational behaviour of sandstones could be evaluated.

In the four sandstones tested, the following parameters are constant; sorting, sphericity, roundness, fracture index and lamellae spacing index (Table III). The influence of specific gravity is ignored as it is a measure of both composition and pore volume. A good correlation between porosity, contacts per grain and calcite content reflects a sample bias in the test materials (Table VI). The real contribution of these parameters may be difficult to establish because of the sampling bias.

2. Strength

The strength of a rock as determined in the laboratory is an average macroscopic property of the material. Consistent values of strength can be obtained only from relatively homogeneous materials. The test materials are reasonably homogeneous on the mesoscopic scale, but microscopically they are heterogeneous. Scatter in the test results usually reflects deviations from homogeneity as the test procedures are carefully standardized.

Table VII tabulates the correlation coefficients between sandstone strengths and the significant fabric parameters. In unconfined tests (1 bar), a negative correlation occurs between contacts per

TABLE VI. SIMPLE CORRELATION COEFFICIENTS BETWEEN SANDSTONE FABRIC PARAMETERS

	Grain Size	Calcite %	Contacts per Grain	Porosity
Grain Size	1.00	-0.141	-0.068	0.05
Calcite %		1.00	-0.859	-0.738
Contacts per Grain			1.00	0.964
Porosity				1.00

TABLE VII. SUMMARY OF SIMPLE CORRELATION COEFFICIENTS BETWEEN SANDSTONE STRENGTHS AND VARIOUS FABRIC PARAMETERS AT DIFFERENT CONFINING PRESSURES

Confining Pressure Bars	Number of Samples	Grain Size	Calcite Percent	Contacts per Grain	Porosity
1	13	0.369	0.578	-0.896	-0.870
500	13	0.742	0.222	-0.365	-0.230
1000	23	0.115	0.012	-0.310	-0.437
1500	23	0.704	-0.372	-0.032	-0.040
2000	25	0.589	-0.533	0.218	0.210
2500	24	0.572	-0.708	0.405	0.366

grain (packing) and strength. This relationship is not real, that is, it reflects the nature of the original starting materials. An increase in the number of grain contacts should lead to an increase in the frictional resistance between grains, which in turn should cause an increase in strength. A positive correlation between contacts per grain and porosity suggests that porosity is the significant and controlling factor influencing unconfined compressive strengths (Figure 29). The profound influence of porosity on the unconfined compressive strengths of other sandstones has also been demonstrated by Price (1963) and Morgenstern and Puhukan (1969). At higher confining pressures, the effect of porosity on strength is minor apparently because of pore collapse and compaction of the specimens (Table VII).

If straight sections of grain boundaries are assumed to be Griffith cracks, the Griffith theory predicts that strength should increase with diminishing grain size. The enhancement of strength with diminishing grain size has been observed in rocks such as marble (Brace, 1961, 1964), granites (Houpert, 1966), loose sands (Krumbein, 1959; Borg et al., 1960; Holmes and Goodell, 1964), mixtures of clay, sand and water (Trask, 1959), and concrete (Hughes and Chapman, 1966). Figure 30 illustrates the effect of mean grain size on the strengths of the different sandstones at various confining pressures. The variation of grain sizes between samples is small (250μ to 125μ), therefore the magnitude of the grain size effect is small.

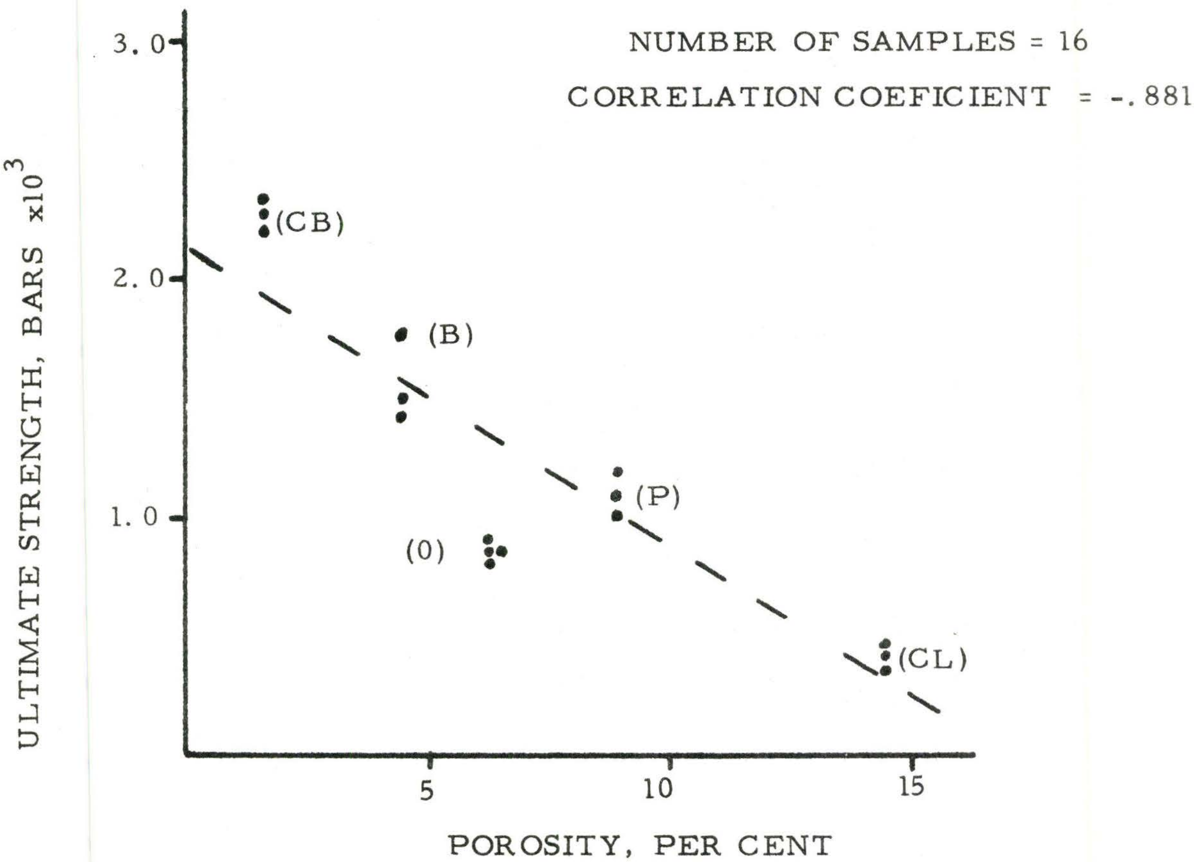

Figure 29. Variation of unconfined compressive strength with porosity

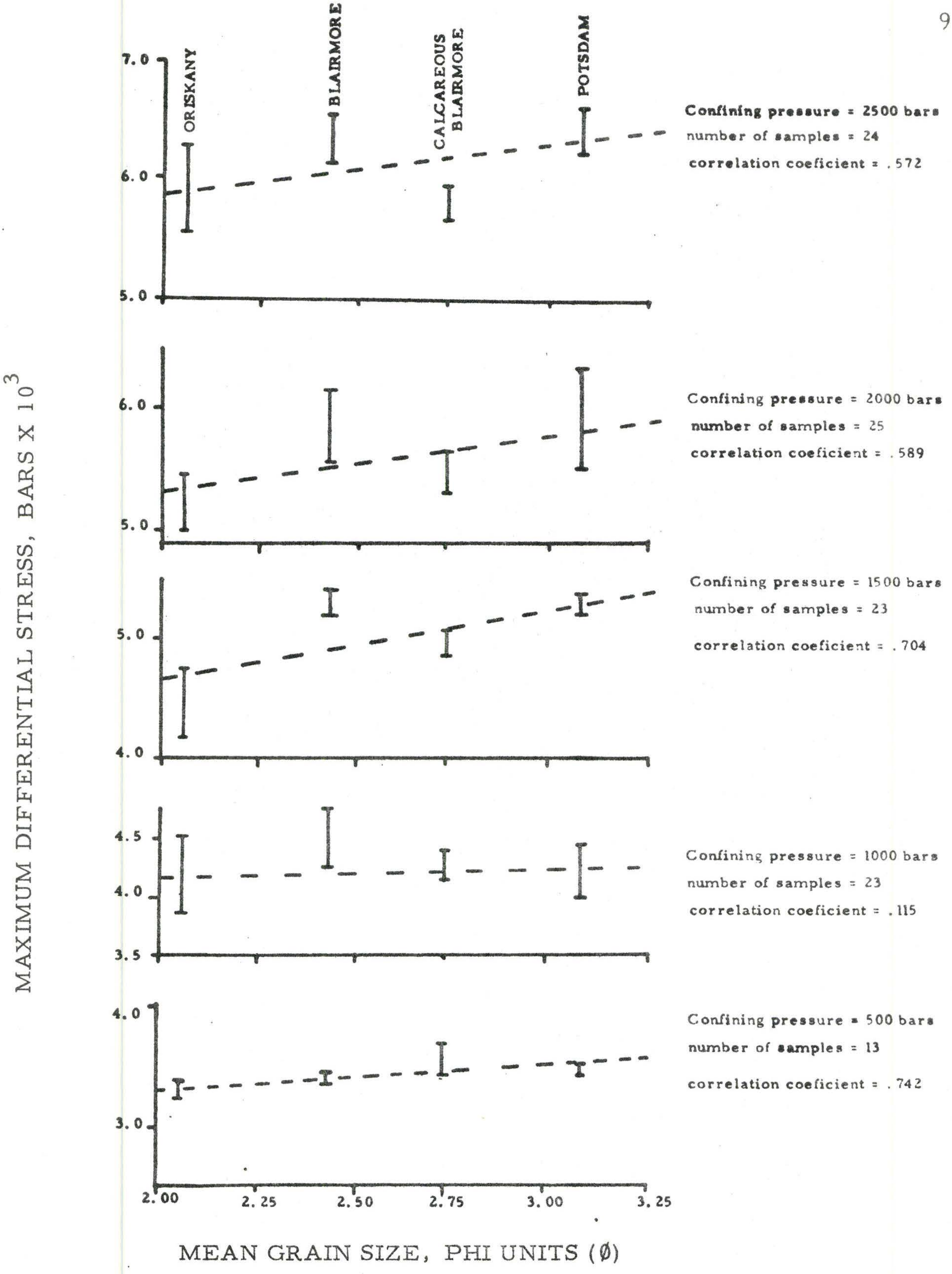

Figure 30. Maximum differential stress as a function of grain size at various confining pressures

Variation in rock composition should lead to differences in strength. Previous work by Price (1960, 1963) has shown that the strengths of sandstones and siltstones with clay matrices and low porosity (<3.5%), are largely controlled by their quartz content and the degree of compaction. The four sandstones in this investigation have a wide compositional range, but the mechanical effects of compositional variation can best be interpreted on the basis of calcite content. Calcite content does not appreciably influence strengths at low confining pressure, but becomes effective at higher confining pressures (Table VII). The influence of calcite content can be related to the activation of additional slip systems in the calcite at elevated confining pressures. Homogeneous deformation of the calcite by intracrystalline gliding and twinning leads to strength reductions in the calcareous sandstones.

The effect of packing (contacts per grain) is masked at low confining pressures by porosity effects. Low correlation coefficients at elevated confining pressures suggest that packing alone is not a significant variable controlling strength variations (Table VII).

To test for the cumulative dependencies of the measured independent variables against a single dependent variable (strength), a multiple linear regression analysis was performed. The resulting data at various confining pressures are summarized in Table VIII. The empirical strength predicting equations are difficult to evaluate

TABLE VIII. SUMMARY OF MULTIPLE LINEAR REGRESSION USING SANDSTONE DATA WITH STRENGTH AS THE DEPENDENT VARIABLE AT VARIOUS CONFINING PRESSURES. (X_1 = grain size, X_2 = calcite percent, X_3 = contacts per grain, X_4 = porosity)

Confining Pressure Bars	Number of Samples	Empirical Strength Predicting Equation	Multiple Correlation Coefficient	Variability Accounted for
1	13	$S_o = 3.77-.62X_3-.02X_2 + .27X_1$	0.99	98%
500	13	$S_o = 2.81 + .24X_1$	0.74	55%
1000	23	$S_o = 4.99-.10X_4-.01X_2$	0.70	49%
1500	23	$S_o = 5.51+.37X_1 -.03X_2-.24X_3$	0.87	76%
2000	25	$S_o = 5.25+.42X_1-.02X_3-.06X_4$	0.82	67%
2500	24	$S_o = 5.42-.02X_2+.36X_1$	0.83	69%

because of the relationships between packing, porosity, and calcite content.

In summary, the following general conclusions can be made:

(1) The unconfined compressive strengths of the sandstones are largely controlled by porosity variations.

(2) Strength is inversely proportional to mean grain size.

(3) At confining pressures greater than 1000 bars, increasing calcite content decreases the observed strength.

(4) In this particular suite of specimens packing does not significantly influence the strength.

3. Elastic Properties

Some calcareous sandstones can be considered as particle reinforced composite materials. Ideally particulate-reinforced composites have a particle volume greater than 25%, and the particle diameter and mean free matrix path exceeds 1μ (Krock and Broutman, 1967). In particulate-reinforced composites both the matrix and the dispersed particles act as load bearing constituents. Strengthening occurs in composites when the dispersed phase resists matrix deformation. The magnitude of the mechanical restraint of a particle to deformation in the matrix is a function of interparticle spacing-to diameter ratio, and the ratio of the elastic properties of the matrix and the particle (Krock and Broutman, 1967). The "rule of mixtures law" can be because of the relationships between packing, porosity, and calcite content.

In summary, the following general conclusions can be made:

(1) The unconfined compressive strengths of the sandstones are largely controlled by porosity variations.

(2) Strength is inversely proportional to mean grain size.

(3) At confining pressures greater than 1000 bars, increasing calcite content decreases the observed strength.

(4) In this particular suite of specimens packing does not significantly influence the strength.

3. Elastic Properties

Some calcareous sandstones can be considered as particle reinforced composite materials. Ideally particulate-reinforced composites have a particle volume greater than 25%, and the particle diameter and mean free matrix path exceeds 1μ (Krock and Broutman, 1967). In particulate-reinforced composites both the matrix and the dispersed particles act as load bearing constituents. Strengthening occurs in composites when the dispersed phase resists matrix deformation. The magnitude of the mechanical restraint of a particle to deformation in the matrix is a function of interparticle spacing-to diameter ratio, and the ratio of the elastic properties of the matrix and the particle (Krock and Broutman, 1967). The "rule of mixtures law" can be applied to predict the elastic modulus of a composite, that is,

$$E_c = V_m E_m + V_p E_p \tag{3.3}$$

where E_c is the elastic modulus of the composite, V_m and V_p are the volume fractions of the matrix and the particles, and E_m and E_p are the elastic moduli of the matrix and the particles (Krock and Broutman, 1967). This expression formulates an upper-bound condition on the composite's elastic modulus.

Theoretical elastic moduli based on equation 3.3 of the five rocks tested are displayed in Figure 31. In the calcareous Blairmore sandstone the elastic modulus of the particles are calculated on the basis of the relative proportions of the different clasts, and their estimated elastic moduli. In the Columbus limestone, both the dolomite and the quartz are considered to be dispersed brittle particles for the purposes of calculating the Young's modulus of the composite. These calculations are influenced by large uncertainties in the elastic moduli of the various constituents (Birch, 1966). However, the calculations provide a reasonable estimate of the composite's predicted elastic modulus.

Experimentally determined static Young's moduli for the various test materials fall well below that predicted by the rule of mixtures law (Figure 31). For comparative purposes, the experimentally

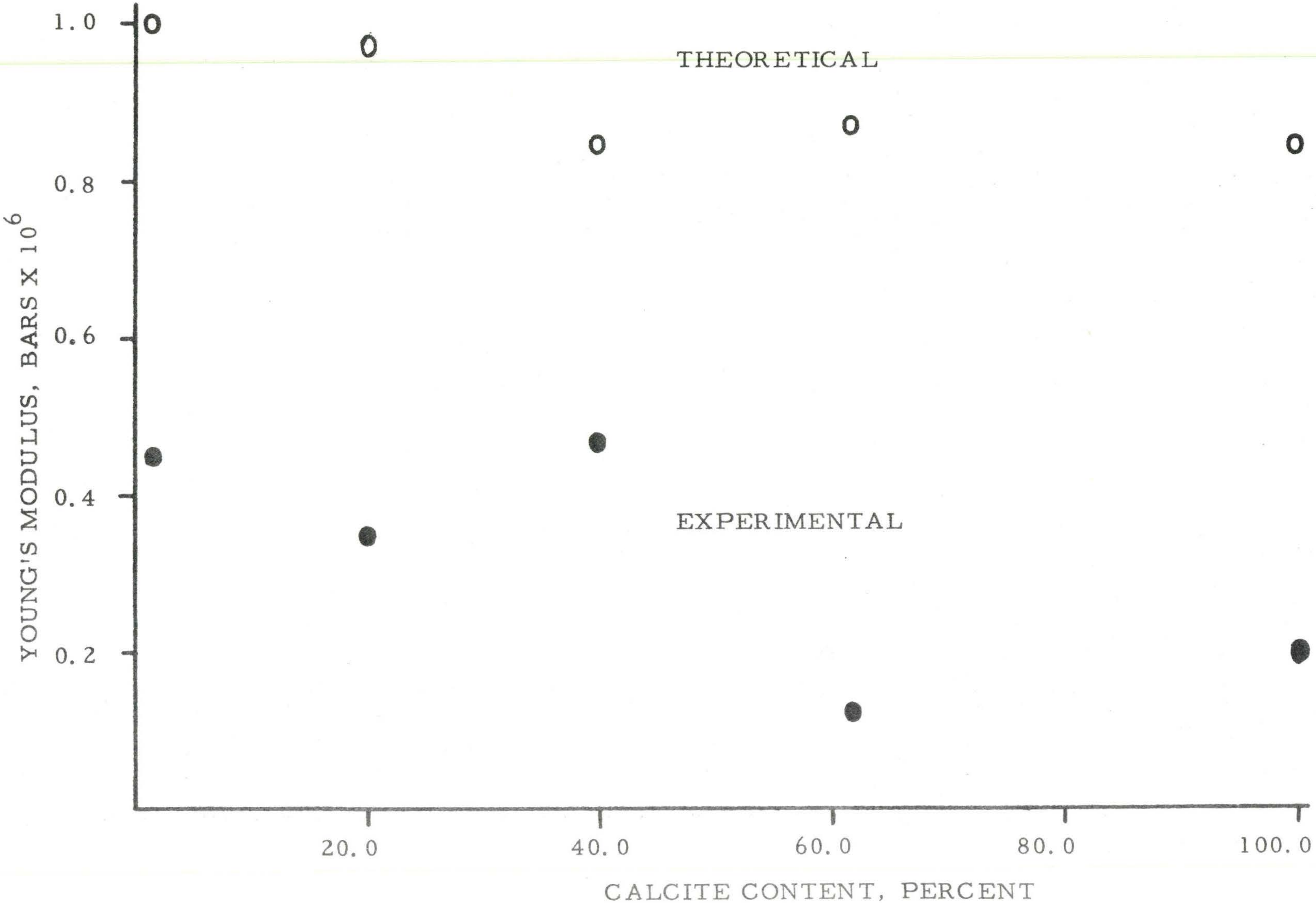

Figure 31. Comparison of experimental composite Young's Moduli with theoretical composite Young's Moduli

determined value of the Young's modulus for the Redwall marble (porosity = 13.9%) has been added to Figure 31 (Birch, 1966). The discrepancy between predicted and determined values of Young's moduli cannot be resolved if lower boundary conditions are imposed in calculating the theoretical composite elastic moduli. The discrepancy can be attributed to porosity effects. Small amounts of porosity have a large effect on experimentally determined elastic moduli (Walsh and Brace, 1966). Pores in rocks can fail under confining pressure when the stress on the pore walls exceeds the local fracture strength, and permanent deformation occurs due to pore collapse (Walsh and Brace, 1966). The combined effect of hydrostatic pressure and the large strain interval used in calculating the elastic moduli significantly lowers the experimentally determined Young's moduli. More precise elastic moduli could be obtained by substantially increasing instrument sensitivity such that total strains of less than 0.1% can be accurately monitored. At this strain level, and at low confining pressures the effects of pore collapse would be minimized. However, even at very low strain levels microscopic and submicroscopic "cracks" play a significant role in reducing elastic moduli in rocks with no pore porosity (Walsh and Brace, 1966).

In summary, the elastic moduli of the sandstones based on the simple rule of mixtures law takes into account only the intrinsic properties of the constituent minerals. Porosity, either as pores or cracks significantly lowers the Young's modulus of rocks.

4. Ductility

Ductility, defined as the percent strain before faulting is also influenced by both environmental and material parameters. Differences in sandstone composition should lead to differences in ductility. The large compositional variations of the test materials are ideally suited for an investigation of compositional, cement, and framework effects on ductility.

Ductilities of the orthoquartzite and the greywacke (Potsdam and Blairmore sandstones respectively) are essentially similar (Figures 25 and 26). This indicates that ductility is not strongly controlled by clast variation in the framework.

Table IX tabulates the simple correlation coefficients between sandstone ductilities and the various material parameters. At confining pressures greater than 1000 bars, ductility is inversely proportional to the strength (Table IX). In general, any material parameter that enhances strength will decrease ductility. Because of this relationship, at elevated confining pressures ductility is directly

TABLE IX. SUMMARY OF SIMPLE CORRELATION COEFFICIENTS BETWEEN SANDSTONE DUCTILITIES AND VARIOUS MATERIAL PARAMETERS AT DIFFERENT CONFINING PRESSURES

Confining Pressure Bars	Number of Samples	Strength	Grain Size	Calcite Content	Porosity	Contacts per Grain
1	13	0.458	0.285	-0.405	-0.274	-0.099
500	13	0.101	0.372	-0.094	0.149	-0.074
1000	23	-0.537	-0.550	-0.292	0.635	0.629
1500	23	-0.743	-0.572	0.584	-0.235	-0.255
2000	25	-0.753	-0.735	0.451	-0.134	-0.110
2500	24	-0.742	-0.577	0.765	-0.441	-0.480

proportional to calcite content and increasing grain size of the framework (Table IX).

Packing and porosity apparently do not significantly influence the ductilities of this particular suite of sandstones.

The influence of calcite content on the ductility at various confining pressures is illustrated in Figure 32. Values of ductility for the limestone end member are based on Donath's (1968) investigation of the Crown Point limestone. Calcite content acting independently has an insignificant effect on ductility at atmospheric confining pressure. At progressively higher confining pressures, significant increases in ductility occur with increasing calcite content. This behaviour can be attributed to the increased ductility of the calcite cement. At elevated confining pressures, the presence of e-twinning and r-translation enables favourably oriented calcite to deform in a ductile manner by intracrystalline deformation. Increasing calcite content provides a greater number of calcite crystals in the favourable orientation.

The effect of material parameters on ductility can be summarized as follows:

(1) Ductility is not strongly influenced by framework variation.

(2) Ductility is directly proportional to calcite content at elevated confining pressures.

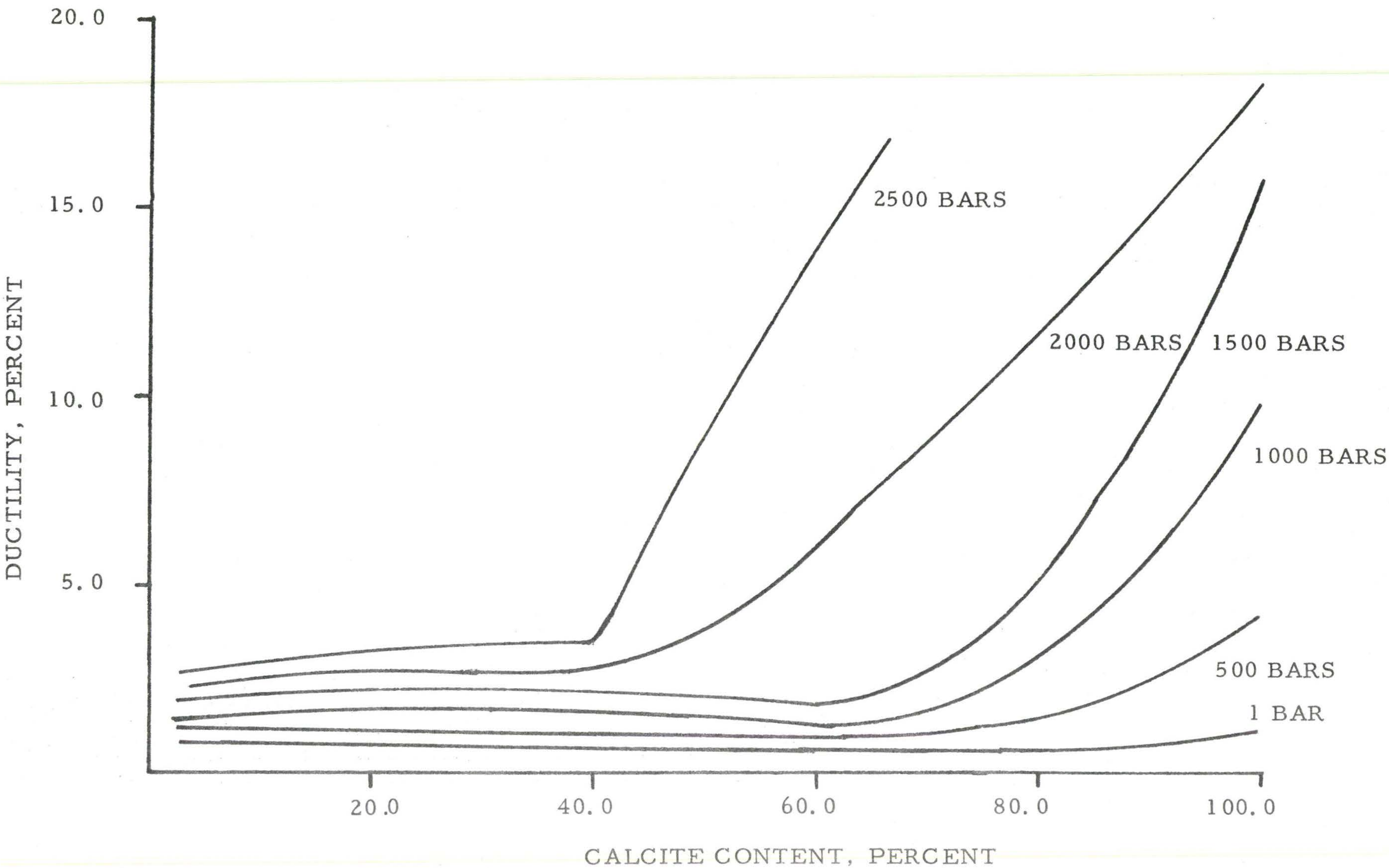

Figure 32. Ductility as a function of calcite content and confining pressure.

(3) Ductility is directly proportional to increasing mean grain size of the framework.

(4) Ductility is not strongly influenced by packing and porosity in this suite of samples.

5. Deformational Modes

Several environmental factors influence the deformational modes of rocks. In this section, the effect of material factors will be discussed.

Deformational modes are strongly related to a rock's ductility, therefore, any material parameter which influences ductility will have an effect on a rock's deformational mode. From the previous discussion on the effect of material factors on ductility, we would predict that increasing calcite content and increasing mean grain size in the framework will decrease the field of brittle behaviour.

It is difficult to evaluate the effects of framework grain size on the ductility without considering the mechanisms of deformation. Qualitatively, we would expect coarse grains to be more susceptible to local fracturing than fine grains. This microfracturing relieves some of the local stresses, lowers the strength, and subsequently increases the ductility of the material. Microfracturing during Region II and just prior to faulting has been acoustically monitored by other workers (Goodman, 1963; Brace, 1964; Chugh and Hardy, 1968; Hardy *et al.*, 1969).

Deformational modes as a function of carbonate (calcite) content and confining pressure at a fixed amount of total strain are diagrammatically illustrated in Figure 33. This diagram is based on the five "sandstones" referred to in this study, and the 100% carbonate end member is based on Donath's (1968) investigation of the Beldens marble. The boundaries in Figure 33 are not rigidly fixed because their position is based on specific samples. If other samples are used, boundaries may shift somewhat, but the general relationships illustrated are still valid. An extension of this diagram in the third dimension (total strain) is shown in Figure 34. The boundaries between deformational mode fields are complex due to the nature of the boundary between elastic and homogeneous deformation. This is a consequence of arbitrarily defining the region of elastic behaviour. Elastic deformation may also be considered as a type of homogeneous deformation. In nature, and in the laboratory it is not feasible to truly delineate the boundary between elastic and homogeneous deformation.

The effect of material factors on the deformational modes of "sandstones" can be summarized as follows:

(1) A sandstone's deformational mode is strongly influenced by its ductility.

(2) The field of brittle behaviour decreases with increasing calcite content.

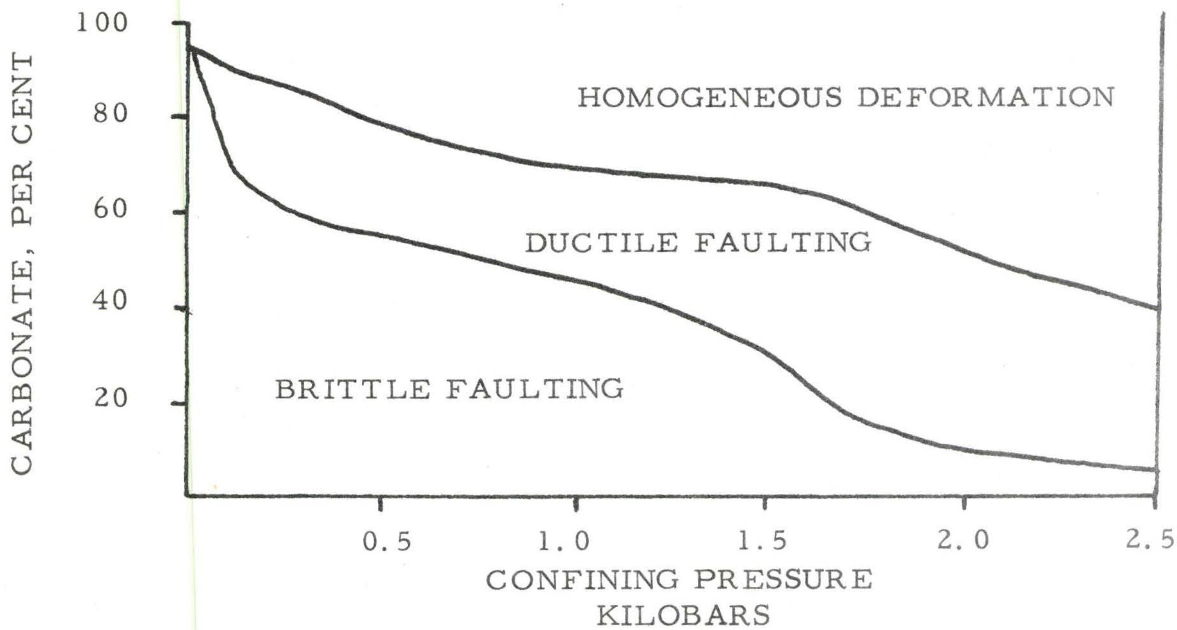

Figure 33. Deformational behaviour as a function of confining pressure and carbonate content at 3% total strain

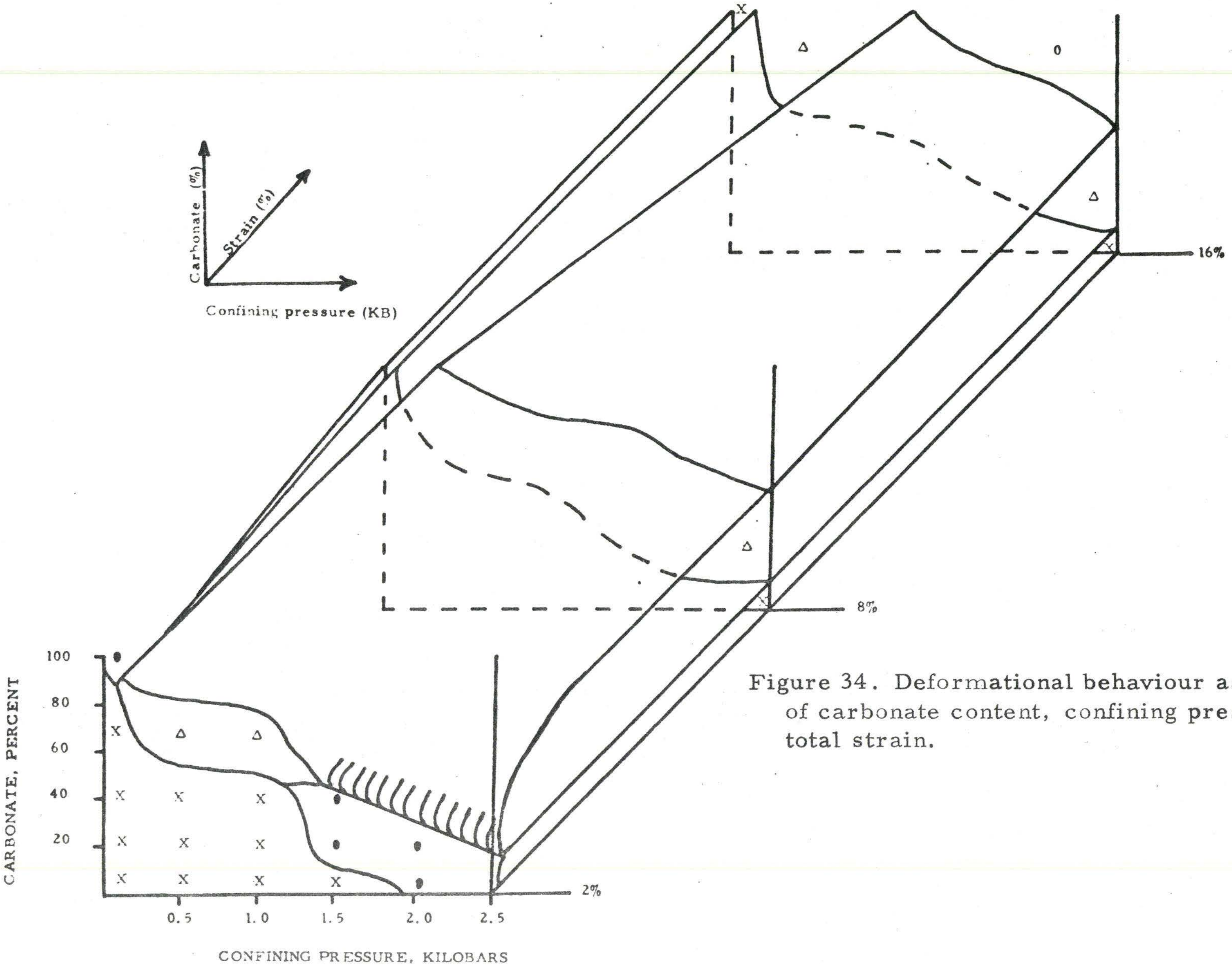

Figure 34. Deformational behaviour as a function of carbonate content, confining pressure, and total strain.

(3) Increasing mean grain size in the framework increases the ductility, and, therefore, decreases the region of brittle behaviour..

6. Deformational Mechanisms

(a) Observed Deformational Features. In an attempt to correlate between experimentally observed deformational features and natural deformation, a series of approximately "iso-strain" thin sections were made (Table X). The selected specimens were intended to be representative of Region V, that is, experimental tests were terminated immediately after fracture, or close to the onset of ductile faulting or homogeneous deformation.

The Potsdam sandstone is brittle at all confining pressures tested. Failure occurs along narrow, well defined faults at 1 bar (Plate 14A). No significant deformation occurs outside the major fault surface, nor is there any significant development of mylonitized material in the shear zone. At 500 bars confining pressure, the fault zone becomes wider (0.5-1mm) and incipient mylonite develops in the shear zone (Plate 14B). At progressively higher confining pressures, the fault zone broadens, or multiple sub-parallel faults are developed. At 2500 bars confining pressure, the major fault zone is a broad cataclastic

TABLE X. SUMMARY OF TOTAL STRAINS OF THIN SECTIONS EXAMINED AT VARIOUS CONFINING PRESSURES

Confining Pressure, Bars	Potsdam	Blairmore	Oriskany	Columbus
1	2.36	3.58	2.26	1.08
500	4.89	4.27	3.62	1.69
1000	3.60	3.87	4.39	2.20
1500	4.74	4.49	4.43	2.51
2000	3.59	5.12	5.08	3.51
2500	4.17	4.81	4.22	3.37

Plate 14

A. Potsdam sandstone deformed at 1 bar confining pressure to 2.36 percent strain. Note narrow well defined fault and the lack of deformation outside the major fault zone (polarized light, X 55).

B. Potsdam sandstone deformed at 500 bars confining pressure to 4.89 percent strain. Note the development of crushed material in the two fault zones (polarized light, X 55).

C. Potsdam sandstone deformed at 2500 bars confining pressure to 4.17 percent strain. The major fault zone is a broad cataclastic zone of crushed and fractured quartz grains encompassing the entire field of view (polarized light, X 55).

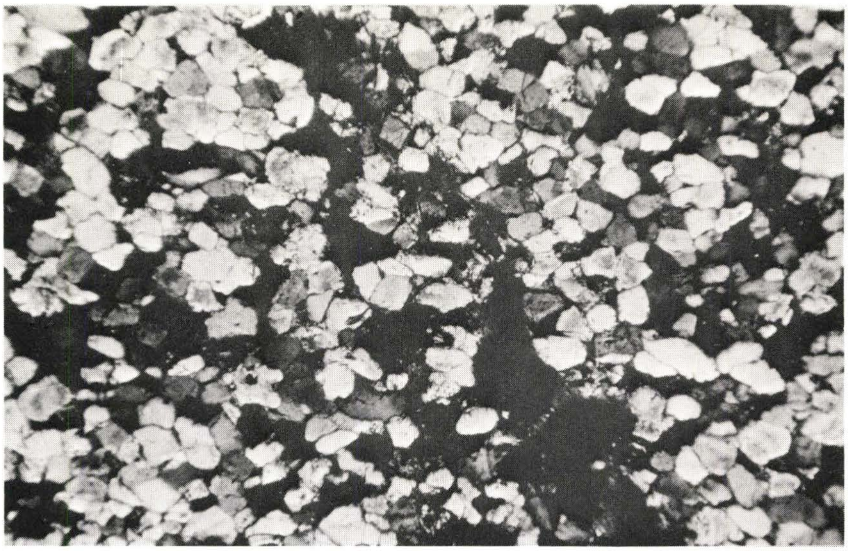

A

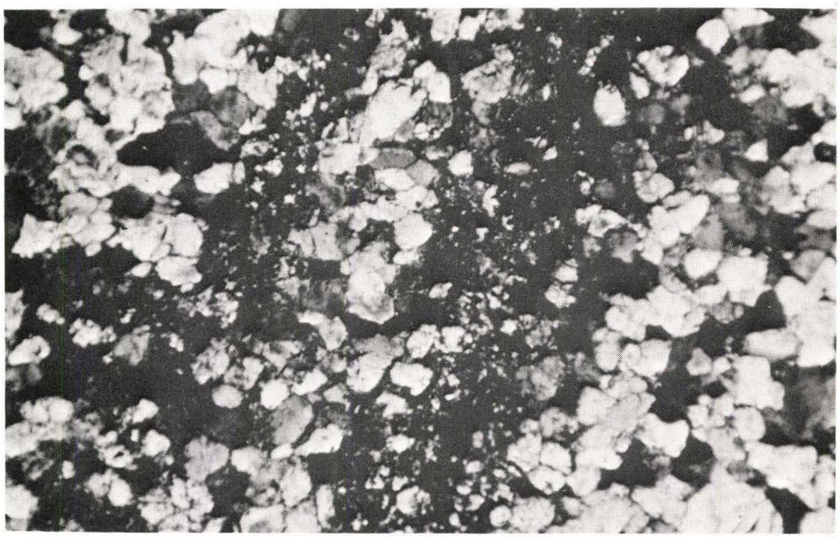

B

C

zone (1.5-2mm), but the deformation is still restricted to the major macroscopic shear zone (Plate 14C). This sequence of deformational features is similar to that observed in the Berea sandstone at low and intermediate effective confining pressures (Handin et al., 1963).

The Blairmore sandstone is brittle at all confining pressures and the macroscopic and microscopic faults are narrow, and well defined, but they contain little or no fault gouge (Plates 15A). In some thin sections "step features" on the fault surface oppose the sense of displacement on the fracture (Plate 15B). Currie (1969) suggests that stepped fracture surfaces are developed in a specific range of confining pressures. The sense of displacement on the microscopic level is marked by drag features developed in biotite grains adjacent to the rupture surface (Plate 15C). At confining pressures less than 1500 bars, no significant grain fracturing occurs away from the major macroscopic shear surface. At higher confining pressures, microfracturing occurs preferentially in the quartz grains with only minor fracturing in the other framework clasts.

At low confining pressures (1-500 bars), fracture surfaces in the Oriskany sandstone are marked by a zone ($<$1mm) of cataclastically deformed calcite and quartz grains. Microfractures are most prevalent in coarse grains and are strongly oriented sub-parallel to σ_1

Plate 15

A. Blairmore sandstone deformed at 500 bars confining pressure to 4.27 percent strain. The fault zone is narrow and well defined but contains little fault gouge (polarized light X 135).

B. Blairmore sandstone deformed at 1000 bars confining pressure to 3.87 percent strain. Note the "step features" on the fault surface which oppose the sense of displacement (polarized light, X 135).

C. Blairmore sandstone deformed at 1000 bars confining pressure to 3.87 percent strain. Note that the sense of displacement on the fault surface is marked by drag features in the biotite grains adjacent to the fault surface (polarized light, X 37).

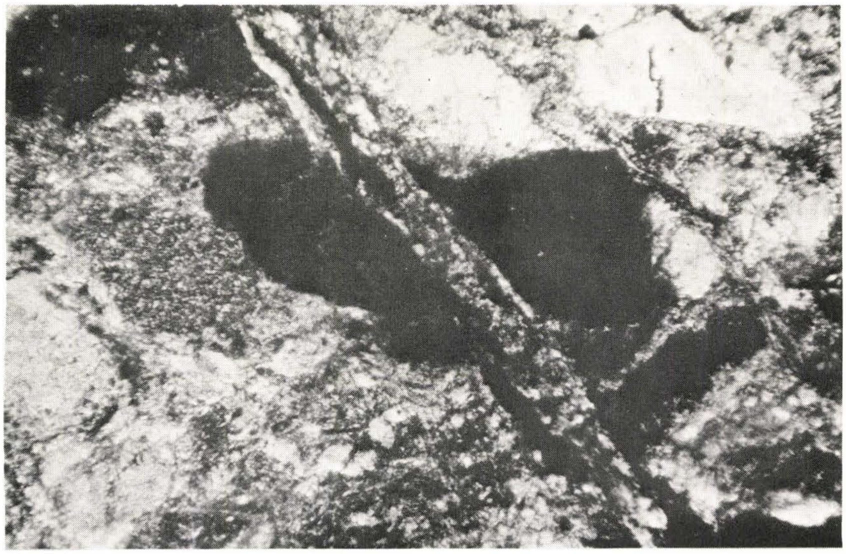

A

B

C

Plate 16A & B). At 1000 bars confining pressure, the fault zone is similar in nature to that observed at 500 bars, but fractured quartz grains now occur up to 5mm away from the fracture surface. At higher confining pressures, no faults are visible in thin section, but microfracturing in the quartz grains now occurs throughout the specimen (Plate 16C). Some of the microfractures in the quartz grains are short and apparently do not have any specific orientation with respect to the applied stress field but the majority of the microfractures are sub-parallel to σ_1 (Plate 16C).

The arenaceous Columbus limestone is brittle at low confining pressures (1-100 bars); the observed mechanism of deformation is cataclasis. Cataclastic deformation of the calcite causes a darkening in the appearance of the calcite in the vicinity of the fault surface (Plate 17A). In the region of ductile faulting and homogeneous deformation no visible faults occur in the thin section, but the calcite is darker in color and more intensely twinned than the undeformed material (Plate 17B). Microfracturing in the quartz and dolomite is minimal even at total strains up to 10% (Plate 17C).

Deformational features observed in thin sections can be summarized as follows:

Plate 16

A. Oriskany sandstone deformed at 500 bars confining pressure to 3.62 percent strain. Microfractures are most prevalent in the coarse quartz grains and are strongly oriented sub-parallel to the applied stress (north-south) (polarized light, X 37).

B. Enlargement of Plate 16A showing the nature of the shear fault zone and the orientation of the micro-fractures (polarized light, X 110).

C. Oriskany sandstone deformed at 2500 bars confining pressure to 4.22 percent strain. Note the nature and the orientation of the quartz microfractures (polarized light, X 120).

A

B

C

Plate 17

A. Arenaceous Columbus limestone deformed at 100 bars confining pressure to 1.32 percent strain. The fault zone contains cataclastically deformed calcite and quartz. Cataclastic deformation of the calcite causes a general darkening in the appearance of the calcite in the vicinity of the fault surface (polarized light, X 57).

B. Arenaceous Columbus limestone deformed at 500 bars confining pressure to 2.20 percent strain. Note that the deformational strain in this specimen is accommodated by twinning (and intracrystalline gliding) in the calcite. Quartz and dolomite (rhombohedral form) remain unfractured (polarized light, X 450).

C. Arenaceous Columbus limestone deformed at 2000 bars confining pressure to 10.26 percent strain. Note that microfractures are not well developed even at relatively high total strains (polarized light, X 450).

A

B

C

(1) The Potsdam sandstone is characterized by cataclastic fault zones which broaden with increasing confining pressure. Most of the permanent deformation occurs in the major zone of movement beyond which there is little or no grain fracturing.

(2) The Blairmore sandstone ruptures along narrow, well defined faults which contain little or no fault gouge. Microfracturing of the quartz grains becomes prevalent at confining pressures greater than 1500 bars.

(3) The Oriskany sandstone is characterized by cataclastic fault zones at low confining pressures. Microfracturing occurs preferentially in the large quartz grains. The extent of microfracturing is governed by the confining pressure.

(4) The macroscopic shear surfaces in the arenaceous Columbus limestone are characterized by granulated calcite and quartz. At elevated confining pressures no visible faults occur in thin section, but the calcite is darker in appearance and more intensely twinned tha the undeformed material. Microfracturing in the quartz grains is rare.

(b) Interpretation of Deformational Features. The differences in the observed deformational features can be related to the character of the test materials. In the Potsdam sandstone frictional resistance between grains is relatively low because of the initial porosity.

Porosity facilitates intergranular movements and grain fracturing in the fault zone. At low confining pressures, friction on the fault surface is low with the result that only minimal amounts of cataclastic material are formed. At higher confining pressures, frictional resistance to movement is larger, but some granulation of the grains has already been initiated by the original porosity. Grain breakage reduces the grain size and hence increases the frictional resistance between the grains. It becomes mechanically easier to granulate previously uncrushed material, of relatively coarse grain size, than to continue to comminute the material already granulated. Hence the zone of cataclasis broadens.

In contrast to the Potsdam sandstone, the Blairmore sandstone has a low porosity and therefore the frictional resistance (cohesion) between grains is relatively large. Once a rock's cohesive strength is exceeded, the rock ruptures on macroscopic shear surfaces, but no significant movement occurs on the fault surface because of high frictional resistance on the fault surface. This is reflected on the stress-strain record by a renewed increase in the differential stress sustained by the specimen (Figure 5).

In the Oriskany sandstone, the observed mechanism of deformation at confining pressures between 1-1000 bars is cataclasis. At elevated confining pressures the deformational mechanism reflects a change in the deformational mode. In this case, the deformation occurs by intracrystalline deformation in the calcite and grain fracturing throughout the framework.

At low confining pressures, cataclasis is the principal deformational mechanism in the Columbus limestone, although some intracrystalline deformation in the calcite is also present. At elevated confining pressures, the major mechanism of deformation is twinning and intracrystalline gliding in the calcite, and perhaps some basal slip in the dolomite grains. At room temperature the critical resolved shear stress for basal translation in dolomite crystals is about 1 kilobar (Higgs and Handin, 1959).

Many of the observed deformational features in the Columbus limestone and the Oriskany sandstone can be interpreted in terms of recent theoretical studies on composite materials. The following discussion on elastic-plastic stress analysis of the constituents of a composite material is based on the work of Drucker (1965, 1966). Drucker, using the principles of continuum mechanics, has analyzed the influence of the volume fraction of brittle inclusions in an elastic-plastic matrix. The matrix may be perfectly plastic or become so by work hardening. A small volume fraction of dispersed inclusions has only a small effect on the overall plastic stress-strain behaviour of the composite, that is, the stress-strain relations for the composite are almost identical to those of the matrix alone.

The application of a small amount of stress, for example, bending of a beam containing a small volume fraction of inclusions in a ductile work hardening matrix, has little effect on the deformational behaviour. With the continued application of stress, the inclusions remain elastic, deform less than the matrix, and therefore carry more than their share of the load. The inclusions on the compressional side of the bending beam do not expand laterally as much as the ductile matrix. This generates a tensile stress in the particles which is balanced by a compressional stress in the matrix (Drucker, 1966). At some advanced stage in the loading, the tensile stress in the inclusion exceeds the tensile strength of the particle, resulting in extensional fracturing of the inclusion.

When the composite contains a large volume fraction of brittle particles, the ductile matrix that surrounds the particles is relatively small compared to the particle size. Drucker (1965, 1966) analyzes this situation by assuming a two dimensional model of hexagons (particles) joined together by a "cement" of uniform thickness, h. In a composite with a large volume fraction of particles, the thickness h, is small when compared to the length of the side of each hexagon, a. Figure 35 sketches the distribution of normal stresses on the sides of the hexagons in uniaxial compression with different "cements". Local

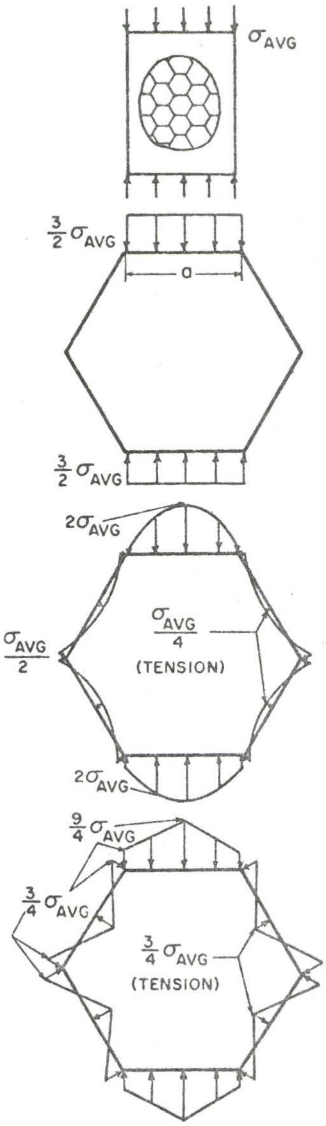

Figure 35. Stress distribution on rigid "grains" with different "cements". h $\ll$ a in vertical uniaxial compression. After Drucker (1965).

stress discontinuities at the corners are ignored. The main features of Figure 35 are that the peak stresses are of the order of twice the applied stress σ_{AVG}, stresses of opposite sign to the applied stress are about equal in magnitude to that of the applied stress, and the magnitude and distribution of the stresses are essentially insensitive to the type of "cement".

If the inclusions are strong and brittle, extensional fractures will occur at some stage in the plastic deformation of the composite in a manner similar to that for a low volume fraction composite. When the volume fraction exceeds 50%, the inclusions become the main load bearing constituents of the material. Fracturing of the inclusions in an appreciable amount will lead to the ultimate failure of the composite no matter how ductile the matrix. At high volume fractions, strain in the matrix is several times the nominal strain of the aggregate. At these volume fractions, if fracture of the inclusions occurs in a work hardening matrix, the failure of the composite as a whole will be brittle (Drucker, 1966).

The continuum theories of elasticity and plasticity contain no scale effect, that is, no distinction is made between large and small particles. However, in metal composites large inclusions have little effect, whereas, small particles will significantly harden the composite. The major role of particles in metals is to act as barriers to dislocation motion and to generate slip in the matrix on planes of high resolved shear stress. The generated slip planes intersect and multiply with increasing stress; the intersecting slip planes then provide the main barriers to further slip and the particles themselves become irrelevant (Drucker, 1966). Decreasing grain size of the inclusions and an increasing volume fraction would enhance the early generation and multiplication of intersecting slip planes.

The preceding discussion on the deformational behaviour of composite materials has important implications regarding the deformation of calcite cemented sandstones. If the composite model is to apply to calcite cemented sandstones, large differences in the elastic moduli of quartz and calcite are required. The Young's moduli of quartz and calcite are not significantly different (1.03 and 0.85 X 10^6 bars respectively), but large differences in the Poisson's ratio (approximately 0.12 for quartz and 0.25 for calcite) fulfil the requirement.

In the composite material model, generation of tensile stresses on the brittle inclusion approximately equal to the applied compressive stress, readily explains the observed extensional microfractures in the quartz grains of deformed calcite cemented sandstones. The lack of fracturing in the quartz grains of the arenaceous Columbus limestone even at relatively high strains (10%) can be attributed to the low volume fraction of quartz grains. On the basis of studies in composite materials, the quartz fraction would have to exceed 40% before it becomes effectively stressed by the matrix at relatively low strains (Corten, 1967). Microfracturing which does occur in the arenaceous Columbus limestone can be related to local increases in the volume fraction of quartz grains.

The Oriskany sandstone can be considered as a composite material containing a high volume fraction of dispersed brittle inclusions (80%). In this case, the strain in the matrix may be several times the nominal strain of the aggregate (Drucker, 1966). Extensive microfracturing of the quartz grains, occurs in a work hardening matrix at relatively low total strains (Plate 16C), with the result that the ductility of the composite as whole is low (brittle to moderately brittle (Figure 27)).

Friedman (1963) has proposed an alternative hypothesis to explain the deformational features observed in calcite cemented sandstones. In calcite sand crystals which have been loaded unfavourably for the development of twin lamellae, Friedman (1963) attributed the presence of twin lamellae in calcite to movement on extensional microfractures in the detrital grains. Movement on the extensional microfractures in the detrital grains would generate local stress conditions such that σ_1 is oriented to produce a resolved shear stress parallel to the twin plane. This interpretation contrasts with

Drucker's hypothesis in which the extensional microfractures in the detrital grains are a direct result of the ductile deformation of the calcite. Drucker's hypothesis is favoured for the following reasons:

(1) the large differences in the Poisson's ratio of quartz and calcite is sufficient to cause local stress situations in which σ_1 is oriented to produce twinning even in unfavourably loaded calcite grains;

(2) the critical resolved shear stress to produce twin lamellae in calcite ($\approx$ 80 bars) is less than the tensile strength of quartz. (Unconfined, room temperature tensile strength of the Cheshire quartzite as determined by indentation hardness tests is approximately 300 bars (Brace, 1964).) It is reasonable to conclude that twinning would occur in the calcite prior to microfracturing of the quartz grains.

Extensional microfractures produced in experimentally deformed calcite cemented sandstones have their counterparts in natural deformational textures. Stauffer (1970) describes micro-boudinage (pull-apart) textures in a number of deformed metamorphic rocks. He concludes that the most significant process producing microboudinage is "... movement within the matrix material under conditions such that a moderate to high intergranular cohesion was maintained between the matrix and the strain marker (though not necessarily between the matrix granules).". This implies that deformation of the matrix primarily is responsible for the observed microboudinage texture.

Chapter 4

SUMMARY AND CONCLUSIONS

General Summary

The influence of environmental, compositional, and fabric parameters have been investigated in a series of triaxial compression experiments on four sandstones and an arenaceous carbonate. Standardized and quantitative descriptions of the test materials have been made using basic rock properties, such as, particle composition, size, sorting, shape, orientation, and packing. Other properties such as porosity, fracture index, twin lamellae index of the calcite, and anisotropy orientation also have been determined to fully specify the undeformed materials. The sorting, sphericity, roundness, fracture index, and twin lamellae index are essentially similar in all the sandstones. Influence of anisotropy is minimized because all specimens have been compressed normal to bedding.

The study of environmental, compositional, and fabric effects on the deformational properties of the sandstones and the arenaceous limestone tested in this investigation can be summarized as follows:

1. <u>Strength Variations</u>

(1) The strengths of the test materials increase with increasing confining pressure.

(2) The unconfined compressive strengths of the test materials are inversely proportional to the porosity. At elevated confining pressures, porosity is not a significant variable controlling strength variations.

(3) Strength increases with diminishing mean grain size of the framework.

(4) Calcite content does not appreciably influence strength at low confining pressures, but at higher confining pressures, strength is inversely proportional to the calcite content.

(5) The effect of packing (contacts per grain) is masked at low confining pressures by porosity effects. At elevated confining pressures, packing alone is not a significant variable in controlling strength variations in this suite of sandstones.

(6) The Mohr-Coulomb failure criterion is useful for depicting experimental results but predicted fracture angles do not agree with those observed. The octahedral shear stress criterion is a useful empirical criterion for failure of the sandstones, namely, linearity of the octahedral shear stress with mean pressure. The modified Griffith criterion is the best mechanistic criterion for prediction of experimental failure strengths.

2. Elastic Properties

The static Young's modulus is significantly lowered by porosity. None of the rocks tested approached the theoretical values of the Young's modulus predicted by the rule of mixtures law and the intrinsic properties of the constituent minerals.

3. Ductility Variations

(1) Ductility is directly proportional to increasing confining pressure.

(2) At confining pressures greater than 1000 bars, ductility of the sandstones is inversely proportional

to strength, and therefore, ductility is directly proportional to increasing mean grain size of the framework.

(3) Ductility is not influenced by framework variation.

(4) Ductility is greatly enhanced by increasing calcite content at elevated confining pressures.

(5) Ductility is not strongly influenced by porosity and packing in this suite of sandstones.

4. Deformational Modes

(1) The deformational mode of a specimen is primarily controlled by ductility. Therefore, any property which enhances ductility will decrease the field of brittle behaviour.

(2) The deformational mode is strongly dependent on the amount of strain to which a rock is subjected.

5. Deformational Mechanisms

(1) The Potsdam sandstone ruptures at low confining pressures. Cataclastic fault zones which broaden with increasing confining pressure characterize the Potsdam at elevated confining pressures.

(2) The Blairmore sandstone ruptures or faults at all confining pressures along narrow, well defined faults with little or no development of fault gouge.

(3) Cataclasis along faults characterizes the Oriskany sandstone at confining pressures below 1000 bars. At elevated confining pressures, deformation occurs by intracrystalline gliding and twinning in the calcite, and grain fracturing of the framework.

(4) The arenaceous Columbus limestone is characterized by cataclastic fault zones at confining pressures below 250 bars. At higher confining pressures, the major mechanism of deformation is twinning and intracrystalline gliding in the calcite. Quartz remains relatively unfractured even at relatively high total strains (10%).

(5) The deformational features observed in the Oriskany sandstone and the arenaceous Columbus limestone can best be explained by Drucker's analysis of brittle inclusions in an elastic-plastic matrix. The presence of extensional microfractures in quartz can be attributed to tensile forces generated by the large differences in the Poisson's ratio of quartz and calcite. The lack of microfracturing in the quartz grains of the Columbus

limestone can be attributed to the low volume fraction of quartz grains in the ductile calcite matrix. Drucker's analysis would predict microfracturing in these quartz grains at some higher value of total strain.

Geological Implications

The behaviour of quartz grains in a plastic or work hardening matrix can be used as a model for interpretation of some deformed conglomerates. Extensional fractures are commonly observed in competent granitic pebbles in a matrix of highly deformed volcanic pebbles and "greenstone" matrix (Plate 18).

The 'Seine' conglomerate, a deformed Precambrian conglomerate near Fort Frances, Ontario, consists of 70% pebbles and 30% matrix (M. Y. Hsu, personal communication). Granitic pebbles form less than 20% of the conglomerate. A study of the deformed volcanic pebbles indicates a total shortening of 60%, but the granitic pebbles have homogeneously deformed only 0-20% (mean 10%) (M. Y. Hsu, personal communication). The granitic pebbles can be considered to be undeformed, brittle inclusions in a highly ductile matrix. In one area, most of the granitic pebbles have extensional fractures which are sub-normal to the maximum elongation, that is, sub-parallel to the inferred direction of σ_1 (Plate 18). Generally, fractures of this type

Plate 18

Deformed Precambrian conglomerate showing the development of extensional fractures in granitic pebbles, Fort Frances, Ontario (photograph courtesy of M. Y. Hsu).

are considered to be brittle extensional fractures which post date the major deformation. On the basis of Drucker's analysis (1965, 1966), and the observed deformational features of quartz grains in calcite cemented sandstones, an alternative interpretation may be proposed. During deformation the brittle and elastic granitic pebbles do not expand laterally as much as the ductile matrix. This generates a tensile stress in the granitic pebbles, which, at some stage exceeds the tensile strength of the granitic pebbles resulting in extensional fracturing. A large amount of deformation (in this case 60% shortening) is required to achieve this result because of the low volume fraction of granitic pebbles. In areas of large volume fraction of granitic pebbles, one would predict that extensional fracturing in the pebbles would occur at lower total strains, and be more extensively developed. This interpretation implies that the extensional fracturing in this example does not post date the major deformation but is syntectonic.

Recommendations for Future Work

Results from the experimental aspects of this investigation suggest that the experimental facilities and techniques should be utilized to carry out an extensive program of experiments to fully evaluate the continuum mechanics approach to the deformation of calcareous sandstones.

It is suggested that the initiation of microfracturing in quartz as a function of total strain, strain rate, confining pressure, and such fabric properties as volume fraction, grain size, and sphericity can be usefully studied with the aid of the experimental facilities and techniques developed during this investigation. Volume fractions of quartz grains should be below 60% to minimize grain contacts and provide good grain-cement bonding.

It is recommended that an extensive study of the microscopic relations of the deformed specimens be carried out in order to examine deformational features and to apply the recent developments of numerical approaches for continuum mechanics problems (Voight and Dahl, 1970).

BIBLIOGRAPHY

Adams, F. D., 1912, An experimental contribution to the question of the depth of flow in the Earth's crust. J. Geol., 20:97-118.

Bieniawski, Z. T., 1967a, Mechanism of brittle fracture of rock: Part I. Theory of the fracture process. Internat. Jour. Rock Mech. Min. Sci., 4:395-406.

________, 1967b, Mechanism of brittle fracture of rock: Part II. Experimental studies. Internat. Jour. Rock Mech. Min. Sci., 4:407-423.

________, 1967c, Mechanism of brittle fracture of rock: Part III. Fracture in tension and under long term loading. Internat. Jour. Rock Mech. Min. Sci., 4:425-430.

________, Denkhaus, H.G. and Vogler, U.W., 1969, Failure of fractured rocks. Internat. Jour. Rock Mech. Min. Sci., 6:323-341.

Birch, F., 1966, Compressibility, Elastic Constants: in Handbook of Physical Constants, editor S.P. Clark, revised edition, Geol. Soc. Amer. Memoir 97, 97-174.

Bombolakis, E.G., 1968, Photoelastic study of the initial stages of brittle fracture in compression. Tectonophysics, 6:461-473.

Borg, I. & Handin, J., 1967, Torsion of calcite single crystals. J. Geophys. Res., 72:641-669.

________, Friedman, M., Handin, J. & Higgs, D.V., 1960, Deformation of St. Peter sand: a study of cataclastic flow: in Rock Deformation, editors D. Griggs and J. Handin, Geol. Soc. Amer. Memoir 79, 133-193.

Brace, W.F., 1960, An extension of the Griffith theory of fracture to rocks. J. Geophys. Res., 65:3477-3480.

________, 1961, Dependence of fracture strength of rocks on grain size. Penn. State Univ. Mineral Industries Experimental Station Bull., 76:99-103.

________, 1964, Brittle fracture of rocks: in Proc. Internat. Conf. on State of Stress in the Earth's Crust, editor W.R. Judd, American Elsevier, N.Y., 110-178.

Brady, B.T., 1969a, A statistical theory of brittle fracture for rock materials: Part I. Brittle failure under homogeneous axisymmetric states of stress. Internat. Jour. Rock Mech. Min. Sci., 6:21-42.

Brady, B.T., 1969b, The non-linear mechanical behaviour of brittle rock: Part I. Stress-strain behaviour during Regions I and II. Internat. Jour. Rock Mech. Min. Sci., 6:211-225.

__________, 1969c, A statistical theory of brittle fracture for rock materials: Part II. Brittle failure under homogeneous tri-axial states of stress. Internat. Jour. Rock Mech. Min. Sci., 6:285-300.

__________, 1969d, The non-linear mechanical behaviour of brittle rock: Part II. Stress-strain behaviour during Regions III and IV. Internat. Jour. Rock Mech. Min. Sci., 6:301-310.

Bredthauer, R.O., 1957, Strength characteristics of rock samples under hydrostatic pressure. Amer. Soc. Mech. Engineers Trans., 79:695-708.

Boyd, J.M. & Currie, J.B., 1969, Fracture porosity in Alabaster; an experimental model of rock deformation. Canad. Petr. Geol. Bull., 17:117-132.

Cherry, J.T., Larson, D.B., & Rapp, E.G., 1968, A unique description of the failure of a brittle material. Internat. Jour. Rock Mech. Min. Sci., 5:455-463.

Chugh, Y.P. & Hardy, R.E., 1968, An investigation of the frequency spectra of microseismic activity in rock under tension. Tenth Symp. on Rock Mechanics, Univ. Texas, Austin, May 20-22, 1968, 45 p.

Coates, D. F., 1965, Rock mechanics principles. Dept. Mines & Techn. Surveys, Ottawa, Mines Branch Monograph 874, 338 p.

Corten, H. T., 1967, Micromechanics and fracture behaviour of composites, in Modern Composite Materials, editors Broutman and Krock, Addison-Wesley, Reading, Mass., 27-105.

Currie, J. B., 1969, Discussion of "Structural analysis of features on natural and artificial faults": a paper by Norris and Barron (1969), in Proc., Conference on Research in Tectonics, Kink Bands and Brittle Deformation, editors A. J. Baer & D.K. Norris. Geological Survey of Canada Paper 68-52, 136-174.

Donath, F. A., 1964, Strength variation and deformational behaviour in anisotropic rock, in Proc. Internat. Conf. on State of Stress in the Earth's crust, Editor W.R. Judd. American Elsevier, New York, 281-300.

________, 1968, Experimental rock deformation in dynamic structural geology. Rock Mechanics Seminar, editor R. E. Riecker. Air Force Cambridge Res. Lab., 2:355-438.

________, 1969, Rock deformation apparatus and experiments for dynamic structural geology. Jour. Geol. Educ., 18, 1: 3-12.

Drucker, D.C., 1954, Coulomb friction, plasticity, and limit loads. Jour. Appl. Mech., 21:71-74.

________, 1965, Engineering and continuum aspects of high-strength materials, in High Strength Materials, editor V.F. Zackay, John Wiley & Sons, New York, 795-832.

________, 1966, The continuum theory of plasticity on the macroscale and the microscale. Jour. of Materials, 1, 4:873-910.

________, and Prager, W., 1952, Soil mechanics and plastic analysis or limit design. Quart. Appl. Mathematics, 10:157-165.

Finn, Liam, W.D., 1967, Applications of limit plasticity in soil mechanics. Jour. Soil Mechanics & Foundations Division, Proc. ASCE, 5:101-120.

Folk, R.L., 1961, Petrology of Sedimentary rocks. Hemphills, Austin, Texas, 154 p.

Friedman, M., 1963, Petrofabric analysis of experimentally deformed calcite-cemented sandstones. J. Geol., 71:12-37.

Goodman, R.E., 1963, Subaudible noise during compression of rocks. Geol. Soc. Amer. Bull., 74:487-490.

Green, H.W., II, 1967, Quartz: extreme preferred orientation produced by annealing. Science, 157, 3795:1444-1447.

Griffith, A.A., 1921, The phenomena of rupture and flow in solids. Phil. Trans. R. Soc., A, 221:163-198.

Griffiths, J C., 1961, Measurement of the properties of sediments. J. Geol., 69:487-498.

Griffiths, J.C., 1967, Scientific method in analysis of sediments. McGraw Hill Book Co., New York, 508 p.

Griggs, D.T. and Handin, J., 1960, Observations on fracture and a hypothesis of earthquakes, in Rock Deformation, editors D. Griggs and J. Handin, Geol. Soc. Amer. Mem. 79, 133-193.

________, Turner, F.J. and Heard, H.C., 1960, Deformation of rocks at 500° to 800°C, in Rock Deformation, editors D. Griggs and J. Handin, Geol. Soc. Amer. Mem. 79, 39-105.

Groves, G.W. and Kelly, A., 1963, Independent slip systems in crystals. Phil. Mag., 8:877-887.

Handin, J., 1966, Strength and ductility, in Handbook of Physical Constants, editor S.P. Clark, revised edition, Geol. Soc. Amer. Mem. 97, 223-290.

________ and Hager, R.V., Jr., 1957, Experimental deformation of sedimentary rocks under confining pressure: tests at room temperature on dry samples. Amer. Assoc. Petr. Geologists Bull., 41:1-50.

________ and ________, 1958, Experimental deformation of sedimentary rocks under confining pressure: tests at high temperature. Amer. Assoc. Petr. Geologists Bull., 42:2892-2934.

Handin, J., Hager, R.V , Friedman, M., Feather, J.N., 1963, Experimental deformation of sedimentary rocks under confining pressure; pore pressure tests. Amer. Assoc. Petr. Geologists Bull., 47, 5:717-755.

________, Heard, H.C. Magouirk, J.N., 1967, Effects of the intermediate principal stress on the failure of limestone, dolomite and glass at different temperatures and strain rates. J. Geophys. Res., 72:611-640.

Hardy, H.R., Kim, R.Y., Stefanko, R., Wang, Y.J., 1969, Creep and microseismic activity in geologic materials. Eleventh Symposium on Rock Mechanics, Univ. of Calif., Berkeley, Calif., June 16-19, 1969, 45 p.

Hatano, T., 1969, Theory of failure of concrete and similar brittle solid on the basis of strain. Internat. J. of Fracture Mech., 5:73-79.

Heard, H.C., 1960, Transition from brittle to ductile flow in the Solenhofen limestone as a function of temperature, confining pressure and interstitial fluid pressure, in Rock Deformation, editors D. Griggs and J. Handin, Geol. Soc. Amer. Mem. 79:193-227.

________, 1963, The effect of large changes in strain rate in the experimental deformation of rocks. J. Geol., 71, 2:162-195.

Heard, H. C., 1968, Experimental deformation of rocks and the problem of extrapolation to nature, in Rock Mechanics Seminar, editor R. E. Riecker, Air Force Cambridge Res. Lab., 2:439-508.

________ and Carter, N. L., 1968, Experimentally induced "Natural" intergranular flow in quartz and quartzite. Amer. J. Sci., 266:1-42.

Higgs, D. V. and Handin, J., 1959, Experimental deformation of dolomite single cryatals. Geol. Soc. Amer. Bull., 70:245-278.

Hoek, E. and Bieniawski, Z. T., 1965, Brittle fracture propagation in rock under compression. J. Fracture Mech., 1, 3:137-155.

________ and ________, 1966, Fracture propagation mechanism in hard rock. Proc. First Congress of the Internat. Soc. of Rock Mech., Lisbon, September, 1966, 1:243-249.

Holmes, C. W. and Goodell, H. G, 1964, The prediction of strength in the sediments of St. Andrew Bay, Florida. J. Sed. Petr., 34: 134-143.

Hoskins, J. R. and Horino, F. G., 1968, Effect of end conditions on determining compressive strength of rock samples. U. S. Dept. Int. Rept., RI 7171, 22 p.

Houpert, R., 1966, Mécanique des roches. Relation entre la résistance à la rupture des roches et la dimension de leurs minéraux. C.R. Acad. Sci. Paris, t. 263, 516-519.

Hughes, B.P. and Chapman, G.P., 1966, The deformation of concrete and microconcrete in compression and tension with particular reference to particle size. Mag. of Concrete Res., 18, 54:19-24.

Hull, D., 1965, Introduction to dislocations. Pergamon Press Ltd., London, 259 p.

Jaeger, J.C. and Cook, N.G.W., 1969, Fundamentals of rock mechanics. Methuen & Co. Ltd., London, 513 p.

Karman, Th. Von, 1911, Festigkeitsversuche unter allseitigem druck. Z. Ver. dt. Ing., 55:1749-1757.

Krock, R.H. and Broutman, L.J., 1967, Principles of composites and composite reinforcement, in Modern Composite Materials, editors L.J. Broutman and R.H. Krock, Addison-Wesley, Reading, Mass., 3-26.

Krumbein, W.C., 1959, The "sorting out" of geological variables illustrated by regression analysis of factors controlling beach firmness. J. Sed. Petr., 29, 4:575-587.

_________ and Sloss, L.L., 1963, Stratigraphy and sedimentation, 2nd edition, W.H. Freeman & Co., San Francisco, 660 p.

Lundborg, N., 1968, Strength of rock-like materials. Internat. J. Rock Mech. Min. Sci., 5:427-454.

McClintock, F.A. and Walsh, J.B., 1963, Friction on Griffith cracks in rocks under pressure. Proc. Fourth U.S. Congress on Appl. Mech., ASME, New York, 1015-1021.

McLamore, R. and Gray, K.E., 1966, The mechanical behaviour of anisotropic sedimentary rocks. Trans. ASME Jour. of Engineering for Industry, 89, Series B, 62-73.

Mellon, G.B., 1964, Discriminatory analysis of calcite- and silicate-cemented phases of the Mountain Park sandstones. J. Geol., 72:786-809.

________, 1967, Stratigraphy and petrology of the Lower Cretaceous Blairmore and Mannville groups, Alberta Foothills and Plains. Res. Council of Alberta, Bull. 21:270 p.

Middleton, G.V., 1962, Size and sphericity of quartz grains in two turbidity formations. J. Sed. Petr., 32, 4:725-742.

Mogi, K., 1967, Effect of the intermediate principal stress on rock failure. J. Geophys. Res., 72, 20:5117-5131.

Morgenstern, N.R. and Phukan, A.L.T., 1969, Non-linear stress-strain relations for a homogeneous sandstone. Internat. J. Rock Mech. Min. Sci., 6:127-142.

Murrell, S. A. F., 1963, A criterion for brittle fracture of rocks and concrete under triaxial stress and the effect of pore pressures on the criterion, in Proc. Fifth Rock Mech. Symposium, Univ. of Minn., editor C. Fairhurst, Oxford, Pergamon, 563-577.

________, 1966, The effect of triaxial stress systems on the strength of rocks at atmospheric temperatures. Geophys. J. of the Roy. Astronomical Soc., 10, 3:231-281.

Nabarro, F.R.N., Basinski, Z.S. and Holt, D.B., 1964, The plasticity of pure single crystals. Advances in Phys., 13:193-323.

Naidai, A., 1950, Theory of flow and fracture of solids. McGraw-Hill Book Co. Inc., New York, 572 p.

Parkash, B., 1968, A Fortran IV program for grain size data from thin sections. Tech. Memo 68-2, Geology Dept., McMaster Univ., Hamilton, Ontario, 11 p.

Parker, E.R., 1963, Plastic flow and fracture of crystalline solids, in Mechanical Behaviour of Crystalline Solids, Nat. Bureau Standards Monography 59, 1-12.

Paterson, M.S., 1958, Experimental deformation and faulting in the Wombeyan marble. Geol. Soc. Amer. Bull., 69:465-475.

Paterson, M.S., 1969, The ductility of rocks, in Physics of Strength and Plasticity, editor A.S. Argon, M.I.T. Press, Cambridge, Mass., 377-392.

Price, N.J., 1960, The compressive strength of coal measure rocks. Colliery Engineering, 283.

________, 1963, The influence of geological factors on the strength of coal measure rocks. Geol. Mag., 100:428-443.

Rinehart, J.S., 1966, Fracture of rocks. Internat. J. Fracture Mech. 2:534-551.

Robertson, E.C., 1955, Experimental study of the strength of rocks. Geol. Soc. Amer. Bull., 66:1275-1314.

Stauffer, M.R., 1970, Deformation textures in tectonites. Can. J. Earth Sci., 7, 2 (Pt. 1):498-511.

Stearns, D.W., 1969, Fracture as a mechanism of flow in naturally deformed layered rocks, in Proc. Conf. on Res. in Tectonics, Kink Bands and Brittle Deformation, editors A.J. Baer and D.K. Norris, Geol. Surv. Can. Paper 68-52, 79-95.

Taylor, G.I., 1938, Plastic strain in metals. J. Inst. Metals, 62: 307-324.

Trask, P.D., 1959, Effect of grain size on the strength of mixtures of clay,sand and water. Geol. Soc. Amer. Bull., 70: 569-580.

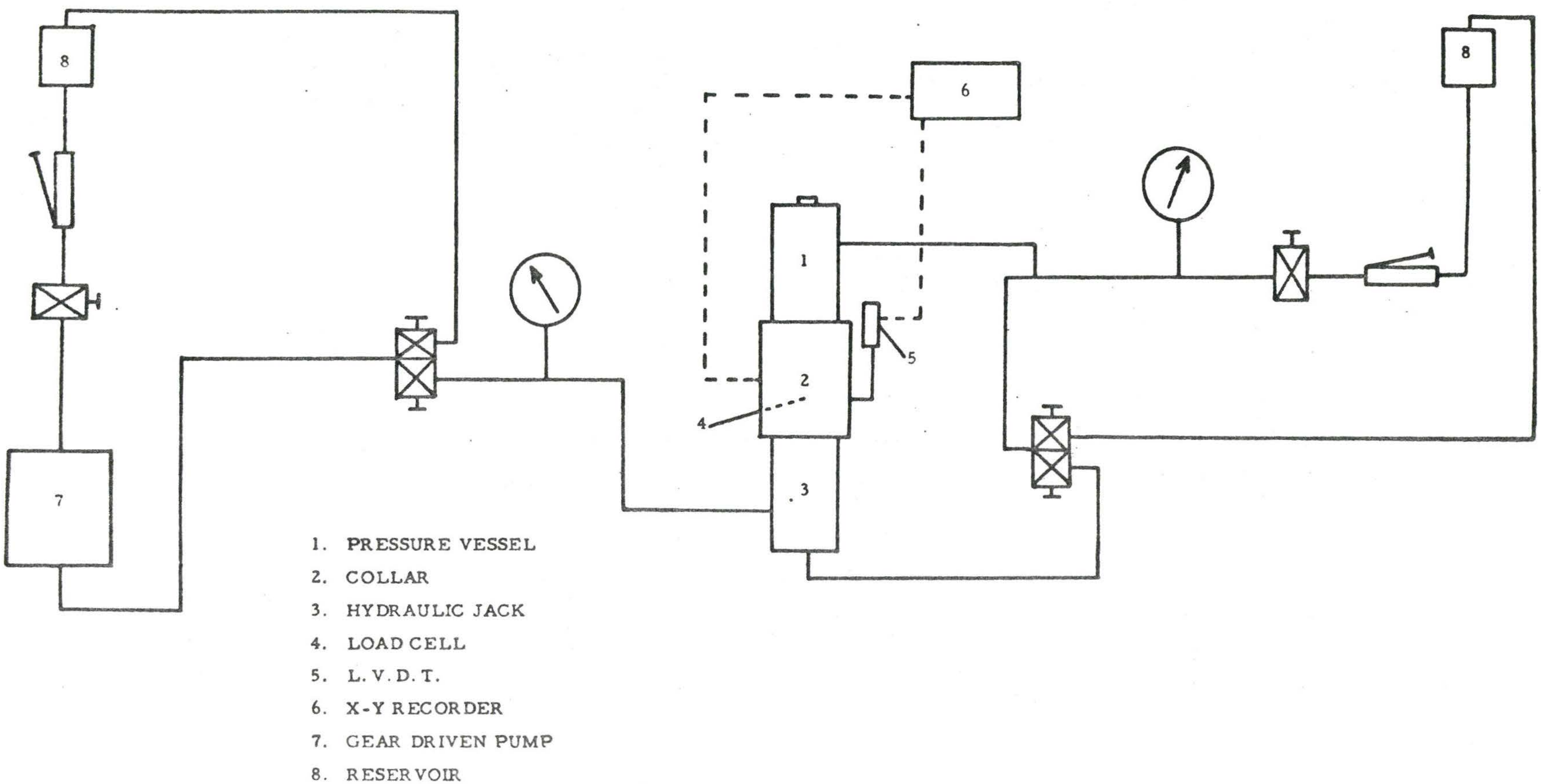

Figure 36. Schematic diagram of triaxial test apparatus.

2. Pressure Vessel

An exploded photograph and a schematic diagram of the pressure vessel are given in Plate 20 and Figure 37. The pressure vessel, designed to withstand confining pressures of 2500 bars, is made from a cylindrical piece of steel which has been machined and hardened. Upper and lower retaining plugs, and neoprene O-rings provide a pressure seal for the confining fluid. The upper plug is mechanically linked to the anvil and the test specimen. In a similar manner, the piston is mechanically linked to the hydraulic ram through the lower retaining plug. A small port in the wall of the test chamber allows the passage of confining fluid (kerosene). The anvil is drilled to allow passage of fluid to the specimen for pore pressure experiments. The specimen is removed through the top of the pressure vessel by unscrewing the upper retaining plug.

3. Confining Pressure System

Confining pressures are generated using a manual Enerpac model P228 hydraulic jack rated at 40,000 psi. Movement of the piston into the test chamber causes an increase in the confining pressure and it is, therefore, necessary to regulate this increase. This is accomplished by:

Plate 20

Exploded photograph of the pressure vessel showing the piston, specimen, anvil, upper and lower retaining plugs, piston rod, and the load cell.

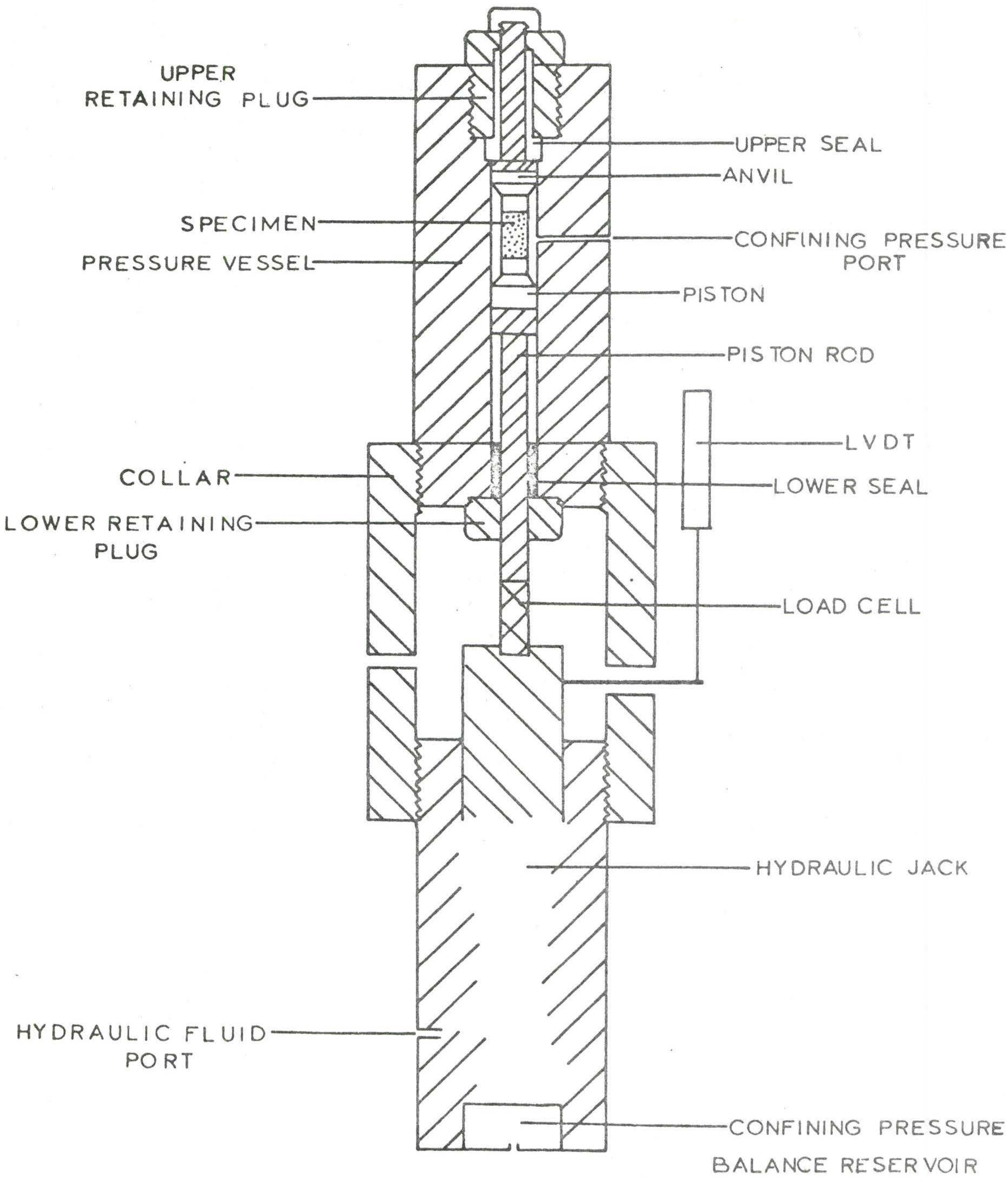

Figure 37. Schematic diagram of pressure vessel-press assembly.

(1) a balance overflow system which allows excess kerosene to flow into a reservoir in the hydraulic jack behind the advancing ram,

(2) a small hole in the piston which allows kerosene to flow behind the advancing piston.

A temperature compensated (-25° to 125°F) Heise gauge calibrated in bars is used for monitoring the confining pressure. During an experimental test small drops in confining pressure, due mainly to apparatus distortion, occur in the initial loading stages. These are easily corrected by making minor adjustments with the hand jack. Small increases in confining pressure (approximately 5 bars) occur when the specimens fail. This increase can be attributed to specimen dilatancy at failure.

4. Loading System

The loading system consists of a 20 ton Enerpac hydraulic ram which is held to the pressure vessel by a cylindrical steel collar (Figure 37). The ram is mechanically linked to the test specimen via a load cell, piston rod, and the piston. Variation in loading rates is achieved by a gear train in a motor-driven hydraulic pump (Plate 21). Although a mechanical loading system would provide constant strain rates, a hydraulic system allows one to investigate strain rate changes related to deformational modes.

Plate 21

A close-up view of the gear train of the strain pump. The strain pump provides constant pumping rates over a range of strain rates from 10^{-2} per second to 10^{-8} per second.

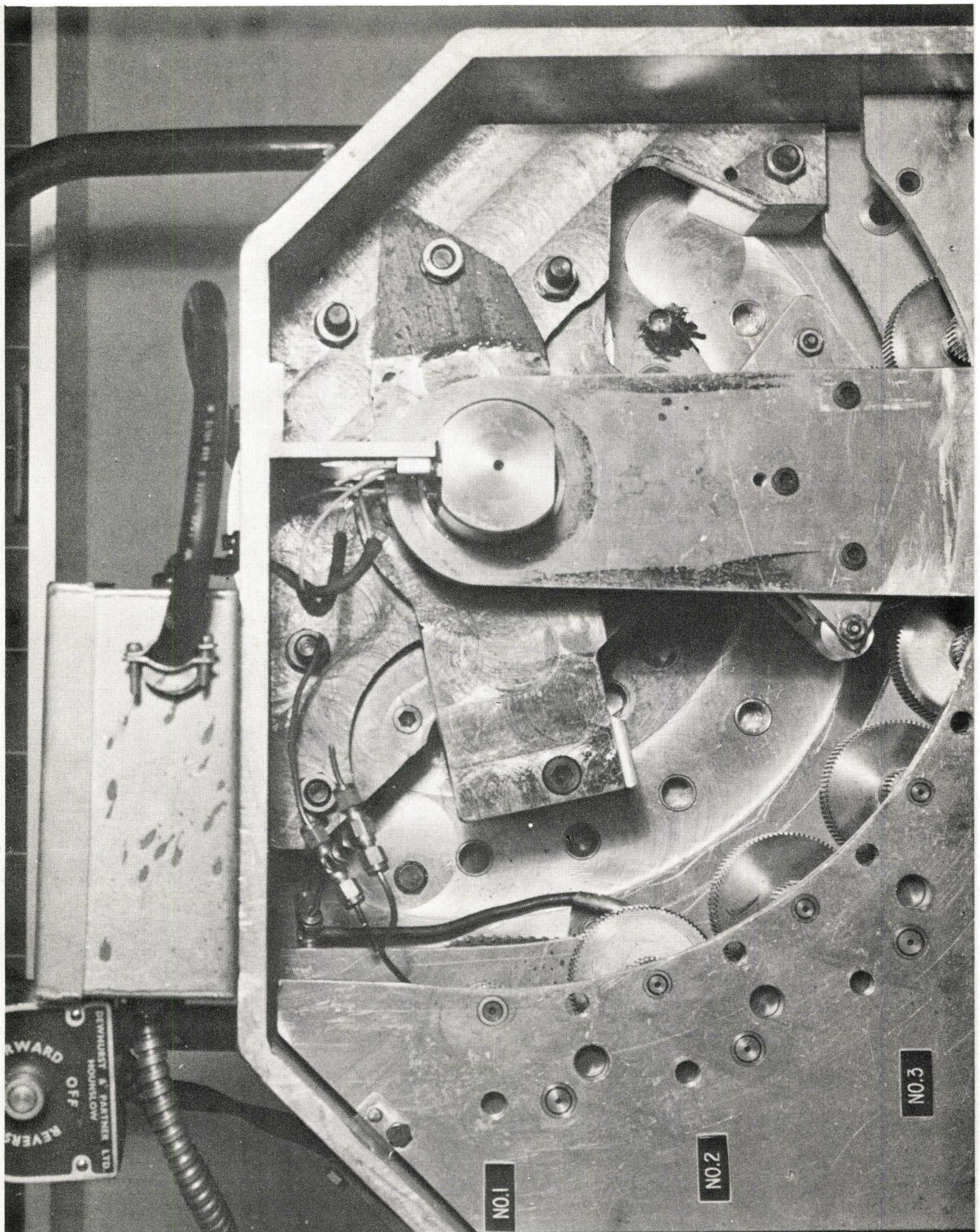
NO.1
NO.2
NO.3
OFF
DEWHURST & PARTNER LTD.
HOUNSLOW

5. Instrumentation

A Hewlett-Packard model 2D-2A, X-Y recorder is used to record the axial load and the piston displacement. A Cramer electric motor and a switching device interrupts the Y-axis to provide a time signal during the test and monitor changes in strain rate. Strain rates for any particular experiment are specified only for the elastic portion of the stress-strain curve.

Load cells were made by mounting in series four Budd strain gauges (Type C-6-141-B) on 1-1/2 by 1/2 inch cyclinders of "Ultimo 200" steel. These gauges have a high resolution and are virtually temperature insensitive between 62° and 100°F. The load cells are calibrated by applying known loads in a Tinius Olsen testing machine. A Budd P-350 Strain Indicator is used to calibrate the load cell and amplify the signal from the load cell to the X-Y recorder. The axial stress in the specimen can be calculated from the axial load after corrections for the confining pressure, frictional contributions of the ram and piston, and changing cross sectional area of the specimen have been made.

Displacement of the piston is measured by a Sanborn LVDT which is mechanically linked to the ram. Output from the LVDT is fed to the X-axis of the X-Y recorder. Piston displacement is converted to specimen strain after corrections have been made for the elastic distortion of the apparatus. An accurate strain measurement system for triaxial tests on rock materials is difficult to obtain. Most workers record compressive strain by external measurement of the loading piston displacement. A major difficulty of an external measuring system is encountered when small strains (0.5%) are being studied. The majority of experiments in this study were terminated at total strains greater than 1%, therefore minimizing errors due to strain measurement.

Elastic distortion of the apparatus for various axial loads and confining pressures was determined by using a steel blank of known Young's modulus as the test specimen. It was found that the apparatus distortion, as determined by axial loading, differed slightly from that obtained by applying different confining pressure loads. These differences are accounted for in reduction of experimental data.

Specimen Preparation

Specimens used for triaxial compressive tests were cored perpendicular to bedding from blocks of material using a half inch I. D. diamond bit. Specimen ends were cut by a diamond saw to an approximate length of slightly greater than one inch, and then were ground plane-parallel to within 1/1000 of an inch. Extrapolation of Hoskins and Horino's (1968) experiments on the influence of end conditions on the determination of compressive strength of various rocks indicates that non-parallelism of less than 0.0012 inches for half inch diameter specimens would not significantly alter specimen strength. Plane-parallel ends were obtained by using a thin section grinder in earlier experiments, but in later experiments a lathe and tool post grinder was used. The specimens were air dried in an oven at 200°F for a period of at least one week. Weighing of test samples showed no significant water loss after three days.

The test specimen is sealed from the enclosing confining pressure fluid by a thin copper or polyethylene jacket such that the strain is achieved in dry material. During initial tests on the Oriskany sandstone, thin copper jackets in confjunction with Tygon tubing was used for specimen jacketing. In later experiments, 6 mil polyethylene and translucent polyethylene tape was used for jacketing. Although different jacket techniques apparently did not influence the outward appearance of the stress-strain curve, the distribution of strain in some materials is significantly different.

After deformation, test specimens were photographed on one to four sides in their jackets. After jacket removal, specimens were impregnated with epoxy cement and the specimen sawed in half. One sawed half is used for this sectioning, the other half is retained as a permanent record of the tested core and is used as an opaque section.

Test Procedure

The test specimen within its polyethylene jacket is taped between the anvil and the piston with polyethylene tape. The upper retaining plug with the attached specimen assembly is secured into the top of the pressure vessel. Priming of the loading system is achieved by means of a small hand jack until the ram and the piston rod seat against the specimen assembly. An arbitrary zero is set on the X-Y recorder and designated as seating at atmospheric pressure. Confining pressure is then applied using the appropriate hand jack to the desired level. A calibration of the load axis, Y is made at this point using the Budd Strain Indicator.

Application of the confining pressure usually drives the piston rod down slightly off the specimen assembly. Reseating is achieved by using the gear driven pump. When the specimen assembly is reseated, the gear driven pump is not stopped but allowed to load the specimen to failure or to a predetermined strain level. The axial force required to overcome frictional resistance and reseat the specimen under confining pressure is later subtracted when calculating the applied load at any point.

When a test has reached the desired strain, the gear driven pump is shut off and a second calibration of the Y-axis is made. The load is removed at the same rate at which it was applied by putting the strain pump into the reverse position. After the load is removed, the seating displacement under confining pressure is noted such that permanent strain under confining pressure can be calculated. The confining pressure is then allowed to drop to atmospheric pressure, the specimen assembly is reseated, and the final displacement on the X-axis is recorded. When the specimen is removed from the pressure vessel, a final micrometer length measurement is made and used to check the electronic calculation of permanent strain.

Data Processing

Values of load and displacement are picked from the X-Y recorder record with special care taken to choose inflection points on the load-displacement curve. These values and pertinent constants are recorded and later punched on IBM cards.

The stress-strain relations for each test are determined using a computer program which corrects for the elastic distortion of the apparatus and provides true strain based on changes in cross-section of the test specimen on the assumption that the strain is homogeneously distributed (Appendix B).

The calculation of the differential stress after the specimen has failed can be complicated by the deformational mode. It must be considered that the strain may be concentrated in a narrow or wide zone depending on the confining pressure. If a specimen deforms homogeneously the cross-sectional area over which the force acts is determined by assuming that the specimen has remained cyclindrical. However, if shortening occurs by movement along a fracture, then the material deformed homogeneously only to the point of failure and all subsequent observable shortening is related to displacement on the fracture. Therefore, any subsequent calculation of strain should be based on the cross-sectional area just prior to faulting (Donath, 1968). If a specimen deforms by ductile faulting, the strain is distributed over a much larger area, but it is necessary to assume a changing mean cross-sectional area. However, a number of experiments on the brittle sandstones used in this study which were terminated at various strains indicated that rather than considerable movement taking place along the fault plane after faulting, the differential stress rose and a second fault was generated. It was, therefore, concluded that a uniformly changing cross-section area was a valid assumption even for specimens which have undergone brittle deformation.

In order to facilitate interpretation and comparison of several tests, a number of subroutines have been added to the main program. One subroutine provides interpolated values of stress for 0.2% increments of strain. These values of stress are used in another program to compute an average stress-strain curve for a number of tests run under identical experimental conditions. Values for each test are then compared to the computed average for every 0.2% of finite strain, and its deviation from the average is calculated and listed. If the average deviation for an entire test is greater than 10%, data from this test are rejected and the analysis is repeated. A deviation of less than 10% is accepted and inferred to be due to sample variation. Due to difficulties in measuring strains of less than 1%, no tests with less than 2% total strain were rejected.

A plot program and subroutine plots the corrected stress-strain curve for individual tests and for the computed average stress-strain curve.

A listing of computer programs used in this study is given in Appendix B.

Appendix B

COMPUTER PROGRAMS

General Statement

The computer programs used in this investigation have been written in Fortran IV for a CDC6400 computer. Programming assistance was provided by Mr. Julian Coward of the Geology Department. A slightly modified program of Parkash (1968) is used to calculate the standard statistical measures from grain size data obtained in thin section.

Calculation of the Stress-Strain Relations

Fortran Program No. 1 (Table XI) corrects for the elastic distortion of the apparatus and provides differential stress (based on changes in cross-sectional area) and specimen strain at any time or point N during a test. It can be used in conjunction with the plot and the interpolation subroutine.

Interpolation Subroutine

Fortran Program No. 2 (Table XII) interpolates for differential stress for specified increments of 0.2% strain.

TABLE XI. FORTRAN PROGRAM NO. 1 - CALCULATION OF STRESS-STRAIN RELATIONS

```
      DIMENSION TITLE(4),D(100),F(100),ED(100),RLS(100),AN(100)
      DIMENSION YDD(100),XDD(100)
      DIMENSION YD(100),YAX(100),NO(100),S(100)
      COMMON/AXS/PC
      CALL IDPLOT
  1   READ(5,101)TITLE,DATE
 101  FORMAT(5A10)
      READ(5,102)CA,CB,CCI,FMI,RLI,RDI,PC,FR1
 102  FORMAT(8F10.0)
      RLO=RLI*2.54
      RDO=RDI*2.54
      CC=CCI*2.54
      FML=FMI*2.54
      READ(5,103)DSAT,DSCP,DRSAT,DRSCP,ORIEN,CF
 103  FORMAT(6F10.0)
      READ(5,104)DO,FO,DN1,DN2,T,DCP1
 104  FORMAT(7F10.0)
      N1=DN1
      N2=DN2
      I=1
 110  READ(5,105)NO(I),DN,FN
      D(I)=DN
      FR=FR1-FO
      F(I)=FN-FO
105   FORMAT (5X,A5,2F10.0)
      ISTART=NO(I)
      IF(NO(I).EQ.5H88888)GO TO 200
      IF(NO(I).EQ.5H99999)GOTO200
      I=I+1
      GOTO110
 200  ITOT=I-1
      CE=CA*CB/CC
      DO210 I=1,ITOT
 210  ED(I)=CE*F(I)
      RLCP=RLO-CC*(DCP1-DSAT)+DSCP
      DO220 I=1,ITOT
      RLS(I)=RLO-CC*(D(I)-ED(I)-DSAT)+CF
 220  S(I)=100.*(RLCP-RLS(I))/RLCP
      SCP=(RLO-RLCP)/RLO
      VO=3.14159*RLO*(RDO/2.)**2.
      VCP=VO*((1.-SCP)**3)
      BM=-(PC*VO/(VCP-VO))
      XK=(1/BM)
      DO 230 I=1,ITOT
      AN(I)=VCP/RLS(I)
      YD(I)=CB*(F(I)-FR)/AN(I)
 230  YAX(I)=YD(I)+PC
```

```
      WRITE(6,310)PC,DRSCP
      WRITE(6,312)SR,SN,SP
      WRITE(6,313)E,SPM
      WRITE(6,314)BM,XK
  302 FORMAT(16H0ORIGINAL LENGTH,15X,F10.5,4H CM.26X,25HK1 (ELAST DISORT
     2 APPAR)    ,5X,E10.4, 7H CM/BAR)
  320 WRITE(6,321)
  311 FORMAT(16H0LENGTH UNDER CP,15X,F10.5,3H CM, 27X,18HK2 (LOAD CONSTA
     1NT),12X,F10.0,9H BARS/DIV)
  304 FORMAT(18H0ORIGINAL DIAMETER,13X,F10.5,3H CM,27X,26HK3 (DISPLACEME
     1NT CONSTANT),4X,F10.4,7H CM/DIV)
  305 FORMAT(16H0ORIGINAL VOLUME,15X,F10.5,6H CM(3),24X,23HK4(DISTORTION
     1 CONSTANT), 7X,F10.5,14H DIMENSIONLESS)
  306 FORMAT(16H0VOLUME UNDER CP,15X,F10.5,6H CM(3),24X,15HREFERENCE FOR
     1CE,15X,F10.2,4H DIV)
  307 FORMAT(23H0ANISOTROPY ORIENTATION,8X,F10.0,8H DEGREES,22X,20HSEATI
     1NG DISPLACEMENT,10X,F10.2,4H DIV)
  308 FORMAT(26H0DISPLACEMENT AT ZERO (DO),5X,F10.2,4H DIV,26X,29HSEATIN
     1G DISPLACEMENT UNDER CP,1X,F10.2,4H DIV)
  309 FORMAT(27H0FORCE DISPLACEMENT AT ZERO,4X,F10.1,4H DIV,26X,22HRESEA
     1TING DISPLACEMENT,8X,F10.2,4H DIV)
  310 FORMAT(19H0CONFINING PRESSURE,12X,F10.0,5H BARS,25X,23HRESEATING D
     1SPL UNDER CP,7X,F10.2,4H DIV)
  312 FORMAT(12H0STRAIN RATE,4X,E11.4,11H PER SECOND,8X,7H LOG SR,2X,F10
     2.3,6X,17H PERMANENT STRAIN,4X,F10.2,9H PER CENT)
  313 FORMAT(16H0YOUNG'S MODULUS,4X,E10.4,5H BARS,20X,16H MEASURED STRAI
     1N,4X,F10.2,9H PER CENT)
  314 FORMAT(13H BULK MODULUS,4X,E11.4,5H BARS,8X,15H COMPRESSIBILTY,4X,
     1E11.4,7H 1/BARS)
  321 FORMAT(1H0,18X,5HCHART,11X,5HCHART,9X,8HSPECIMEN,8X,8HPER CENT,5X,
     112HDIFFERENTIAL,4X,5HAXIAL/8H   POINT,11X,4HLOAD,12X,5HDISPL,9X,6H
     2LENGTH,10X,6HSTRAIN, 7X,6HSTRESS,10X,6HSTRESS //)
  341 FORMAT(1X,I5,10X,F10.3,6X,F10.3,4X,F10.5,6X,F10.2,2X,F10.0,4X,F10.
     10)
          I=1
  340 WRITE(6,341)I,F(I),D(I),RLS(I),S(I),YD(I),YAX(I)
          I=I+1
          IF(I.LE.ITOT)GOTO340
      SR=(S(N2)-S(N1))/(T*6000)
      SN=ALOG10(SR)
      SP=100*(DRSAT-DSAT)*CC/RLO
      E=(YD(N2)-YD(N1))/(RLS(N1)-RLS(N2))
      SPM=100.*(RLO-FML)/RLO
      WRITE(6,301)TITLE,DATE
  301 FORMAT(1H1, 8HSPECIMEN,12X,4A10,10X,12HDATE OF TEST,18X,A10)
      WRITE(6,302)RLO,CA
      WRITE(6,311)RLCP,CB
      WRITE(6,304)RDO,CC
      WRITE(6,305)VO,CE
      WRITE(6,306)VCP,FR
      WRITE(6,307)ORIEN,DSAT
      WRITE(6,308)DO,DCP1
      WRITE(6,309)FO,DRSAT
```

```
401   CONTINUE
      CALLPLOTSS(S,YD,ITOT,TITLE,DATE)
      IF(ISTART.EQ.5H88888) GO TO 1
      CALL PLOT(0.0,0.0,999)
      STOP
      END
```

TABLE XII. FORTRAN PROGRAM NO. 2 - INTERPOLATION SUBROUTINE

```
      SUBROUTINE INTRPL (XX,XDD,YDD,YY,N,ICK)
C    THIS SUBROUTINE GIVES LINEAR INTERPOLATION BETWEEN THE TWO
C     NEAREST POINTS  IN ARRAYS XDD(N), AND YDD(N) OF SIZE N
C      XX IS THE INPUT QUANTITY CORROSPONDING TO ARRAY XDD
C     YY IS THE OUTPUT QUANITITY  FRON THE POINT XX
C      ICK IS A TEST. IF ICK =0 THEN INTERPOLATION IS OK. IF ICK= 1 THEN
C     THE INPUT POINT XX DOES NOT LIE BETWEEN ANY OF THE POINTS IN ARRAY
C      XDD(N)
      DIMENSION XDD(N),YDD(N)
      XHG=XDD(N)
      XLW=XDD(1)
      YHG=YDD(N)
      YLW=YDD(1)
      ICK=0
      ICK1=0
      ICK2=0
      XHG=1000000.0
      XLW=-1000000.0
C    TO FIND THE TWO NEAREST POINTS IN ARRAY XDD
      DO 300 I=1,N
      IF(XDD(I).GT.XX)ICK1=1
      IF(XDD(I).LT.XX)ICK2=1
      IF(XDD(I).GT.XX.AND.XDD(I).LT.XHG) GOTO 100
      IF(XDD(I).LT.XX.AND.XDD(I).GT.XLW) GOTO 200
      GOTO 300
 100  XHG=XDD(I)
      YHG=YDD(I)
      IHG=I
      GOTO 300
 200   XLW=XDD(I)
      YLW=YDD(I)
      ILW=I
 300  CONTINUE
      YY=YLW+(YHG-YLW)*(XX-XLW)/(XHG-XLW)
      IF(ICK1.EQ.0.OR.ICK2.EQ.0) GOTO 400
      RETURN
 400   ICK=1
      RETURN
      END
```

Plot Subroutine

Fortran Program No. 3 (Table XIII) plots a curve of the differential stress (axial stress minus confining pressure) versus strain for individual tests. With minor modifications the program is also used to plot averaged stress-strain curves.

Test Comparison Program

Fortran Program No. 4 (Table XIV) provides the average values of differential stress in 0.2% increments of strain for a number of tests run under identical conditions. The program then compares the individual tests with the computed average for each 0.2% increment of strain.

Grain Size Study

Fortran Program No. 5 (Table XV) calculates the standard statistical measures using the method of moments from grain size data obtained in thin section. Also, this program calculates the mean and variance of sphericity, roundness, and packing of the grains studied in thin section.

TABLE XIII. FORTRAN PROGRAM NO. 3 - PLOT PROGRAM

```
      SUBROUTINE PLOTSS(S,YD,ITOT,TITLE,DATE)
      REAL MAXSS,MAXSN
      DIMENSION S(100),YD(100),TITLE(4),MAXSN(2),MAXSS(2)
      COMMON/AXS/PC
      ENCODE(8,105,APC)PC
  105 FORMAT(F8.0)
      CALL PRELIM(SIZSN,SIZSS,MAXSN,MAXSS,XTICKS,YTICKS,
     2XTICSZ,YTICSZ)
      CALL AXISS(MAXSN,MAXSS,XTICKS,YTICKS,XTICSZ,YTICSZ)
C     DRAW IN SPOTS AT POINTS
      CALL PLT MSP(S,YD,0.12,1H+,0.0,ITOT)
C     DRAW IN LINES BETWEEN POINTS
      DO100I=2,ITOT
  100 CALL PLTLN(S(I-1),YD(I-1),S(I),YD(I))
C     TITLE GRAPH
      CALL LETTER (10,0.12,0.0,1.0,0.2,10HSPECIMEN= )
      CALL LETTER (40,0.12,0.0,3.0,0.2, TITLE)
      CALL LETTER (10,0.12,0.0,1.0,0.0, 10HDATE=          )
      CALL LETTER(13,0.12,0.0,1.0,0.4,13HCONFINING P= )
      CALL LETTER(8,0.12,0.0,3.0,0.4,APC)
      CALL LETTER(10,0.12,0.0,3.0,0.0, DATE)
C     MOVE TO NEW PLOT
      CALL PLOT(SIZSN,0.0,-3)
      CALL PLOT(2.0   ,0.0,-3)
      RETURN
      END
      SUBROUTINE AXISS(MAXSN,MAXSS,XTICKS,YTICKS,XTICSZ,YTICSZ)
C     THIS SUBROUTINE DEFINES AXIS
      REAL MAXSS,MAXSN
      DIMENSION MAXSN(2),MAXSS(2)
C     DRAW IN AXIS LINES
      CALL PLTLN(0.0,0.0,MAXSN(1),0.0)
      CALLPLTLN(0.0,0.0,0.0,MAXSS(1))
C     PUT IN TICKS ON X AXIS AND LABEL XTIC=0.0
      XTIC=0.0
  100 CALL PLTLN(XTIC,0.0,XTIC,XTICSZ)
      ENCODE(4,101,AXX)XTIC
  101 FORMAT(F4.1)
      CALL PLTLET(4,0.12,-90.,XTIC,XTICSZ,AXX)
      XTIC=XTIC+XTICKS
      IF(XTIC.LT.MAXSN(1))GO TO 100
C     PUT IN TICKS ON YAXIS AND LABEL YTIC=0.0
      YTIC=0.0
  200 CALL PLTLN(0.0,YTIC,YTICSZ,YTIC)
      YYT=YTIC/1000.0
      ENCODE(4,101,AYY)YYT
      CALL PLTLET(4,0.12,0.0,-1.7,YTIC,AYY)
      YTIC=YTIC+YTICKS
```

```
      IF(YTIC.LT.MAXSS(1)) GO TO 200
C     LABEL AXISES
      CALL LETTER  (10,0.18,0.0,2.0,0.7,10HSTRAIN O/O)
      CALL LETTER(25,0.18,90.0,0.1,3.7,25HDIFFERENTIAL STRESS KBARS)
      RETURN
      END
      SUBROUTINE PRELIM(SIZSN,SIZSS,MAXSN,MAXSS,XTICKS,YTICKS,
     2XTICSZ,YTICSZ)
      REAL MAXSS,MAXSN
      DIMENSION MAXSS(2),MAXSN(2)
C     THIS SUBROUTINE INITILIZES THE PLOT SIZE ETC.
      SIZSS=10.0
      SIZSN=8.0
      MAXSS(1)= 7000.0
      MAXSN(1)=20.0
      MAXSS(2)=-1000.0
      MAXSN(2)=-2.0
      LTMARG=1.0
      BOTMG=1.0
      XTICKS=1.0
      YTICKS =1000.0
      XTICSZ=-200.0
      YTICSZ=-0.4
C     NOTE STRAINEQSN PUT ON X AXIS
C     STRESS EQ. SS PUT ON Y AXIS
      CALL FACTOR(2,MAXSN,MAXSS,SIZSN,SIZSS,LTMARG,BOTMG)
      RETURN
      END
```

TABLE XIV. FORTRAN PROGRAM NO. 4 - TEST COMPARISON

PROGRAM

```
      DIMENSION STSAV(100),DEV(10,100),DEVSUM(10),DEVAVE(10)
      DIMENSION TITLE(10,4),DATE(10),STN(10,100),STS(10,100),JJ(10)
      READ(5,100)NSTOP
C     JJ=NUMBER OF READINGS
  100 FORMAT(I2)
      JJMAX=0
      JJMIN=1000000
C     NUMBER OF TESTS IN COLUMN 2
      DO 50 J=1,100
      STSAV(J)=0.0
      DO 50 I=1,10
      STS(I,J)=0.0
   50 DEV(I,J )=0.0
      DO 300 II=1, NSTOP
      READ(5,101)(TITLE(II,J),J=1,4),DATE(II),JJ(II)
  101 FORMAT(4A10,20X,A10,5X,I5)
      JSTOP=JJ(II)
      IF(JJMAX.LT.JJ(II)) JJMAX=JJ(II)
      IF(JJMIN.GT.JJ(II)) JJMIN=JJ(II)
      DO 200 K=1, JSTOP
  200 READ(5,201) STN(II,K),STS(II,K)
  201 FORMAT(2F10.2)
  300 CONTINUE
      DO 400 I=1,JJMAX
      STOP=0.0
      SUM=0.0
      DO 400 J=1,NSTOP
      IF(JJ(J).GE.I) STOP=STOP+1.0
      SUM=SUM+STS(J,I)
  400 STSAV(I)=SUM/STOP
      DO 500 I=1, NSTOP
      DO 500 J=1, JJMAX
      DIFF=STSAV(J)-STS(I,J)
  500 DEV(I,J)=DIFF*100.0/STSAV(J)
      DO 450 I=1,NSTOP
      JIJ=JJ(I)+1
      DO 450 K=JIJ,JJMAX
  450 DEV(I,K)=0.0
      DO 620 I=1,10
  620 WRITE(6,621) (TITLE(I,J),J=1,4),DATE(I)
  621 FORMAT(1X,4A10,10X,A10)
      WRITE(6,600)
  600 FORMAT(7H STRAIN,3X,9HAVE STRSS,37X,8HSTRESSES,40X,14HDEVIATIONS 0
     1/0)
      WRITE(6,601)
```

```
601 FORMAT(20X,110H1        2         3         4         5         6         7         8         9
  1   10          1         2         3         4         5         6         7         8         9         10)
    SSSS=0.2
    DO609 K=1,JJMAX
    WRITE(7,611)SSSS,STSAV(K)
    WRITE(6,610)SSSS        ,STSAV(K),(STS(I,K),I=1,10),(DEV(I,K),I=1,10)
    SSSS=SSSS+0.2
609 CONTINUE
610 FORMAT(1X,F6.2,4X,F6.0,10F6.0,4X,10F5.1)
611 FORMAT(1X,F6.2,4X,F6.0)
    DO 701 J=1,NSTOP
    DEVSUM(J)=0.0
    DO 700 I=1,JJMAX
700 DEVSUM(J)=ABS(DEV(J,I))+DEVSUM(J)
701 DEVAVE(J)=DEVSUM(J)/JJ(J)
    WRITE(6,710)(DEVAVE(J),J=1,NSTOP)
710 FORMAT(50H DEV SUM=

  2                 10F5.1)
    STOP
    END
```

TABLE XV. FORTRAN PROGRAM NO. 5 - GRAIN SIZE STUDY

```
C     GRAIN SIZE STUDY
      DIMENSION A(500), B(500),C(500) , KFRE(30), KF(30), KLONG(30) ,
     1SP(500),KACUM(30),D1(500),D2(500),D3(500),D4(500),FMT(8),
     2 IDENT(2) ,FACT(500),SPE(500),RO(500),GC(500)
      REAL KF,KSUM,KFRE,LSUM,KACUM,KLONG
      READ (5,101 )  KPROS
      DO61 KK= 1,KPROS
      READ (5, 102) IDENT
      WRITE ( 6, 103 ) IDENT
      READ ( 5, 104) FMT
      N=1
    1 READ(5,FMT) A(N),B(N),FACT(N),SPE(N),RO(N),GC(N)
      IF(A(N).LT.0.0) GO TO 2
      N=N+1
      GO TO 1
    2 N=N-1
      AN=N
      DO 3 I = 1,N
      IF(FACT(I).EQ.0)FACT(I)=FACT(I-1)
      A(I)= A(I)* FACT(I)
      B(I)= B(I)* FACT(I)
      C (I)  = -(ALOG10 (   SQRT (   A(I) * B(I) ) ))/ 0.30103
    3 CONTINUE
      S1= 0.0
      DO 4 I= 1,N
      D1 (I) = C(I)
      S1  = S1+ D1(I)
    4 CONTINUE
      S2=0.0
      DO 71  I=1,N
       D2(I) = (   C(I) )**2
      S2 = S2 + D2(I)
   71 CONTINUE
      S3=0.0
      DO 72  I= 1,N
      D3(I) = (   C(I)  )**3
      S3=   S3+D3(I)
   72 CONTINUE
      S4= 0.0
      DO 73  I=1,N
      D4(I) = (   C(I)    )**4
      S4  = S4+ D4(I)
   73 CONTINUE
      SS2 =0.0
      SS3  = 0.0
      SS4  = 0.0
      SS2  = S2 -((  S1  ) ** 2) /AN
      SS3  = S3 - S2 *S1*3.0/AN +(2.0*(S1)**3   ) /AN**2
```

```
      SS4 = S4 - S3* S1* 4.0/ AN + S2* S1* S1* 6.0/ AN**2    - ( (S1)**4
     1  )*3.0 / AN** 3.0
      AK1 =0
      AK2= 0
      AK3=0
      AK4=0
      AK1 = S1/AN
      AK2 = (1.0/ (AN-1.0))*SS2
      AK3 = (AN/( (AN-1.0) *(AN-2.0)))*SS3
      AK4 = (AN/( (AN-1.0)*(AN-2.0)*(AN-3.0))) * ( (AN+1.0)*SS4-(3.0*
     1(AN-1.0)/AN)*(SS2)**2)
      AM1 = AK1
      AM2 = AK2*( AN-1.0) / AN
      AM3 = AK3*(AN-1.0) * (AN-2.0)/ AN**2.0
      AM4 = ( (AN-1.0) /((AN+1.0)*(AN**2.0)))*((AN-2.0)*(AN-3.0)*AK4 +
     1      3.0* ( (AN-1.0)**2.0) *AK2**2)
      GG1 =0.0
      GG2 = 0.0
      GG1 = AK3/(AK2)**1.5
      GG2 = AK4 /(AK2)**2
      SG1 = SQRT
     1      (6.0* AN*(AN-1.0)/((AN-2.0)*(AN+1.0)*(AN+3.0)) )
      SG2 = SQRT(
     1      24.0*AN*((AN-1.0)**2.0)/((AN-3.0)*(AN-2.0)*(AN+3.0)*(AN+5.0))
     2 )
      TG1 = GG1/SG1
      TG2 = GG2/SG2
C     SORT IN TO QUARTER PHI CLASSES
      TOP = - 0.25
      DO 6 NCLSS= 1,25
      KS= 0
      DO 7 I= 1,N
      IF (C(I).LT.TOP.AND. C(I).GE.(TOP-0.25)) KS = KS+1
    7 CONTINUE
      TOP = TOP+ 0.25
      KF (NCLSS)=KS
    6 CONTINUE
      KFRE(1)=KF(1)
      KSUM=0.0
      DO201NCLSS=1,25
  201 KSUM=KF(NCLSS)+KSUM
      DO202 NCLSS=1,25
  202 KF(NCLSS)=100.0*KF(NCLSS)/KSUM
      DO 203 NCLSS=2,25
      NCLSX=NCLSS-1
  203 KFRE(NCLSS)=KF(NCLSS)+KFRE(NCLSX)
C     SPHERICITY DETERMINATIONS
      DO 9 I = 1,N
      SP(I) = B(I)/A(I)
      IF ( SP(I) .GT. 1.00) GO TO 23
      GO TO 9
   23 SP(I) = 1.0/ SP(I)
    9 CONTINUE
C SORT INTO 0.1 SPHERICITY CLASSES
```

```
      TOP = 0.1
      DO 10 NLASS= 1,10
      KP = 0
      DO 11 I = 1,N
      IF ( SP(I) .LE. TOP. AND. SP(I).GT.(TOP-0.1)) KP=KP+1
   11 CONTINUE
      KLONG (NLASS) = KP
      TOP = TOP + 0.1
   10 CONTINUE
      KACUM(1)=KLONG(1)
      LSUM =0.0
      DO301NLASS=1,10
  301 LSUM=KLONG(NLASS)+LSUM
      DO 302 NLASS=1,10
  302 KLONG(NLASS)=100.0*KLONG(NLASS)/LSUM
      DO 303 NLASS=2,10
      NLASSX=NLASS-1
  303 KACUM(NLASS)=KLONG(NLASS)+KACUM(NLASSX)
      P1 = 0.0
      P2 = 0.0
      DO 50 I = 1, N
       R1 = SP(I)
       R2 = R1*SP(I)
      P1 = P1 + R1
      P2 = P2+R2
      R1=0.0
      R2=0.0
   50 CONTINUE
      SPMEA = P1/AN
      SPSTA = ( P2 - (P1*P1/AN))/ (AN-1.0)
      WRITE(6,105)  S1, S2, S3, S4, SS2, SS3, SS4, AK1, AK2, AK3, AK4,
     1 AK1, AM2, AM3, AM4,GG1,GG2, SG1, SG2,SPMEA,SPSTA,TG1,TG2
      WRITE (6,106)
      SPH=0.0
      DO 41 NLASS= 1,10
       SPH= SPH+ 0.1
      WRITE(6,107)  SPH, KLONG(NLASS), KACUM(NLASS)
   41 CONTINUE
      WRITE (6,108)
      PHI = 0.0
      DO 31 NCLSS= 1,25
      PHI= PHI+ 0.25
      WRITE(6,109)  PHI, KF(NCLSS), KFRE(NCLSS)
   31 CONTINUE
      WRITE(6,110)
   61 CONTINUE
  101 FORMAT (I3)
  102 FORMAT ( 2A6, 8X, I3, 7X, F5.4 )
  103 FORMAT ( // 40X, 9H ********, 2A6, 9H ******** //45X,17H GRAIN SIZ
     1E STUDY )
  104 FORMAT (8A10)
  105 FORMAT ( 10X, 4H S1=, F8.3, 10X,  4H S2=, F8.1, 10X,4H S3=, F8.1,
     1 10X , 4H S4=,F8.1/10X,5H SS2=, F8.3, 10X, 5H SS3=,F8.3, 5H SS4=,
     2 F8.3/  10X, 4H K1=, F8.3, 10X, 4H K2=, F8.3, 10X, 4H K3=, F8.3,
```

```
    3 10X, 4H K4=, F8.3,  /10X, 4H M1=, F8.3, 10X, 4H M2=, F8.3, 10X,
    4 4H M3=, F8.3, 10X, 4H M4=, F8.3/    20X, 4H G1=,F8.3,10X,4H G2=,
    5 F8.3/ 20X, 5H SG1=, F8.3, 10X, 5H SG2=,F8.3/
    6 20X, 18H MEAN SPHERICITY =,F8.3,19H SPH. STAN. DEV.  =, F8.3/
    7      15X, 5H TG1=, F8.3,15X,5H TG2=,F8.3)
  106 FORMAT ( // 40X, 17H SPHERICITY STUDY/ 50X, 10H FREQUENCY, 10X,
    1 21H CUMULATIVE FREQUENCY)
  107 FORMAT ( 23H CLASS WITH UP. LIMIT =, F5.2, 28X,F5.2,24X,F5.2)
  108 FORMAT (//40X, 11H SIZE STUDY/ 50X, 10H FREQUENCY, 10X, 21H CUMULA
    1TIVE FREQUENCY)
  109 FORMAT ( 23H CLASS WITH UP. LIMIT =, F7.3,28X, F5.2,24X,F5.2)
  110 FORMAT ( 1H1)
C      CALCULATIONS WITH ESTIMATED VALUES OF SPHERICITY,ROUNDNESS
C     CALCULATION AVERAGE ESTIMATED SPHERICITY AND STANDARD DEVIATION
      SSPE=0.0
      DO 800 I=1,N
  800 SSPE=SSPE+SPE(I)
      ASPE=SSPE/N
      DSPE=0.0
      DO 801 I=1,N
  801 DSPE=DSPE+ (ASPE-SPE(I))**2
      AN=N-1
      STDS=(DSPE/AN)**0.5
      WRITE(6,802)ASPE,STDS
  802 FORMAT(1X,15HAVERAGE EST SPH,4X,F10.2,4X,3HSTD,1X,F10.4)
C     CALCULATION OF MEAN ESTIMATED ROUNDNESS AND ITS DEVIATION
      SRO=0.0
      DO 900 I=1,N
  900 SRO=SRO+RO(I)
      ARO=SRO/N
      DRO=0.0
      DO 901 I=1,N
  901 DRO=DRO+ (ARO-RO(I))**2
      AN=N-1
      DRO=(DRO/AN)**0.5
      WRITE(6,902)ARO, DRO
  902 FORMAT(1X,21HAVERAGE EST ROUNDNESS,4X,F10.4,4X,3HSTD,1X,F10.4)
C     CALCULATION OF MEAN CONTACTS PER GRAIN AND ITS DEVIATION
      SGC=0.0
      DO500 I=1,N
  500 SGC=SGC+GC(I)
      AGC=SGC/N
      DGC=0.0
      DO 501 I=1,N
      DGC=DGC+(AGC-GC(I))**2
  501 CONTINUE
      AN=N-1
      SDGC=(DGC/AN)**0.5
      WRITE(6,502)AGC,SDGC
  502 FORMAT(1X,26HAVERAGE CONTACTS PER GRAIN,4X,F10.2,4X,3HSTD,1X,F10.4
    1)
      STOP
      END
```

Appendix C

SUMMARY OF EXPERIMENTS

The pertinent experimental data of the triaxial compression tests on the Potsdam sandstone, Blairmore sandstone, Oriskany sandstone, and the arenaceous Columbus limestone at room temperature and strain rates of the order of 10^{-5} per second are summarized in Tables XVI, XVII, XVIII, and XIX. Experimental results on the Oriskany sandstone deformed at strain rates of the order of 10^{-6} and 10^{-7} are summarized in Tables XX and XXI.

TABLE XVI. SUMMARY OF TRIAXIAL COMPRESSION TESTS ON POTSDAM SANDSTONE, BLOCK 71-A, AT ROOM TEMPERATURE AND STRAIN RATES OF THE ORDER OF 10^{-5} PER SECOND

Experiment Number	Confining Pressure KB	Ultimate Strength, KB	Mean Pressure, KB	Octahedral Shear Stress, KB	Total Strain Percent	Ductility, Percent	Fracture Angle to σ_1, degrees	Deformational Mode
5.1	Atmospheric	1.00	0.33	0.47	2.22	0.62	2	Extensional fault
6.9	Atmospheric	1.25	0.40	0.56	2.51	0.63	0	"
6.4	Atmospheric	1.11	0.37	0.52	2.36	0.61	0	"
4.6	0.50	3.54	1.68	1.67	4.26	1.39	28	Brittle fault
6.6	0.50	3.44	1.65	1.62	8.15	1.30	29	"
6.7	0.50	3.53	1.68	1.66	4.89	1.25	21	"
4.7	1.00	4.11	2.37	1.94	9.75	1.91	32	"
4.8	1.00	4.42	2.47	2.08	6.41	1.72	30	"
4.9	1.00	3.90	2.30	1.84	3.60	1.64	32	"
4.10	1.00	3.90	2.30	1.84	3.21	1.56	33	"
4.11	1.00	-	-	-	0.84	-	-	Elastic
5.2	1.50	5.37	3.29	2.53	4.74	1.72	35	Brittle fault
5.4	1.50	5.24	3.25	2.47	16.47	1.87	NM*	"
5.5	1.50	5.19	3.23	2.44	7.53	1.90	36	"
5.6	1.50	5.22	3.24	2.46	3.59	1.60	24	"
5.8	1.50	-	-	-	1.48	-	-	Elastic
5.9	2.00	5.81	3.94	2.74	9.57	1.86	35	Brittle fault
5.10	2.00	5.42	3.81	2.56	4.93	1.70	36	"
5.11	2.00	6.07	4.02	2.86	3.31	1.97	31	"
5.12	2.00	5.93	3.97	2.80	3.59	2.24	34	"
6.1	2.00	6.32	-	-	1.69	-	-	Elastic
4.1	2.50	6.37	4.62	3.00	4.17	2.55	36	Brittle fault
4.3	2.50	6.60	4.70	3.11	8.71	2.53	31	"
4.4	2.50	6.23	4.58	2.94	7.00	2.01	41	"
4.5	2.50	6.50	4.67	3.06	2.39	2.39	33	"
6.2	2.50	6.49	4.78	3.23	2.76	2.16	33	"

NM* Not measurable

TABLE XVII. SUMMARY OF TRIAXIAL COMPRESSION TESTS ON BLAIRMORE SANDSTONE, BLOCK 51A, AT ROOM TEMPERATURE AND STRAIN RATES OF THE ORDER OF 10^{-5} PER SECOND

Experiment Number	Confining Pressure KB	Ultimate Strength, KB	Mean Pressure, KB	Octahedral Shear Stress, KB	Total Strain Percent	Ductility, Percent	Fracture Angle to σ_1, degrees	Deformational Mode
1.7	Atmospheric	1.54	0.52	0.73	4.24	0.90	0	Extensional fault
1.8	"	1.43	0.48	0.68	3.58	0.84	0	"
2.1	"	1.80	0.60	0.85	4.31	0.98	10	"
3.8	0.50	3.37	1.62	1.59	4.27	1.48	26	Brittle fault
4.6	0.50	3.44	1.65	1.62	8.96	1.35	24	"
4.7	0.50	3.36	1.62	1.58	8.17	1.39	28	"
1.5	1.00	4.77	2.59	2.25	14.33	1.33	30	"
1.9	1.00	4.49	2.50	2.11	14.24	1.49	25	"
1.11	1.00	4.49	2.50	2.12	3.87	1.51	33	"
3.4	1.00	4.26	2.42	2.01	7.52	1.62	27	"
3.6	1.00	4.35	2.45	2.05	1.61	1.61	-	Elastic
3.7	1.00	-	-	-	0.62	-	-	Elastic
2.4	1.50	5.38	3.29	2.54	4.49	1.85	32	Brittle fault
2.7	1.50	5.29	3.27	2.49	9.96	1.82	30	"
2.9	1.50	5.20	3.23	2.45	13.55	1.81	27	"
3.3	1.50	5.19	3.23	2.44	1.84	-	-	Elastic
1.4	2.00	6.15	4.05	2.90	5.12	1.95	30	Brittle fault
1.6	2.00	6.15	4.05	2.90	1.93	1.93	-	Elastic
1.12	2.00	5.72	3.91	2.70	13.89	1.98	35	Brittle fault
3.5	2.00	5.53	3.84	2.61	8.95	2.49	34	"
2.1-A	2.50	6.56	4.69	3.09	4.58	2.62	32	"
2.2	2.50	6.28	4.59	2.96	13.89	2.80	31	"
2.3	2.50	6.29	4.60	2.96	4.81	2.65	36	"
2.5	2.50	6.35	4.62	2.99	2.48	2.48	-	Elastic
2.6	2.50	-	-	-	1.03	-	-	Elastic
2.10	2.50	6.13	4.54	2.89	7.97	2.57	32	Brittle fault
3.2	2.50	6.14	4.55	2.89	8.44	2.71	37	"

TABLE XVIII. SUMMARY OF TRIAXIAL COMPRESSION TESTS ON THE ORISKANY SANDSTONE, BLOCK 61-A, AT ROOM TEMPERATURE AND STRAIN RATES OF THE ORDER OF 10^{-5} PER SECOND

Experiment Number	Confining Pressure Kb	Ultimate Strength, Kb	Mean Pressure, Kb	Octahedral Shear Stress, Kb	Total Strain Percent	Ductility, Percent	Fracture Angle to σ_1, degrees	Deformational Mode
2.5	Atmospheric	0.92	0.31	0.44	2.26	0.52	0	Extensional fault
3.9	"	0.86	0.29	0.40	1.72	0.49	0	"
5.10	"	0.92	0.31	0.43	1.61	0.40	0	"
5.11	"	0.89	0.30	0.47	1.65	0.41	0	"
2.9	0.25	2.10	0.95	0.99	3.82	0.55	22	Brittle fault
5.4	0.25	2.36	1.05	1.11	3.66	0.96	14	"
5.12	0.25	2.21	0.99	1.04	7.36	0.79	26	"
5.6	0.50	3.25	1.58	1.53	2.69	0.93	18	"
5.7	0.50	3.23	1.58	1.52	3.25	1.16	24	"
5.8	0.50	3.37	1.62	1.59	3.62	0.94	27	"
2.1	1.00	4.13	2.38	1.95	4.39	2.05	27	"
2.4	1.00	4.50	2.50	2.12	4.72	1.97	32	"
3.2	1.00	3.94	2.31	1.86	4.54	1.95	28	"
3.3	1.00	3.91	2.31	1.85	4.48	2.22	28	"
3.5	1.00	3.99	2.33	1.88	15.04	1.84	37	"
6.1	1.00	4.10	2.37	1.94	15.05	1.91	30	"
7.11	1.00	3.89	2.30	1.83	1.96	1.96	-	Elastic
7.12	1.00	-	-	-	0.79	-	-	"
3.10	1.10	3.98	2.43	1.88	15.41	1.89	37	Brittle fault
4.3	1.10	4.02	2.44	1.89	9.45	1.60	42	"
4.7	1.10	4.13	2.48	1.95	5.74	2.27	33	"
6.2	1.10	3.99	2.43	1.88	15.70	1.83	36	"
2.10	1.25	4.23	2.66	1.99	15.91	2.59	NM*	"

Experiment Number	Confining Pressure Kb	Ultimate Strength, Kb	Mean Pressure, Kb	Octahedral Shear Stress, Kb	Total Strain Percent	Ductility, Percent	Fracture Angle to σ_1, degrees	Deformational Mode
2.12	1.25	3.81	2.52	1.80	15.87	2.50	NM	Brittle fault
4.10	1.25	3.95	2.57	1.86	12.96	1.97	NM	"
4.12	1.25	4.23	2.66	1.99	8.13	2.09	NM	"
6.6	1.25	4.33	2.69	2.04	4.71	2.17	37	"
3.5	1.50	5.11	3.20	2.41	14.50	2.09	34	"
3.6	1.50	4.66	3.05	2.20	14.20	2.53	33	"
3.11	1.50	4.47	2.99	2.11	5.33	2.26	27	"
4.6	1.50	4.66	3.05	2.20	6.15	2.40	30	"
4.11	1.50	4.15	2.88	1.96	5.97	2.45	NM	"
5.9	1.50	4.50	3.00	2.12	5.80	1.98	NM	"
6.5	1.50	4.70	3.07	2.22	15.02	2.54	37	"
7.7	1.50	4.48	2.99	2.11	4.43	2.71	42	Ductile fault
7.8	1.50	4.67	3.06	2.20	2.65	2.34	43	"
7.9	1.50	-	-	-	1.73	-	-	Elastic
2.7	2.00	5.22	3.74	2.46	10.74	3.21	37	Ductile fault
2.11	2.00	5.29	3.76	2.49	5.08	3.13	42	"
4.1	2.00	5.21	3.74	2.46	9.06	2.85	30	"
4.2	2.00	5.26	3.75	2.48	18.39	3.58	40	"
4.9	2.00	4.99	3.66	2.35	8.53	3.97	37	"
5.3	2.00	5.10	3.67	2.40	10.12	3.01	35	"
6.3	2.00	5.43	3.81	2.56	13.43	2.20	37	"
7.4	2.00	5.34	3.78	2.52	4.71	2.99	NM	"
7.5	2.00	5.39	3.80	2.54	3.36	3.14	NM	"
7.6	2.00	-	-	-	2.85	-	-	Elastic
2.6	2.50	6.26	4.59	2.95	7.08	3.07	42	Ductile fault
2.8	2.50	5.72	4.41	2.69	6.16	3.30	$\approx$ 40	"
3.7	2.50	5.57	4.36	2.63	15.34	3.57	NM	"
4.4	2.50	6.10	4.53	2.87	15.17	3.36	33	"
4.8	2.50	5.91	4.47	2.79	8.40	3.65	NM	"
5.2	2.50	5.71	4.40	2.69	7.91	3.38	NM	"
6.4	2.50	5.97	4.49	2.81	4.22	3.28	41	"

Experiment Number	Confining Pressure Kb	Ultimate Strength, Kb	Mean Pressure, Kb	Octahedral Shear Stress, Kb	Total Strain Percent	Ductility, Percent	Fracture Angle to σ_1, degrees	Deformational Mode
7.1	2.50	5.68	4.39	2.68	4.93	4.13	43	Ductile fault
7.2	2.50	5.53	4.34	2.61	2.95	2.95	-	Elastic
7.3	2.50	-	-	-	1.33	-	-	Elastic

*NM = Not measurable

TABLE XIX. SUMMARY OF TRIAXIAL COMPRESSION TESTS ON THE COLUMBUS LIMESTONE, BLOCK 81A, AT ROOM TEMPERATURE AND STRAIN RATES OF THE ORDER OF 10^{-5} PER SECOND

Experiment Number	Confining Pressure Kb	Ultimate Strength, Kb	Mean Pressure, Kb	Octahedral Shear Stress, Kb	Total Strain Percent	Ductility, Percent	Fracture Angle to σ_1, degrees	Deformational Mode
1.1	Atmospheric	0.46	0.15	0.21	1.08	0.34	10	Extensional fault
1.3	"	0.45	0.15	0.21	1.37	0.34	2	"
1.6	"	0.41	0.14	0.19	0.99	0.35	NM*	"
2.2	0.10	0.75	0.35	0.35	7.86	0.56	28	Brittle fault
2.3	0.10	0.85	0.38	0.40	1.32	0.48	33	Brittle fault
3.12	0.10	0.70	0.33	0.33	1.19	0.54	NM	"
1.5	0.25	0.97	0.57	0.46	4.53	0.84	32	Ductile fault
1.9	0.25	0.94	0.56	0.44	1.30	0.84	40	"
2.1	0.25	0.99	0.58	0.47	0.83	0.83	-	Elastic
3.1	0.50	1.02	0.84	0.48	1.69	1.13	NM	Ductile fault
3.2	0.50	1.08	0.86	0.51	18.56	0.97	36	"
3.3	0.50	1.18	0.89	0.56	7.92	1.13	44	"
3.4	0.50	1.31	0.81	0.62	0.93	0.83	-	Elastic
2.11	0.50	1.04	0.85	0.49	12.72	1.74	$\approx$ 40	Ductile fault
2.4	1.00	-	-	-	2.20	-	NM	"
2.5	1.00	-	-	-	1.42	1.42	-	Homogeneous
3.6	1.00	1.90	-	-	17.75	-	40	Ductile fault
3.7	1.00	-	-	-	7.30	-	NM	"
3.11	1.00	-	-	-	0.64	0.64	-	Elastic
2.7	1.50	2.69	-	-	16.95	-	$\approx$ 40	Ductile fault
2.10	1.50	-	-	-	0.69	0.69	-	Elastic
3.9	1.50	-	-	-	10.77	-	NM	Ductile fault
3.10	1.50	-	-	-	2.51	2.51	-	Homogeneous

Experiment Number	Confining Pressure Kb	Ultimate Strength, Kb	Mean Pressure, Kb	Octahedral Shear Stress, Kb	Total Strain Percent	Ductility, Percent	Fracture Angle to σ_1, degrees	Deformational Mode
4.9	1.50	-	-	-	7.59	-	$\approx$ 40	Ductile fault
1.11	2.00	-	-	-	11.07	-	NM	"
3.5	2.00	-	-	-	15.61	-	$\approx$ 40	"
4.1	2.00	3.14	-	-	16.01	-	$\approx$ 40	"
4.2	2.00	-	-	-	11.21	-	NM	"
4.3	2.00	-	-	-	7.08	7.08	-	Homogeneous
4.4	2.00	-	-	-	3.15	3.15	-	"
4.5	2.00	-	-	-	1.10	1.10	-	"
4.6	2.50	3.76	-	-	15.93	15.93	-	"
4.7	2.50	-	-	-	7.44	7.44	-	"
4.8	2.50	-	-	-	3.37	3.37	-	"
4.10	2.50	-	-	-	1.38	1.38	-	"
4.12	2.50	-	-	-	10.26	10.26	-	"

NM* Not measurable

TABLE XX. SUMMARY OF TRIAXIAL COMPRESSION TESTS ON ORISKANY SANDSTONE, BLOCK 61-A, AT ROOM TEMPERATURE AND STRAIN RATES OF THE ORDER OF 10^{-6} PER SECOND

Experiment Number	Confining Pressure Kb	Ultimate Strength, Kb	Mean Pressure, Kb	Octahedral Shear Stress, Kb	Total Strain Percent	Ductility, Percent	Fracture Angle to σ_1, degrees	Deformational Mode
6.7	1.00	3.71	2.24	1.75	4.29	1.98	31	Brittle fault
6.8	1.00	3.57	2.19	1.68	4.44	1.93	33	"
6.9	1.00	3.57	2.19	1.68	4.41	1.87	32	"

TABLE XXI. SUMMARY OF TRIAXIAL TEST ON ORISKANY SANDSTONE, BLOCK 61-A, AT ROOM TEMPERATURE AND A STRAIN RATE OF THE ORDER OF 10^{-7} PER SECOND

Experiment Number	Confining Pressure Kb	Ultimate Strength, Kb	Mean Pressure, Kb	Octahedral Shear Stress, Kb	Total Strain Percent	Ductility, Percent	Fracture Angle to σ_1, degrees	Deformational Mode
6.11	2.50	5.89	4.46	2.78	9.36	5.76	≈ 40	Ductile fault